Micro Systems for Bio-Enzymatic Reaction Detection

AMRITSAR JEETENDER SINGH

A Thesis

In

The Department

of

Mechanical and Industrial Engineering

Presented in Partial Fulfillment of the Requirements for the

Degree of Master of Applied Science

at

Concordia University

Montreal, Quebec, Canada, H3G 1M8

November 2005

Your file Votre référence
ISBN: 0-494-14294-4
Our file Notre référence
ISBN: 0-494-14294-4

Abstract

Micro Systems for Bio-Enzymatic Reaction Detection

Amritsar Jeetender Singh

In recent years a great deal of scientific research has been devoted to fabrication of microdevices for continuous monitoring of biological samples. These samples require easy-to-use, low cost and highly sensitive methods for their identification. Micro Electro Mechanical Systems (MEMS) or Microsystem Technology (MST) are considered to be ideal candidates for such applications. Biosensing applications is one of the fields where MEMS are promising to revolutionize both industrial and consumer products. Micro-cantilever beams are one of the MEMS devices that are used to sense enzymatic reactions using Micro Opto Mechanical Systems (MOEMS) and that concept is studied in this thesis. Detection of enzymatic reactions needs analytical modeling to validate with the experimental work done in this thesis. Enzymatic detection is carried under various conditions associated with the surrounding electrostatic field. The basic principles of measurement are then formulated.

In the present work, Poly Vinyl Dichloro Fluoride (PVDF) small size cantilever beams are analyzed under the influence of the extra mass which is due to the enzyme droplet on one segment of the beam. The superficial tension developed on the surface due to the enzymatic interaction was evaluated from the tip deflection of the cantilever beam in order to validate the signature reaction obtained from the experiments. The variation of natural frequency with the position of the load is pivotal to understand the dynamics of the beam was done using the Finite Element Analysis (FEA). The stress produced by the

enzyme droplet on the segment of the beam created a significant deflection which is amply exhibited in this thesis. Static equilibrium analysis on the cantilever beam was carried out. Further, Rayleigh-Ritz method was used to evaluate the dynamic changes that would occur in a vibrating cantilever on which a bio-chemical reaction takes place.

Experimental analysis was done on PVDF cantilever beams under the influence of two sets of enzymes to quantify the results for enzymatic detection. In this experimental work, the enzymatic detection on cantilever beams was extended to external electrostatic field to understand the signature of reactions to a higher degree. Optical detection technique was employed to monitor the signature of reactions.

Validation needs further led to the application of other sophisticated techniques like Fourier Transform Infrared Spectrometer (FTIR), Fluorescence Spectrometer (FS) and Mass Spectroscopy (MS) in order to validate on the experimental approach used in this thesis.

Lastly the possible architecture of the Bio-chip was designed that include the concept of MOEMS and which post great challenges. The application of this work could be led to systems that enable the detection of Acute Myocardial Infarction (AMI, biomedical term for heart attacks) with the help of the Bio-chip.

Dedicated to my parents

The source of my hope

Acknowledgements

The author is deeply privileged to work under the thesis supervision of Dr. Ion Stiharu. It was Dr. Stiharu's invaluable thoughts at the macro level which helped the author to mould his thoughts on a technical plane. The author is deeply indebted to him for providing an opportunity to work under him. It was Dr. Stiharu's vision and ideas that provided the foundation for this thesis.

The author would also like to express his sincere gratitude to Dr. Muthukumaran Packirisamy. The author would like to thank Dr. Packirisamy for his valuable guidance during various stage of this thesis.

It is the author's pleasure to acknowledge the help offered by Mr. Ganesharam Balagopal (Ontario University of Environment), Ms. Julie Bovin and Ms. Neema Chirwa (Biochemistry Department, Concordia University) during the experimental stages of this work.

The author wishes to express his thanks to Mr. Eric Duchesne, of Ecole Polytechnic for his valuable assistance during the taking of Scanning Electron Microscope (SEM) pictures.

It is the author's pleasure to work with colleagues Mr. Avinash Kuppar, Mr. Gino Rinaldi, Mr. Arvind Chandrasekaran, Mr. Jianliang You, Mr. Raghavendra and Mr. Kiran Chatrathy, who provided valuable help during the various stages of this work.

The author would like to express his gratitude to his parents and sister without whose help the dream would not have been possible and Mr. Himanshu Sikka for always being there.

TABLE OF CONTENTS

LIST OF FIGURES

LIST OF TABLES

NOMENCLATURE

α	Angle between normal of the deflection beam and reflected beam in radiance
A	Area of cross-section
Al	Absorbance value
A_k	Constant coefficients in the genaration of deflection function
%A	Percentage Absorbance
AFM	Atomic Force Microscopy
AMI	Acute Myocardial Infarction
Au	Arbitrary units
b	Length of the droplet
Bio-MEMS	Bio-Micro Electro Mechanical Systems
Bi-CMOS	Bi-Complementary Metal Oxide Semiconductor
B_k and C_k	Constant coeffficents in generation of orthogonal polynomial using Gram-Schmidt process
C	Concentration of Melittin
CABG	Coronary Artery Bypass Graft
Ca^{2+}	Calcium ions
CaM	Calmodulin
CaM*	Activated Calmodulin
CK	Creatine Kinase
CMOS	Complimentary Metal Oxide Semi-Conductor
cTnI	Troponin I

cTnT	Troponin T
δ	Tip deflection of the cantilever in microns
$\delta 1$	Deflection of the cantilever from the end of the enzyme droplet to the tip of the beam
δ_{total}	Total deflection including the deflection of the bended portion with the droplet and remaining portion of the beam
D	Laser spot movement in PSD in microns
Da	Dalton
DRIE	Deep Reactive Ion Etching
ε	Strain caused in the bended portion of the beam due to the droplet
E	Young's Modulus
ECG	Electro Cardio Gram
ED	Emergency Department
E_{mi}^{22}	Stiffness matrix in an eigen value equation, where m denotes the number of rows in a matrix and j denotes the number of columns
E_{mi}^{00}	Mass matrix in an eigen value equation with same sufixes as above
F	Force due to the droplet
Fe^{4+}	Ferrous ions
FS	Fluorescence Spectroscopy
FT	Fourier Transform
FTIR	Fourier Transform Infrared Spectrometer
g	Path length
Gpa	Gega Pascals

h	Distance from the neutral axis
HP	Hewlett Packard
HRP	Horse Raddish Peroxide
H_2O_2	Hydrogen Peroxide
i	Angle of Incidence
I	Moment of Inertia
ICU	Intensive Care Testing
IR	Infrared
K_t	Spring stiffness due to translational spring energy
K_r	Spring stiffness due to rotational spring energy
KCl	Pottasium Chloride
KH_2PO_4	Potassium Phosphate
λ	Eigen value
L	Distance from deflected cantilever tp PSD in meters
Li-ion	Lithium Ion
MEMS	Micro Electro Mechanical Systems
MST	Microsystems Technology
Myo	Myoglobin
MI	Myocardial Ischemia
MS	Mass Spectroscopy
ME	Honey Bee Melittin
M	Bneding Moment in the fixed portion of the beam
Mc	Concentrated mass (lumped mass)

M1	Mass of Troponin C
Mpa	Mega Pascals
m/e	Mass-to-charge-ratio
υ	Extinction coefficient or molar absorptivity
OD	Optical Density
OLM	Optical Lever Method
ρ	Density of the material (mass)
$\Phi(x)$	Shape function of a system
POCT	Point-of-Care Testing
PTCA	Percutaneous Transluminal Coronary Angioplasty
PSD	Positive Sensitive Detector
PVDF	Poly Vinyl Dichloro Fluoride
PMT	Photomultiplier Tube
R	Radius of curvature
ROS	Reactive Oxygen Species
σ	Uni-axial stress produced due to the Bending Moment
S	Superficial tension due to the enzyme droplet
SFM	Scanning Force Microscope
SEM	Scanning Electron Microscope
%T	Percentage Transmittance
τ	Change in length in the upper and lower portion of the beam due to strain
T_{max}	Maximum kinetic energy
Tb	Total kinetic energy

Tn	Troponin
TnC	Rabbit Skeletal Muscle Troponin C
Tris-HCL	Tris-Hydrochloric acid
U_{max}	Maximum potential energy
U_b	Strain energy
U_s	Potential enerugy due to springs
UDL	Uniformly Distributed Load
V	Shear in the fixed portion of the beam
ω	Natural frequency of a system
ω_n	Natural frequency of a system with load
W(x)	Deflection function of a system
X	Distance connecting the tip of two imaginary triangles formed due to the bended portion on the beam
XeF_2	Xenon Di-fluoride

CHAPTER 1

INTRODUCTION, RATIONALE, LITERATURE REVIEW, OBJECTIVE, LAYOUT AND SUMMARY

1.1 INTRODUCTION TO MICROSYSTEMS

1.1.1 Micro Electro Mechanical Systems (MEMS)

Miniaturization is often associated with high sensitive systems. The reduced size of the sensor reduces the interaction with the detected phenomenon. The early developments of miniaturization leaded to what has been known for two decades as Micro-Electro Mechanical Systems (MEMS). Apart from a design objective, miniaturization has endorsed the development of specific fabrication processes that enable the integration on the same chip of the micromechanical system the different electronic circuit and the soft ware [1]. This field of MEMS has been growing at a remarkable pace in recent years. They provide point-of-care testing (POCT), on-chip signal processing and reductions in per-unit cost. Along with these advantages the problems associated with them are packaging and process compatibility [2]. With further ever increasing complexity, building Microsystems Technology (MST) is an evolutionary process.

Earlier sensors were merely pressure switches, but later evolved into micromechanical sensors that directly measured pressure. The current generation of sensors combines electronic circuitry with micromechanical sensor to provide a digital output used for self-diagnosis [3]. The future promises to bring innovative and novel MEMS solutions to a

wide variety of applications, ranging from biochemical analysis to wireless optical systems. As the technology matures, MEMS will be more available for integration in consumer's products including bio-kits for diagnostic and testing inside every individual's home at an affordable price. Ongoing research of implementing biosensors to identify DNA signatures and sensing heart attack has gained particular importance in recent times. Though some laboratories have started work in this direction, research has to be intensified for the amplification of sensor response in organic media.

Another challenge for the future for organic phase biosensors is the immobilization of the biocomponent together with the substrate. Although Cornor et al., [4] has already reported immobilization of silicone oil to the substrate, the application of organic media to the substrate still remains a query to be solved. Most of the work has reported applying enzymes on both sides of the microstructures, while only few have been reported on the application of enzymes to one side.

1.1.2 Bio-MEMS (Micro Electro Mechanical Systems)

The vast area of MEMS has been divided after multiple criteria while the devices are classified accordingly. Recent progress in MEMS is being applied to biomedical applications and has become a new field of research known as BioMEMS (Micro Electro Mechanical Systems). BioMEMS is an enabling technology for higher functionality and cost reduction in smaller devices for improved medical diagnostics and therapies. The field of BioMEMS is very promising as it has the capacity to fulfill the demands made by

the pharmaceutical industries in the case of cancer and heart attacks. Clinical diagnosis especially that of heart infarction require rapid and reliable test systems. A great deal of scientific research has been devoted to fabrication of microdevices that are suitable for the identification of DNA molecules and enzymes released due to heart attacks. These microdevices will ideally comprise a sensing element, a sampling surface and a fluidic connection between these two components [5]. This is one of the significant areas where these microdevices are expected to find widespread use. Petrou et al [5]., suggested continuous monitoring of some specific analytes can contribute to more successful treatment of severe diseases like Acute Myocardial Infarction (AMI, the medical name for heart attacks).

1.1.3 Need for New Diagnostic Techniques

New biochemical diagnostic methods and strategies for detection of Acute Myocardial Infarction (AMI) are being identified to treat patients with greater accuracy and rapidity. The early assessments of heart attacks and its subsequent treatment is the key to increasing patient survival rate after chest pain and hence the interest in defining early sensitive biochemical markers [6]. Such detection could be performed by any measurable disturbances in the normal behavior of the microcantilever beam which are used in the detection of enzymes-anti-enzymes reaction pattern. A high degree of parallelization is also desirable because of the present detection demands and these demands can be fulfilled by biomarkers. It is becoming increasingly evident that high-throughput identification and quantification of a large number of biological molecules is important

for continuous monitoring of complex diseases such as AMI when compared to using of Electrocardiogram (ECG)

.

1.2 RATIONALE

1.2.1 Significance of Present Research

Commercial instruments for biochemical and biomedical analysis are already available on the market manufactured by well known companies. They perform a broad range of analytical functions and are built to satisfy the requirements of the bio-test facility. Accurate methods to detect the early markers in AMI are available and operate with extremely high accuracy. However, the available kits require expensive calorimetric reading equipment that is usually afforded by hospitals or health care units. The objective of this research is to investigate the possibility to realize such detection kits that are self-supported and could be handled and read by the layman. Also the present equipment used in the hospitals is large adding to the cost. MEMS technology promises to miniaturize and integrate these instruments [7]. Proof for this is the ongoing significant research activity in the MEMS community and the relevant number of start-up companies, around the globe, trying to implement the portable diagnostic biosensors [7]. These biosensors include diagnosing glucose level in the body [8], DNA sequencing [9] and sensing AMI. The present study deals with experimental and analytical data that could be applied in the sensing of AMI.

Each year, many people visit clinics and emergency departments reporting chest pain and discomfort [10]. These patients must be evaluated precisely in order to find out the real reason for the pain. Figure 1.1 shows the total number of adult men and women of

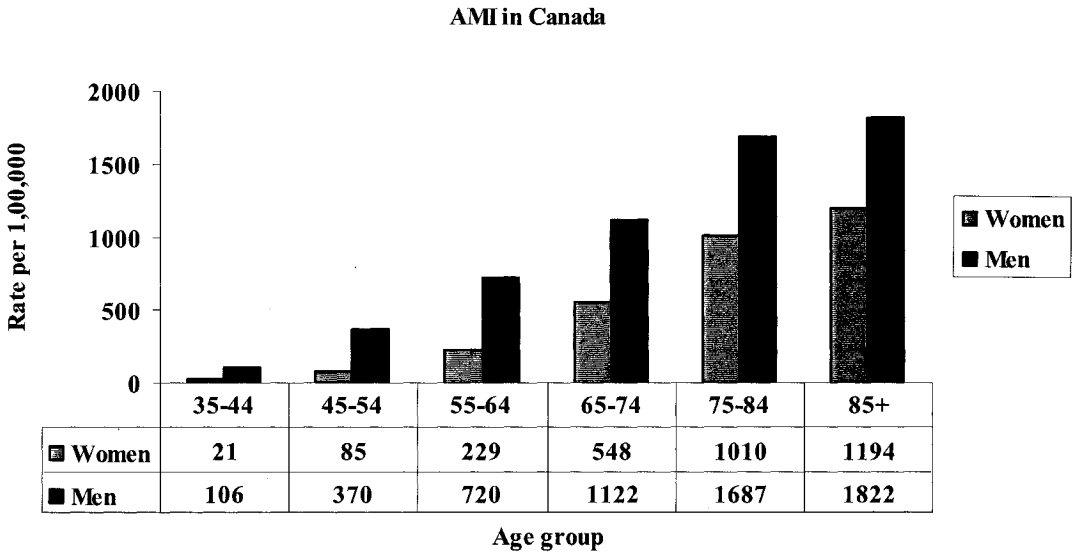

Figure 1.1: AMI hospitalization rate, by age group and sex in Canada [9]

Table 1.1: Per patient in hospital cost of treatment of Acute Myocardial Infarction at 2 Canadian and U.S hospitals [11]

Costs	Canada		United States	
	$	%	$	%
Total direct costs	4796	78	9801	64
Nursing	2547	42	3743	24
Angiography, *PTCA, *CABG	1520	24	3541	23
Pharmacy, laboratory, radiology	663	11	1747	11
Other direct costs	67	1	770	5
Total indirect costs	1385	22	5830	36
Total in-hospital costs	6181	100	15631	100

*PTCA – Percutaneous Transluminal Coronary Angioplasty

*CABG – Coronary Artery Bypass Graft

respective ages (in rate per 1, 00,000) in Canada visiting hospitals due to AMI. Sometimes the pain may be not due to AMI. It could also be due to sleeping over on one side of the body or any other trivial reason. However, this makes people worried and they land up in the emergency rooms. The rising costs of hospital care and the reasonable aim to minimize unnecessary hospital admissions has further heightened the need for bedside biosensor [11] as shown in Figure 1.1 and demonstrated in Table 1.1. In such circumstances it would be ideal to have a portable biosensor that could confirm or rule out the occurrence of AMI. Since most quantitative tests are centralized in hospital laboratories for which highly qualified technical staff are required which add up to the cost, intensive research has been undertaken to decentralize such tests so that they can be performed at the patient's bedside. Therefore, development of rapid and sensitive biosensors, that are also portable, with immediate on the spot interpretation of results is underway [12].

In order to get these biosensors working, it is essential that an ideal blend of biochemical markers need to be used for proper diagnosis. Biochemical markers are of increasing importance in diagnostic strategies for ruling in or out AMI, particularly when electrocardiographic (ECG) findings do not provide proper diagnosis [13]. In addition, the diagnostic sensitivity of ECG is about 50% for detecting AMI [14]. Also ECG findings are rather heterogeneous or produce small changes in the case of micro-infarcts and much more complicated devices have to be brought in.

1.2.2 Significance of Biomarkers

It is time for transition in the area of biomarkers to perform better diagnosis and rely on the science of discipline to be on track. The utility of these biomarkers have evolved from the diagnosis of cardiac injury through the physical assessment of patients with chest pain. While electrocardiogram (ECG) may still be the gold standard for AMI, it is inadequate and late for detecting myocardial damage. The finding of a typical rising and falling pattern of a highly specific biochemical in blood will be the best indicator of AMI. The ideal biochemical marker is one that has both clinical sensitivity and specificity, appears immediately after AMI to facilitate early diagnosis, remains abnormal for several days after AMI, and can be assayed easily with a rapid turn around time [15]. However a marker that is having all the above criteria is still yet to be found. Earlier the considerable variation in the enzymatic levels, encountered after AMI led to the progression from measurements of enzymes like Creatine Kinase (CK) to proteins like Troponins (Tn) (takes more release time after AMI) which are more specific and sensitive compared to the other markers. Real-time sensing of these biological molecules on MEMS devices increase the applicability of these devices [16]. For example, micromachined cantilevers undergo changes in their mechanical behavior when enzymatic reactions of these biomarkers take place on their surface. The reactions can be easily detected optically. Microcantilevers are considered to be highly sensitive MEMS devices as they are the key to advancing sensor performance and utility [17].

Table 1.2: Comparison of cardiac markers for AMI [18]

Characteristic		Creatine Kinase (CK)	Myoglobin (MYO)	Troponin (Tn)
Specificity	**Absence in healthy patients**	No	No	Yes
Sensitivity	**Early rise**	Yes	Yes	No
	Elevated periods	No	No	Yes
Analytical Factors	**Ease of measurement**	Yes	Yes	Yes
	Dynamic range of results	Yes	Yes	Yes
	Excellent precession	No	No	Yes

Knowledge of certain biological and cellular aspects of marker proteins could enable some predictions to be made regarding alterations that can occur after myocardial injury as well as how this could effect their application to clinical practice [19]. Table 1.2 shows the comparison of certain cardiac markers used for diagnostic use. Also the availability of more powerful analytical tools for these highly specific markers of myocardial injury offers a unique opportunity to expand the field of their application and to explore new diseases processes [20]. Studies show that [21] point-of-care testing (POCT) can be done by qualitative bedside tests. But due to the delayed availability of the test results and higher fixed costs pose some disadvantages and also they provide limitations for cardiac marker determination. These tests have to be read within an adequate time interval and

under adequate illumination [22]. In the present study an effort is been made to detect the specific signature of a few biomarkers and their enzymatic reactions optically on MEMS structures such as microcantilevers. These cantilevers tend to act as mechanical transducers for detection of the reaction among these biological molecules that could be incorporated in a biosensor. The high sensitivity and small size of these MEMS structures yields to reduced amount of reactants required for detection. The same concept can be extended to the development of a portable biosensor that could be available to the patient bedside.

1.3 LITERATURE REVIEW

1.3.1 Importance of Biosensors

One of the major goals of biosensor technology is to identify analytes in a chemical reaction. Identification of quantitative immunoassays for rapid on the spot performance in the field is important for clinical diagnostics, biochemical and biotechnological research. A device operating in such remote sites as in the case of emergency department should not only provide fast, sensitive measurements but also simple to operate and inexpensive. In this respect, an electrochemical biosensor presents an attractive option. Consequently, devices with both high sensitivity and relative simplicity are at an initial stage of development.

From a clinical point of view, electrochemical biosensors are well suited for enzymatic detection. Rishpon et al., [23] insisted on the importance of these biosensors as they had the ability of an antibody to inhibit the activity of the labeled enzyme. In support of these biosensors, Athey [24] and Mcneil [25] said that these biosensors are particularly suitable for quantities of such small molecules as drugs. The advantages included in this type of sensor are that there would be no need for pretreatment of the complex samples as in the case of other biosensors. Panos G. Datskos et al., [26] subjected to the use of chemical sensors in the field of medicine. According to them chemical sensors consist of a physical transducer (i.e., a transducer of physical quantities into convenient output signals) and a chemically selective layer so that measurable output signals can be produced in response to chemical stimuli. More recently there is an increasing demand to perform real-time in situ chemical detection in the case of medicine. P.S. Petrou's., [27] work targeted towards continuous monitoring of specific analyte levels so that they can contribute to more successful treatment of both chronic diseases and acute incidents. This idea was extended from Henry et al, [28] in which a sensor system was developed for monitoring of glucose levels in the body.

1.3.1.1 Methodology for Enzymatic Detection using Biosensors

A few approaches have been followed earlier for the on-line monitoring of enzymatic levels in biological fluids. One of the approaches was that the sensor is designed for direct introduction in the human body as employed by George Guilbault et al., [29] who

developed an amperometric immunosensor for the rapid detection of Myoglobin (Myo) in whole blood. The other approach proposed [30] was to connect the biosensor to an

Figure 1.2: Schematic of a micro-cantilever sensor which can be adapted to detect physical, chemical or biological activity [31]

appropriately designed sampling probe. The sampling probe is usually consisted of a membrane not permeable by high molecular weight substances, such as proteins. It permits, however, the fast transport of low molecular weight substances from the surrounding medium (blood) to the fluid running in the membrane (fluid). Also microdialysis membranes connected with biosensors have been used for continuous monitoring of one or more analytes both in-vitro and in-vivo [30]. Nicolini et al., suggest that these enzyme-based biosensors are analytical devices which combine a biologically sensitive element with a physical or chemical transducer to selectively or quantatively detect the presence of specific compounds and can be used for continuous monitoring [32]. Y. Arntz et al., [33] demonstrated continuous label-free detection of multiple proteins using an array of microfabricated cantilevers.

1.3.1.2 Microcantilever Beams for Enzymatic Detection

The use of microfabricated beam structures as a force sensing stimuli in atomic force microscopy (AFM) is a well established application [33]. P. Oden [34] observed that these structures bend upon absorption of optical energy due to temperature changes which can be easily detected. Sensing with macroscopic cantilevered structures was by no means a new area of study. Taylor et al., [35] was the first to utilize cantilevered beam sensors for the detection/sensing and distinguishing of gases through differential-sorption process. Thundat et al., [36] used microcantilevers used in the AFM to sense protein-protein interaction. The molecular adsorption on the surface of the cantilever causes a change in the surface stress. Butt et al., [37] detected the bending of the cantilever due to the differential surface stress caused by the molecular adsorption. The strength of the microcantilever concept, however, is in its ability to work in solutions. Gunanghua Wu et al., [38] was the first to detect DNA sequences simultaneously using an array of microcantilevers. Y. Arntz et al., [32] followed the same concept of microcantilever array, where cantilever beams were functionalized with covalently anchored proteins. Binnig et al., [39] used scanning force microscopy (SFM) to measure forces on beams for biosensing applications. The SFM measures small forces acting between a sample surface and a sharp tip at the apex of the thin beam clamped at one side, the cantilever. The force on the tip bends the cantilever, which acts as a force transducer. Miniaturization and mass-production are the main reasons for the success of SFM in research labs and industrial applications. These lead to cantilevers with low spring constants for a high sensitivity to the applied forces or high resonance frequencies for faster response times

and insensitivity to external disturbances [40]. Scanning Electron Microscope (SEM) images of a couple of microcantilevers structures of different shapes and dimensions used are shown in figure 1.3.

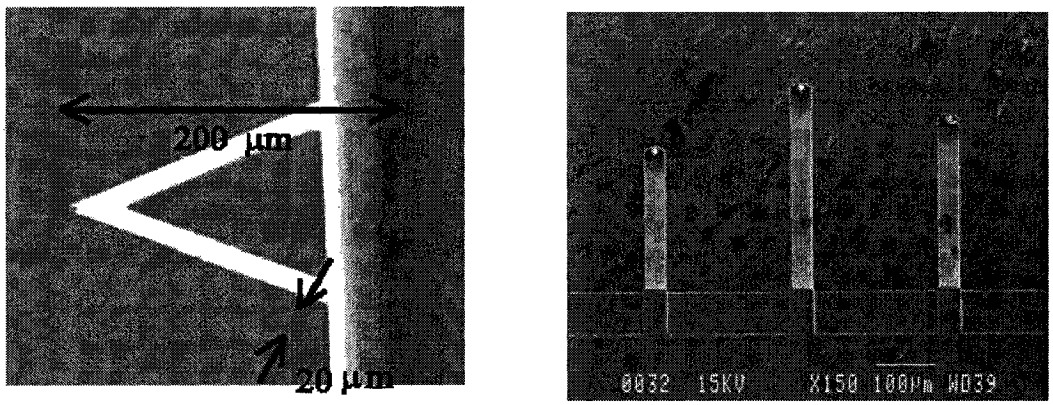

Figure 1.3: SEM images of different microcantilever beams used in biosensors to detect chemicals

For medical applications these microcantilever based sensors would allow life-saving treatments of patients suffering from Acute Myocardial Infarction (AMI).

1.3.2 Acute Myocardial Infarction (AMI)

Detection of AMI in particular requires critical diagnostic and therapeutic monitoring situations with repeated testing and short turnaround times. A crucial step of AMI detection systems is to identify enzymatic reactions within a given sample. This is required in order to reduce false positives, events which can turn out to be extremely costly errors. Christopher T. Bazjer [41] defined AMI as the death or necrosis of myocardial cells. AMI occurs when Myocardial Ischemia (MI) exceeds a critical threshold and over whelms myocardial cellular repair mechanisms that are designed to maintain normal operating function. Ischemia at this critical threshold level for an

extended time period results in irreversible myocardial cell damage or death [42, 43]. The early assessment of the extent of myocardial damage can be done with several confirmatory tests which may not be accurate enough, although they are still been in use [44]. But the principle candidates that are currently vying to capture today's market are tests due to cardiac markers like creatine kinase (CK), myoglobin (MYO) and troponin (Tn). Although creatine kinase is considered traditional biomarker, but troponins lead the head of diagnostic ranks as they represent the latest advance in cardiac patients [45]. Troponin-based diagnostics have revolutionized coronary care. The finding of typical rising and falling pattern of a highly specific biochemical marker in blood will likely be the best indicator for detection of myocardial infarction due to their superior sensitivity and specificity, leading to their rapid acceptance for clinical practice compared to other tests. A typical rise after the onset of infarction and amounts in blood for a few cardiac markers is been shown in Table 1.3.

Table 1.3: Typical rise of cardiac markers and amounts in the blood after infarction [46]

Cardiac Enzyme	**Time for typical rise after the onset of infarction in hours**	**Normal range of distribution in the blood after infarction in ng/ml**
Myoglobin	1 - 2	0 - 85
Creatine Kinase	2 – 4	0 – 7
Troponin	4 – 8	0 – 0.1

The above table clearly shows the initial elevation levels of the enzymes after chest pain with their quantitative measurements. Although the first two markers may die down after the initial onset, troponins get further elevated for larger intervals of time. The range of normal distribution is more specific for troponin due to their wide range of presence in the cardiac, skeletal muscle and kidney bladder [47].

1.3.2.1 Biosensors for Acute Myocardial Infarction (AMI)

With the advancements of microfabrication technology and the integration of micromechanical and electrical components known as microelectromechanical systems (MEMS), it has become a commonplace to construct cantilevered beams and other structures with the dimensions on the micrometer scale and use them with biomarkers [48]. According to Gorgan et al., [49] enzyme-based biosensors can be incorporated with the microcantilever-based sensors, since they are proposed as mechanical transducers for different sensing applications. They have been successfully used to monitor different enzymatic interactions in liquid environment, like antibody-antigen interaction [50]. In the category of chemical-based sensors, enzyme-based biosensors have received more attention than any other type of sensors [51]. The future of MEMS will be greatly influenced by the development of biosensors as these structures provide ideal base for a sensor platform.

Present day enzymatic detection technologies are based primarily on adaptation of laboratory. There have been only few scientific papers describing real-time optical

sensing using proteins. The basic mechanism of detection is based on the fact that whenever an enzymatic interaction takes place on one side of the cantilever surface it undergoes bending due to the local stress developed at the reaction site on the cantilever. The detection is possible only if the response to the antibody-antigen (analyte) is high enough compared to the solid-liquid interface interaction which is the non-specific adsorption.

1.3.3 Optical Detection Techniques for Monitoring of Enzymes

The antigen-antibody reaction on the surface of the cantilever also changes the surface stress of that side of the cantilever depending on the selectivity of the reaction [51]. Analyte A and enzyme A would yield a specific time depending on the signature of the deflection. Any other enzyme that is different from enzyme A will yield a signature that may be very different from the signature given by enzyme A. The difference in the two signatures will give the sensitivity of the cantilever. It is this cantilever bending which is ultimately detected, indicating the presence of enzymes as shown in Figure 1.4.

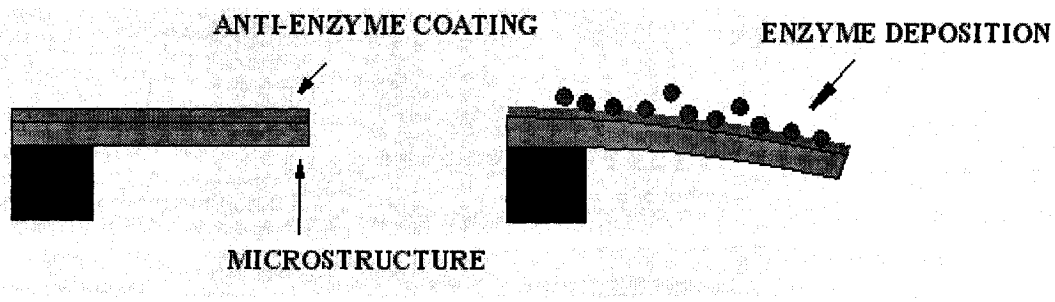

Figure 1.4: Schematic diagram depicting the bending response of a microcantilever to enzymatic reaction

This bending can be detected optically, by focusing the light from a low power laser diode onto the free end of the cantilever and recording the deflection by monitoring the displacements of the reflected laser light on a position sensitive detector (PSD). The optimum deflection response is created when the enzymes react specifically with only one side of the cantilever, which acts as a sensing surface and also prompts the change in surface stress. This specific response is proportional to the mass added onto the cantilever surface [52]. So the concentration and molecular weight should be high, which is not common in practice. The major problems encountered in the optical detection method are reproducibility, long term drifts of cantilever bending, deposition of the antibody-antigen onto the cantilever surface, local noise that further causes vibrations, a clear understanding of the mechanism of binding of the enzymes to the cantilever surface and their enzymatic reactions. Moreover, when these cantilevers are exposed to radiation, the temperature change of the cantilever which may cause further bending due to absorption of energy [52]. In addition to this, a clear understanding is required to determine the lifetime, stability and activity of these enzymes. To understand the stability of these enzymes dynamic tests were performed using the Fourier Transform Infrared Spectrophotometer (FT-IR).

FT-IR is an analytical tool to study protein confirmation in a diverse range of environments like in the case of upon binding to membranes. Pelton et al, [53] demonstrated a method to determine enzymatic reactions using the FT-IR at a relatively low cost, both in solution as well in solid state. Protein solutions of atleast 25 mg/ml were needed to be prepared to get a meaningful spectrum. However, Hiroki Samo et al,

preferred Fluorescence Spectroscopy (FS) to determine enzymatic reactions at much lower concentrations [54]. This finding is very useful for selecting a particular enzyme for reaction with the best possible potential [55]. These optical methods possess several inherent advantages as it based on long wavelength range of radiation, minimizing scattering problems and also it gives a wide range of sampling methods using transmission, reflection or emission techniques [56]. However, the high concentration of solute makes the method less feasible for biomarkers in blood.

1.4 OBJECTIVE OF THE THESIS

1.4.1 Point-of-Care Testing (POCT)

Each year, more than 6 million Americans visit clinics and emergency departments (ED) reporting chest discomfort [57]. These patients must be evaluated early enough to optimize outcomes, conserve health care resources, and minimize the likelihood of litigation for improper diagnosis. It has been reported that each year upto 70% of patients admitted to coronary care units for suspected acute myocardial infraction (AMI) are later discharged with a different diagnosis costing billion of dollars [58] as shown in Figure 1.5.

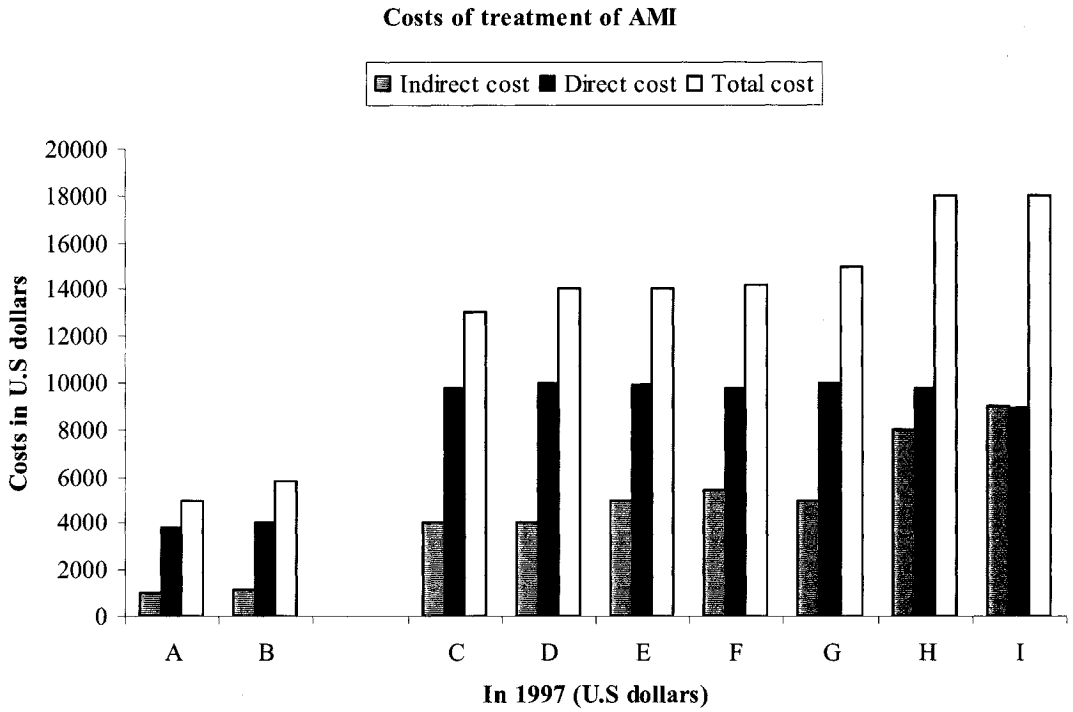

Figure 1.5: Cost of treatment per person of AMI in Canadian hospitals in 2000 (in US dollars) including costs related to diagnostic procedures and emergency rooms [59]. A, B, C, etc denote the hospitals.

This makes point-of-care testing (POCT) even more significant to provide with some means of diagnosis near patient bedside. Point-of care testing (POCT) [59] or near patient testing allows for diagnostic assays to be performed at the site of patient care delivery such as the Emergency Department (ED), chest pain evaluation center, or intensive care unit (ICU). Compared with centralized laboratory testing, POCT provides for rapid clinical decision making by reducing time spent ordering tests, as well as retrieving data. Increasingly, POCT for cardiac markers are being researched, developed, and put into clinical use.

The present thesis aims to do experimental analysis with a couple of proteins that are cardiac specific with cantilever beams in order to understand the behavior of the beams

under the influence of the enzymatic reaction between the proteins. Various optical detection techniques have been put forth to identify the enzymatic reactions. To support the experimental analysis, theoretical work has been demonstrated by standard procedures to support the concepts presented in the thesis. This idea can be put forth to develop cardio specific biosensors.

Full acceptance of this relatively new technology will not be recognized until a comfort level is reached where utilization of these devices is foolproof and they have full confidence in the results. The results included in this thesis provide an opportunity for a new biosensor chip to evolve into the standard of care for evaluating patients presenting with chest discomfort. The decision as to which device to use and what markers to employ must be made by each individual. The remarkable merit of the method consists of the fact that quantitative evaluation on the cardiac enzymes could be provided to the user with minimum knowledge of medicine.

1.5 LAYOUT OF THE THESIS

The major goal for this present work is to prove the detection principle and quantify enzymes optically using microstructures. To achieve this much of the emphasis has been laid on experimental work. Experimental methods and set-ups including Doppler Velocimeter, Fourier Transfer Infrared Spectrophotometer (FTIR), Spectrofluorometer, Mass Spectrometer (MS) and Optical Detection methods using Poly Vinyl Dicholoro Fluoride (PVDF) cantilever beams, Position Sensitive Detector (PSD) and low power

laser source were used. The above experimental methods were tried out with specific enzymes and results obtained were discussed in the different chapters of the thesis.

Chapter one gives the objective of the thesis along with its rationale. The rationale provides the need for such a thesis. The literature review is provided to give a bird's eye view of what is happening in the present area of research followed by the summary.

Experimental validation is done by deriving a relation between superficial tension on the beam (due to the enzymes) and total deflection (which includes the segment on which load is added and the remaining portion from the enzyme deposition to the tip of the beam). The tip deflection is evaluated from the beam geometry from which the superficial tension, which is responsible to move the beam, is calculated in chapter 2.

After calculating the tip deflection it was very evident to find the relation between the ratio of natural frequency and ratio of position of load on the beam is evaluated for different load conditions. An ANSYS model was created based on certain assumptions to evaluate the shift in natural frequency. The stress derived from the beam flexure formula is plotted against tip deflection. Results were obtained for both the set of enzymes and compared. Dynamic analysis was performed on the cantilever beam with and without the extra mass on it. Although vibration experiments were not carried out, vibration problem of the cantilever beam is analyzed using the Rayleigh-Ritz method. The influence due to the extra mass was also included in the Rayleigh-Ritz analysis.

Optical deflection method comprising cantilever beams, PSD, laser source was performed with proteins like Rabbit skeletal muscle Troponin C (TnC) and Honey Bee Melettin (ME) to understand the behavior of the cantilever beams under their reaction. The reactions were also compared with that of TnC and water. The results were compared to another set of enzymes namely, Horse Raddish Peroxide (HRP) and Hydrogen Peroxide (H_2O_2) on PolyvinylDichlorofluoride (PVDF) beams. In order to catalyze the reactions a voltage of 90 volts was applied to the beams and results analyzed. PVDF beams were chosen because of their higher sensitivity to chemical reactions, highly reflective surface and easy availability. The above method and the results comprised of chapter 3 and summarized.

Other optical detection techniques were also carried out to confirm the enzymatic reaction in chapter 3 using cantilever beams. Stability, activity of the enzymes and dynamic analysis were carried out using the FT-IR. The corresponding percentage transmittance and absorbance spectrums were obtained to see the variation for each of the two sets of enzymes in chapter 4. The Fluorescence energy transfer study of the enzymes was carried out to observe the enzymatic reaction at a fixed wavelength and at different ratios of the enzymes. The changes in their molecular weights were observed using the mass spectrometer.

Conclusions and future work are presented in chapter 5.

1.6 SUMMARY

One of the major goals of biosensor technology is to detect and quantify analytes in very complex matrices. To achieve this, much of the emphasis in sensor fabrication has been laid on antibody-antigen interaction. The consequence of this focus of enzyme biosensor studies is the development of many immobilization methods such as coating enzymes on the substrate. The suitability of organic media for enzymatic reactions has led to tremendous advancement in biosynthesis and, more recently, biosensing. Biosensors that operate in organic media combine the high selectivity and specificity of enzymes with the ability to control their reactivity by altering some physiochemical properties of the reaction media, such as the solvent polarity or the degree of hydration. The implication of having an enzyme biosensor as analytical tool is that any analyte can be detected provided there is a suitable biocomponent and a solvent in which the analyte is soluble.

Identification of the enzymatic reactions using different optical methods has been explained in the thesis. An appropriate analysis of current and future biomarkers requires some knowledge of the limitations and advantages of these markers, while understanding the limitations of our current standard diagnostic practices. Use of biomarkers has revolutionized the practice of patient care, but is a revolution in evolution. It is an exciting time as the potential of currently available and new biomarkers to improve

patient care and augment our understanding of underlying medical processes continues to increase. The cardiac troponins are new and promising biochemical markers in patient with AMI. They provide useful clinical information unavailable through other diagnostic techniques. Heart failure is a completely new field of application of these proteins and open hypotheses that deserve further investigation.

In the present work constant rectangular cross-section cantilever beams were considered use in understanding the enzymatic reactions much better as they are considered extremely sensitive to molecular adsorption on its surface. Experiments were conducted with enzyme/anti-enzyme and enzyme/water to show that the bending of the cantilever is not due to the load of the liquids but due to the reaction. The behavior of the cantilever beams were also analyzed under the action of voltage when these enzymes were deposited on the cantilever surface. The findings of this research confirm the enzymatic reactions between more cardiac specific proteins like Troponin C in the detection of AMI.

To compliment the above work, enzymatic reactions were also detected using the FTIR, spectrofluorometer and mass spectroscopy. Further, theoretical analysis was done on the cantilever beams using the classic Rayleigh-Ritz method. The results discussed in the present work suites well in the application of development of a biosensor that could detect AMI on the spot.

CHAPTER 2

DETERMINATION OF THE BEHAVIOR OF A CANTILEVER BEAM UNDER STEADY LOAD AND BIOLOGICAL REACTION

2.1 INTRODUCTION

Modeling and analyzing the static and dynamic performances of Micro Electro Mechanical Systems (MEMS) structures are very important steps in building successful Microsystems. They are subjected to mechanical loads during fabrication [60], buckling [61] and operation [62]. Assessment of the stability of these structures to withstand the mechanical loading requires accurate modeling. Experimental measurements of these structures need to be in accordance with the analytical and numerical modeling for characterizing the local developed stresses.

In miniature structures one could use micro-cantilever beams to sense the existence of bio-materials. Once the bio-material is deposited the cantilever will change the previous position due to:

- The added mass
- The surface stress due to the physical superficial tension
- The surface stress at the contact area of enzyme-cantilever beam due to loading of the bio-material on the surface.

The three influences might change with time but for short periods of time they are in equilibrium. The influence of each of the three is independently and globally is analyzed while attempting to match the experimental results. It is important to mention that the objective of the model is to estimate to some extent the values of the stress-induced bio-reaction.

Apart from the bending, the cantilever beam will exhibit different dynamic characteristics such as the shift of the natural frequency or the subsequent harmonics, the mode shapes and the Q factor may modify. Below, the attempt to quantify the independent influences of the extra-mass and stress are made. At first, the effect of the three causes of deformation on the static deflection of the beam is made. However, the causes are grouped in two; given their action the mass is analyzed separately from the effect of stress induced by the superficial tension and the biological reaction. Further, the influence of the two phenomena on the dynamic performances of the sensing element is evaluated.

The analytical models are developed to understand the extent of the stress produced by the bio-reaction. Since it is very likely that the extra mass consisting of reactive bio-molecules in solution would influence the dynamic characteristics of the beam, the expected change is analyzed using an adequate energy method, in the present thesis the Rayleigh-Ritz is used. Thus, the shift of the natural frequency evolution is modeled and evaluated.

The energy methods are very adequate to carry out this analysis as the strain produced by the bio-molecules might be to some extent evaluated from the static analysis on which the model is calibrated through experimental results. This method not only provides the means of obtaining a more accurate value for the fundamental frequency, but also gives approximations to the higher frequencies [63]. This method can be applied to both a continuous as well as a discrete system. The continuous systems lead to eigen value problems that do not have exact solutions due to non-uniform mass or stiffness distribution [64]. MEMS structures are analyzed in the case of continuous systems due to the influence of various parameters caused by the deposition of enzymes.

While developing a model, one should make assumptions that would enable reasonable results based on acceptable considerations. In the present model the load applied on the cantilever during the experimental analysis was also taken into account and assumed uniformly distributed only on a section and the deflection at the free end of the cantilever due to the mass was calculated to validate the experimental results. The influence of the cantilever geometry, position of the droplet and the mass of the droplet was analyzed. The superficial tension that is localized only on a segment of the beam due to the enzymatic reaction in the droplet is studied. The dynamic behavior of the beam subjected to the bio-reaction was observed. Since the beam produces a quasi-static signature it may produce a dynamic signature as well. The deflection behavior was compared for three cases which include the cantilever alone, the cantilever with the extra mass and the cantilever with the extra mass and bending. A simple relation was also provided to evaluate the tip deflection of the cantilever beam from the angle of incidence and the

distance moved in the PSD. The dynamic analysis of the cantilever beam was done using the Rayleigh-Ritz process.

The vibration problem of a cantilever beam has been investigated by using a set of characteristic orthogonal polynomials in the classic Rayleigh-Ritz method. This method shows that with a reasonable assumption for the shape of the vibration amplitude, it is possible to take into account previously ignored masses and arrive at a better estimate for the fundamental frequency. The extra mass acting on the surface of the cantilever was also incorporated in the equations along with the kinetic energy. Although the formulation is well known, it will be revisited below as a base for future formulations.

2.2 CANTILEVER BEAM ANALYSIS

2.2.1 Deflection at the Free end of the Cantilever Due to the Mass (Calibration against the Experimental Tests)

MEMS structures are often subjected to mechanical loading under various circumstances [65]. To check for the reliability of these structures analytical or numerical modeling has to accompany the experimental results for deformation due to imprecise knowledge of material properties and to assist in microsystem design [66]. The load which is in the present case bio-enzymes actually act as a droplet of certain height and width is applied only on a certain segment of the cantilever beam. The evaporation rate is not taken into

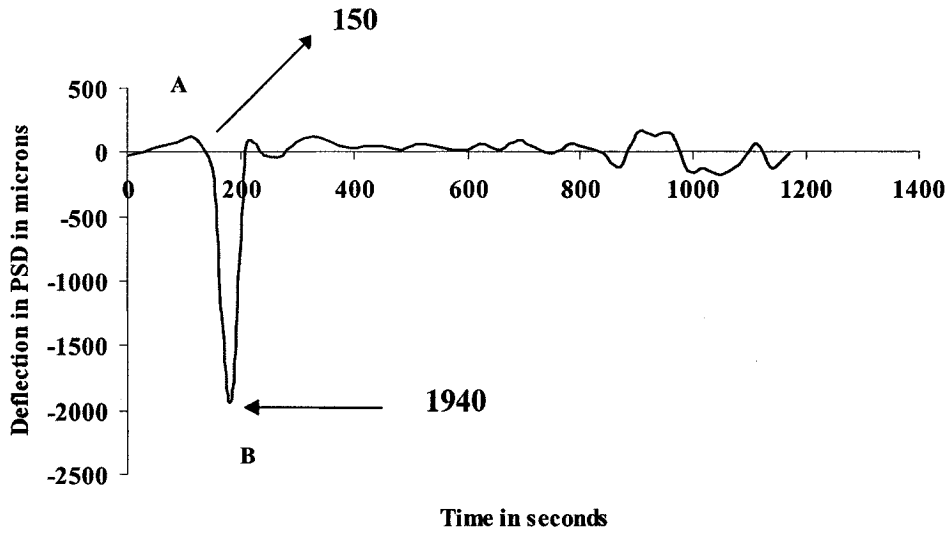

Figure 2.1: PSD reading of cantilever deflection for 40mg/ml TnC-Water showing different peaks of reaction where tension is calculated

consideration because the droplet vaporizes long after the reaction occurs. This can be clearly explained in the experimental results obtained in Figure 2.1 in the case of TnC-water interaction. Initially when 0.4 μl water is deposited on the cantilever beam with the help of the pipette, the cantilever beam moves downward due to the load and the spot in the PSD moves upward. That is the reason for the recorded upward movement of 150 μm on the PSD as illustrated in Figure 2.1. After a period of time the water dries out due to the laser heating and also due to other environmental factors and during the conversion to a solid the water molecules pull the surface of the cantilever (only on the applied segment of the beam) inwards making the beam to move well upwards and the laser spot moves downwards till 1940 μm. When the molecules of water stop pulling the surface of the cantilever, indicating the drying process is complete the beam moves back to its initial position (not exactly though) and remains steady there.

In order to validate this experimental process the tip deflection of the cantilever was evaluated at two peaks of the signature reaction as shown in Figure 2.1 using a relation between distance moved in the PSD, angle of incidence and the tip deflection of the beam shown below [67]:

$$D = \sqrt{[\frac{L\sin i}{\cos 2\alpha} - L\sin(i+2\alpha) - \delta\cos i]^2 + [\frac{L\cos i}{\cos 2\alpha} - L\cos(i+2\alpha) - \delta\sin i]^2} \quad (2.1)$$

Here

D = laser spot movement in the PSD in microns

L = distance from the deflected cantilever to the PSD in meters

i = angle of incidence in radiance

δ = tip deflection of the cantilever beam in microns

α = the angle between the normal of the deflection beam and reflected laser beam in rad.

The model under study is based upon the following assumptions:

1. The load acting on the segment of the cantilever is a uniformly distributed load (UDL)
2. The load is uniformly distributed over the entire width of the beam in that particular segment
3. The standard theory of pure bending of beams is been used
4. The sole cause of the cantilever deflection after the loading is the superficial tension variation related to the biochemical reaction at the interface of bio-fluid-cantilever.

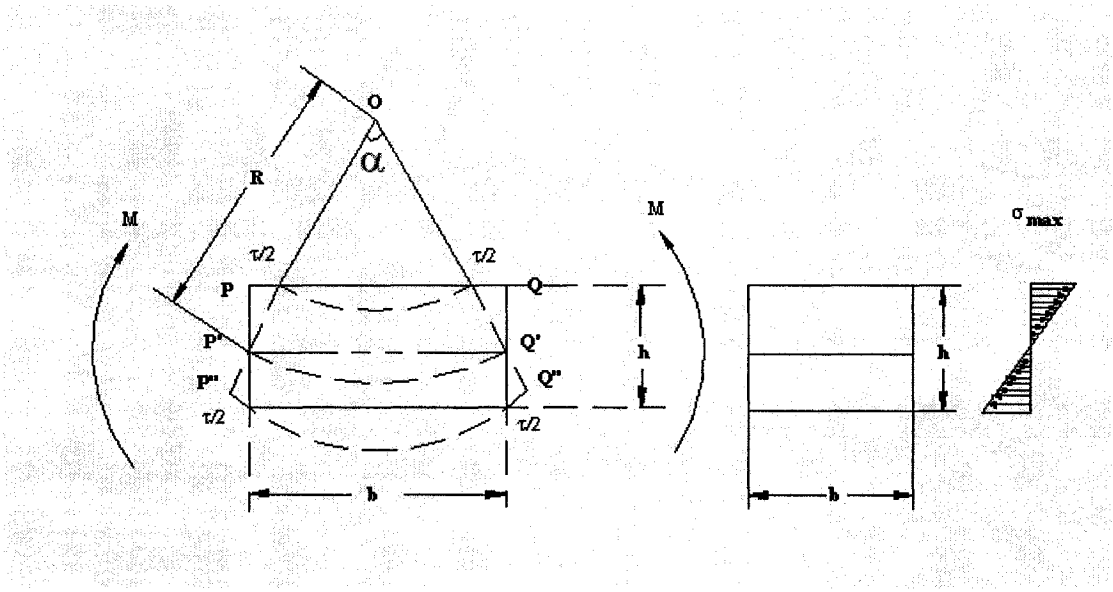

Figure 2.2: Section of the beam undergoing bending due to enzymatic reaction

From the sector OPQ, $\alpha(R-h/2)=b-\tau$ (2.2)

From the sector OP'Q', $\alpha(R+h/2)=b+\tau$ (2.3)

From the sector OP"Q", $\alpha R=b$ (2.4)

From the equations 2.2 and 2.4 it can be formulated that

$$\tau=\frac{b*h}{2*R} and \varepsilon=\frac{\tau}{b}=\frac{h}{2*R} \quad (2.5)$$

where

τ is the change in length in the upper and lower portion of the beam due to strain

h/2 is distance from the neutral axis

R is Radius of curvature

ε is the strain caused in the bended portion of the beam due to the droplet

In the above equation the strain generated due to bending is related to the radius of curvature and geometry of the beam.

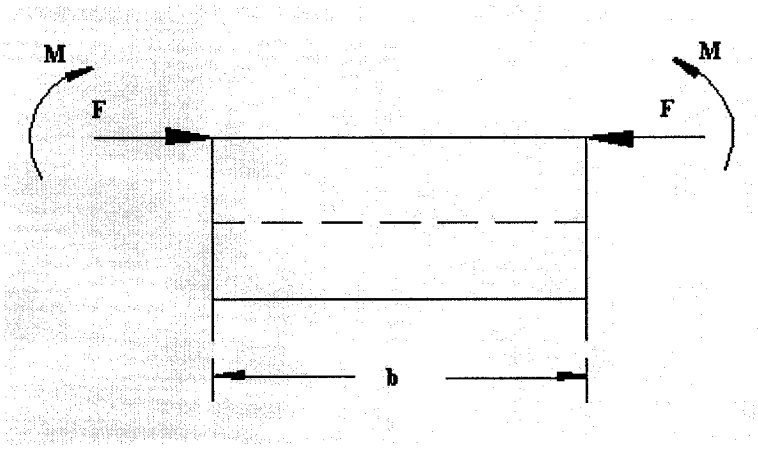

Figure 2.3: The force acting on the surface of the beam is represented in terms of a bending moment

The two equal and opposite forces that are created due to the enzymatic interactions are represented in terms of bending moment. The action of the shear and bending moment are represented in Figure 2.4. The force that acts on the surface of the cantilever is a function of the superficial tension.

$$S * d = F \tag{2.6}$$

Where

d is the width of the droplet

S is the superficial tension

This force is substituted in terms of the bending moment as follows

$$M = \frac{F * h}{2} \tag{2.7}$$

From the beam flexure formula [68, 69] we have the following relation

$$\frac{M}{I} = \frac{\sigma}{h/2} = \frac{E}{R} \tag{2.8}$$

where

M = bending moment created by the surface stress on the cantilever

I = moment of inertia

σ = uni-axial stress produced due to the bending moment

E = Young's Modulus of the cantilever beam

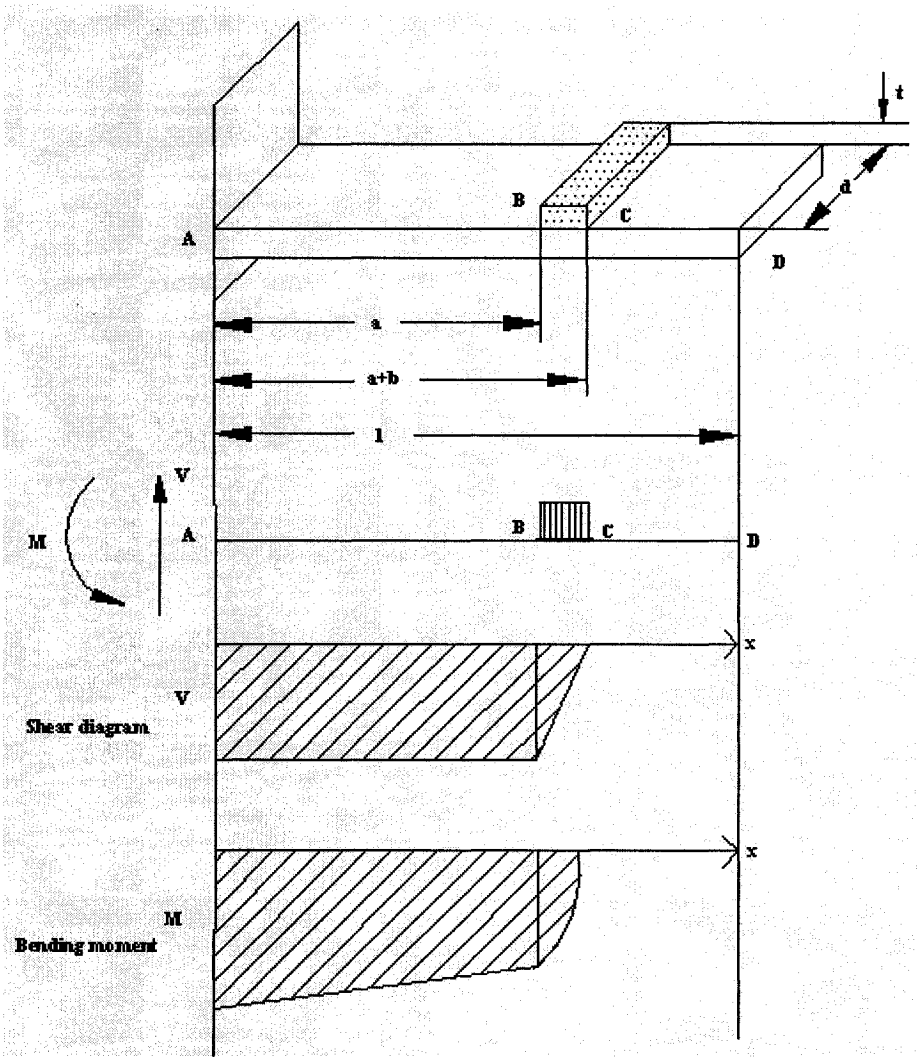

Figure 2.4: Cantilever model showing the shear and bending moment diagrams

The above equation can be adjusted in the following way

$$\sigma_{max} = \frac{M * h}{2 * I} \tag{2.9}$$

by using Hooke's law and equation 2.5 and 2.7 strain can be evaluated as follows

$$\varepsilon = \frac{M * h}{2 * E * I} \tag{2.10}$$

Note: Here σ_{max} is assumed to be due to the effect of the superficial tension. The reason being that, stress is force per unit area and superficial tension is force per unit length. This assumption makes possible correlation between the bending stress and the superficial tension effect.

Substituting the expression for moment of inertia in equation 2.9 the final expression for strain in terms of bending moment can be obtained as follows

$$\varepsilon = \frac{6 * M}{E * d * h^2} \tag{2.11}$$

Clearly strain is a function of the geometric properties of the beam. Once the expression for strain is obtained, substituting for strain in equation 2.5 the radius of curvature is obtained as follows

$$R = \frac{h^3 * E * d}{12 * M} \tag{2.12}$$

Using equation 2.6 and 2.7 the relation between radius of curvature and superficial tension is as follows

$$R = \frac{h^2 * E}{6 * S} \tag{2.13}$$

The above equation is quite appropriate because as the enzymatic molecules interact on the surface of the beam they pull the beam inwards reducing the radius of curvature. This

superficial tension is responsible for bending that portion of the beam where the droplet is applied. The more the superficial tension will tend to bend the more will the radius of curvature decrease. Also the relation between the angle α and superficial tension can be obtained from equation 2.4

$$\alpha = \frac{6 * b * S}{E * h^2} \tag{2.14}$$

From the theorem of sines the following relation can be obtained from Figure 2.5

$$\frac{R}{\sin(90-\alpha)} = \frac{X}{\sin 90}$$

$$X = \frac{R}{\cos\alpha} \tag{2.15}$$

From Figure 2.5 it can be noted that both triangle OMS and triangle NKS are similar triangles and hence,

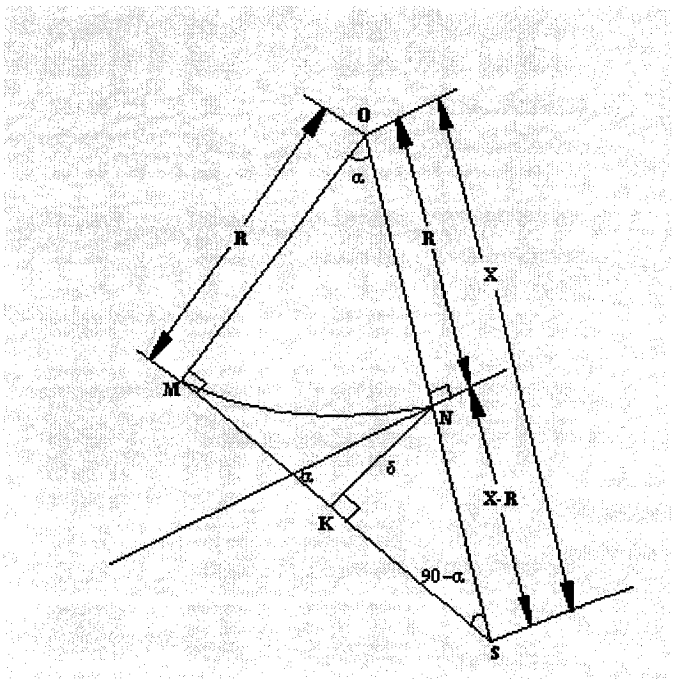

Figure 2.5: Geometrical representation of the bended portion of the beam used to relate radius of curvature with superficial tension

$$\frac{R}{\delta} = \frac{X}{X-R} \Rightarrow \delta = \frac{R(X-R)}{X} \tag{2.16}$$

Substituting equation 2.14 in 2.15 the relation between deflection, radius of curvature and angle α

$$\delta = R(1-\cos\alpha) \Rightarrow \delta = \frac{E*h^2}{6*S}(1-\cos\alpha) \tag{2.17}$$

The deflection δ is the deflection of the bended portion of the beam on which the enzyme droplet was deposited which may not necessarily be at the tip of the beam. The remaining portion of the beam (beyond the droplet) which is dry is also curved up due to the superficial tension. That total deflection is found out as a function of the superficial tension.

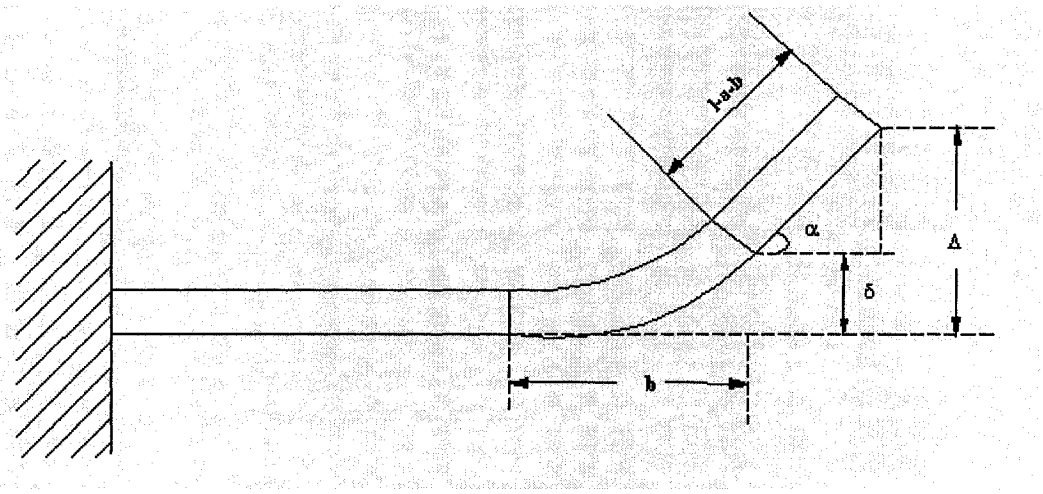

Figure 2.6: Geometrical representation of the entire beam in order to relate total deflection with superficial tension

Another point to keep in mind is that the total deflection is not evaluated exactly at the tip of the cantilever beam, instead it is calculated at the point where the laser beam is flashing on the cantilever. So the total deflection does not take into account the entire length of the cantilever beam.

From Figure 2.6 the relation between total deflection and superficial tension is derived.

$$\Delta = (l - a - b) * \sin\alpha + \delta$$

The final equation can be rearranged as follows

$$\Delta = (l - a - b) * \left(\sin(\frac{6 * b * S}{E * h^2}) \right) + \frac{E * h^2}{6 * S} \left(1 - \cos(\frac{6 * b * S}{E * h^2}) \right) \quad (2.17)$$

For the values of deflection obtained on the PSD for TnC-ME, HRP-H_2O_2 and water the corresponding tip deflection was evaluated using equation 2.1. From that tip deflection and dimensions of the cantilever beam the corresponding superficial tension S was evaluated. This S is responsible to make the beam move positive to negative in the plots shown in Figure 2.1, 2.7 and 2.8 respectively.

This can be clearly understood from the Table 2.1 in which each of the enzymes were deposited on the beam to observe the signature reaction. The tip deflection was evaluated from the PSD values at the different peaks of the signature reaction denoted as A, B, C and D respectively. From these tip deflection values the corresponding superficial tension was evaluated to know as to how much force is needed to lift the beam from -600 microns to 700 microns in case on TnC-ME and from 450 microns to 1500 microns in the case of HRP-H_2O_2.

Table 2.1: Evaluation of superficial tension from the tip deflection of the beam using the PSD reading

Category	Troponin-Water		Troponin-Melittin				HRP-H_2O_2			
Peaks in the plots	**A**	**B**	**A**	**B**	**C**	**D**	**A**	**B**	**C**	**D**
PSD deflection in microns	1940	150	75	200	700	-600	210	450	1500	140
Tip deflection in microns	6.2	.47	.005	.64	.88	.53	.2	.73	4.8	.44
Superficial Tension in $*10^5$ N/m	14.1	.05	.002	.07	1.5	0.06	.03	0.09	12	.04

Table 2.1 shows the comparison that validates the experimental process. The increase in values of tip deflection due to load could be due to the additional mass of water added in

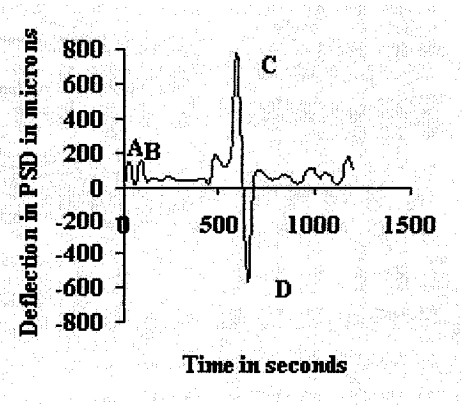

Figure 2.7: PSD reading of cantilever deflection for 25mg/ml TnC-ME showing different peaks of the reaction where the tension is calculated

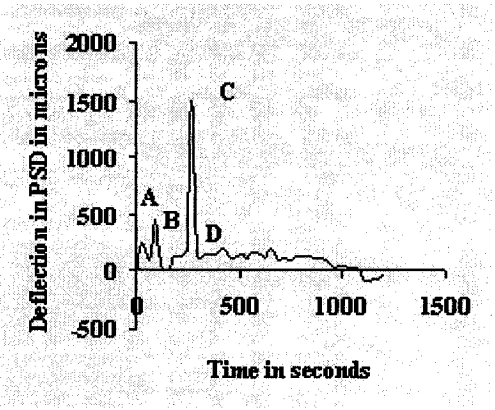

Figure 2.8: PSD reading of cantilever deflection for 25mg/ml of HRP-H_2O_2 showing different peaks of the reaction where the tension is calculated

the enzymes because almost 80% of the enzyme solution contains water. Clearly from the table it can be incurred that as the tip deflection of the cantilever increases the superficial tension also increases due to enzymatic interaction on the surface of the beam.

The same concept can be applied in the two cases given below for Troponin-Melittin reaction and HRP-H_2O_2 reaction. In Figure 2.7 the initial peak of 180 μm is due to the load of the enzyme. After a period of time the chemical reaction between the two proteins takes place with the cantilever beam first moving up to 700 μm and then moving down to 575 μm. In this span the molecules of the two proteins react with each other pulling the surface of the cantilever (the segment alone) inwards. Hence the cantilever moves down and then goes up immediately. When the enzymes dry up the cantilever returns back to the original position and remain steady after that. A similar explanation could be given for HRP-H_2O_2 as well in Figure 2.8.

2.2.2. Influence of the Geometry, Position and Mass on the Drop of Natural Frequency

Due to the addition of this extra mass the natural frequency and second harmonics will go down. A Finite Element Modeling (FEM) is used to analyze the resonant frequency and the second harmonic. This droplet can be assumed to be a concentrated mass at the free end of the cantilever beam while in modeling. In many vibrational systems the mass is assumed to be lumped. A mass-spring-damper system could be taken as a simplest

example to replace the present model. The above situation can be analyzed in the following manner:

The natural frequency is analyzed for both the cases, i.e., for both with and without the application of load with the aid of ANSYS as shown in Figure 2.9. The model was built using SOLID 45 using the material properties of PVDF with a Young Modulus of 2.1GPa, with a Poisons ratio of 0.3 and density of 1780 Kg/m^3. The dimensions of the beam were in the order of length = 2.3mm, width = 0.8mm and thickness = 25 μm respectively.

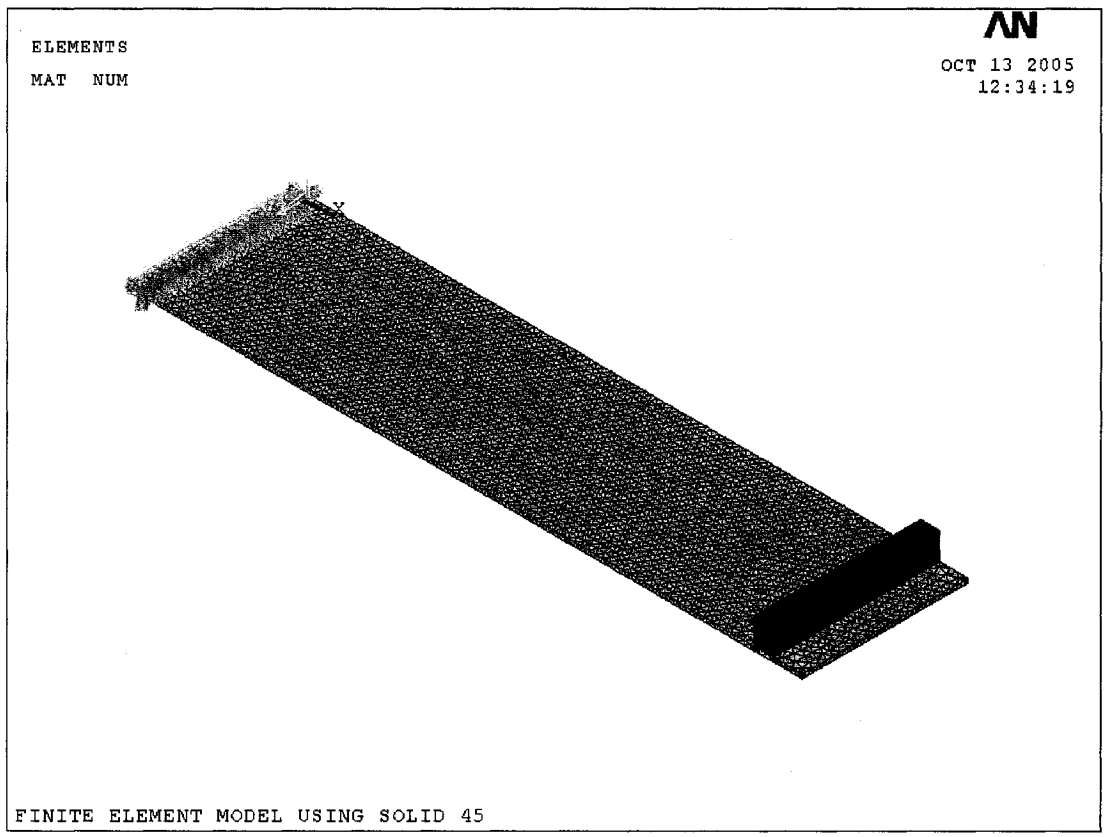

Figure 2.9: Representation of the cantilever model in ANSYS with boundary conditions and extra mass on it

A total of 17000 elements were obtained after meshing. The extra mass was assumed to be a different material but the same element. The other material chosen was rubber with material properties of 2.3 GPa and 0.3 and a density close to that of water 1050 Kg/m^3 respectively. Both the materials are glued to each other in order to perform modal analysis.

The natural frequency is represented in the normalized form in which the plot of the natural frequency (first harmonic) vs. the concentrated mass reported to the mass of the cantilever as shown in Figure 2.10. The ratio of the first natural frequency involves the ratio of frequency of the beam with the mass to the ratio of the beam without the mass. The ratio of the position of the load on the beam is due to the ratio of the load position on the beam to the ratio of the load at the tip of the beam. The mass ratio includes ratio of mass of the liquid to the ratio of the mass of the cantilever at different loads on the cantilever beam. The load is made to move at different positions on the cantilever and correspondingly the natural frequency was calculated. It can be clearly concluded from Figure 2.10 that the natural frequency is maximum at zero load. But when the load increases along with its position on the beam the natural frequency reduces and becomes almost equal to zero although it does not touch zero.

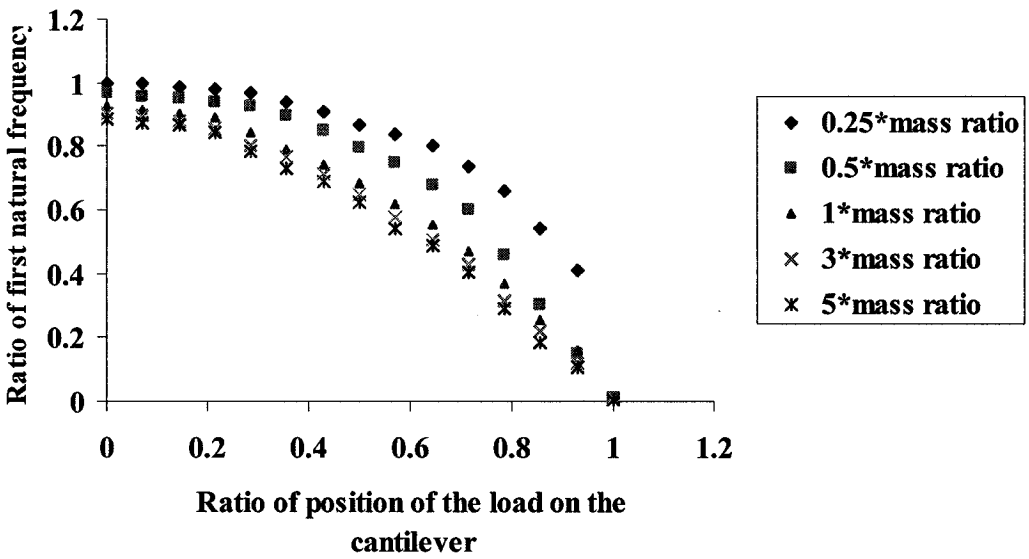

Figure 2.10: Ratio of first natural frequency plotted against ratio position of load on the cantilever

Usually the evaluation of surface stress of a multi-DOF system is often of greater interest and that can be incorporated in the cantilever beam analysis. The variation of stress along the length of the beam provides importance in the design of machine parts subjected to variable external forces and to the reversal of stresses. Changes in surface stress can be the result of an adsorption process or electrostatic interaction between charged molecules on the surface.

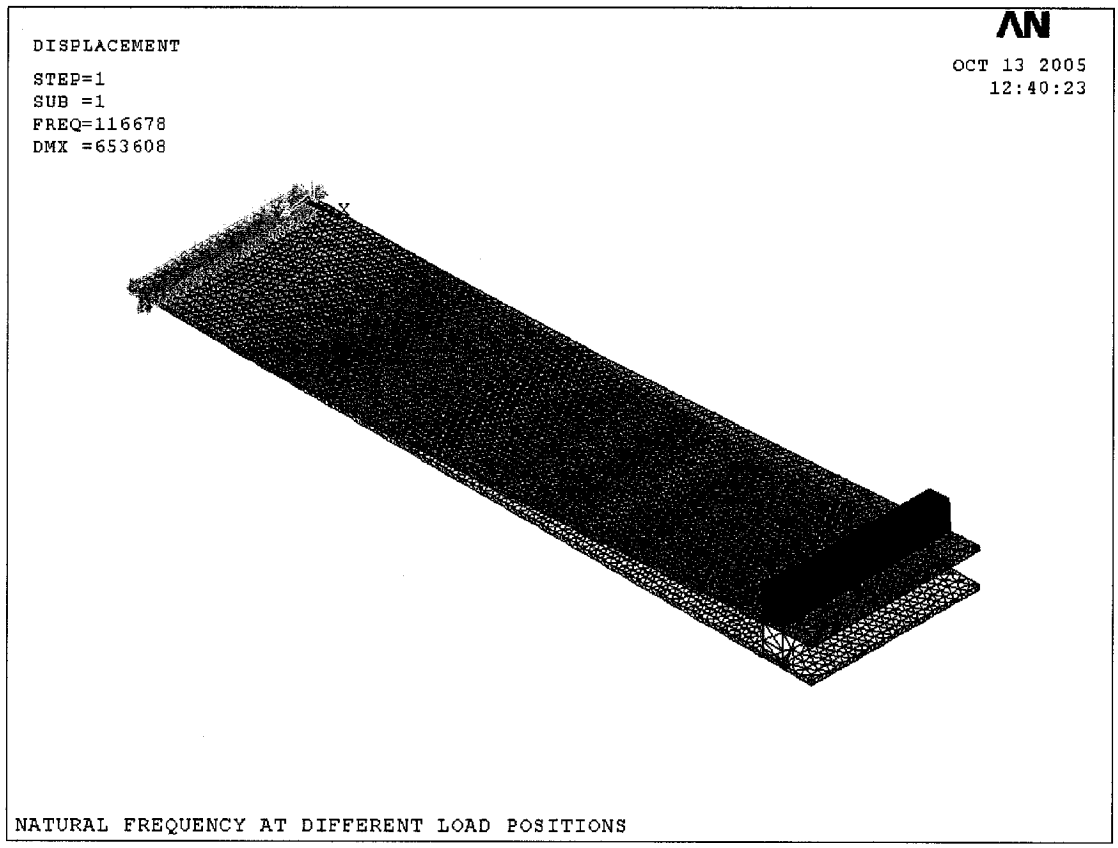

Figure 2.11: ANSYS representation of the cantilever beam with the deformed and un-deformed states

Modal analysis was done to evaluate any anomalies in the natural frequencies. The deformed and un-deformed shape of the cantilever for the first natural frequency due to the extra load added on it as shown in Figure 2.11.

2.2.3 Superficial Tension due to the Enzymes on the Cantilever Surface

2.2.3.1 Relation between Radius of Curvature and Stress

In general, adsorption of molecules to a surface causes a change in the surface energy, also called as surface tension [69]. The cantilever response is caused due to this surface stress. Uniform surface stress acting on an isotropic material increases (tensile stress) or decreases (compressive stress) the cross-section surface area. If this stress is not compensated at the opposite side of the beam, then the whole structure will bend as shown in Figure 2.12. Between the areas of compressive stress and tensile stress, there is a neutral plane which is not deformed. Usually the deformation is assumed to be in pure bending and stress uni-axial, but when dealing with complex molecules like proteins for biochemical sensing, there are several other possible sources of stresses than simple ion adsorption onto a clean crystal surface which are ignored.

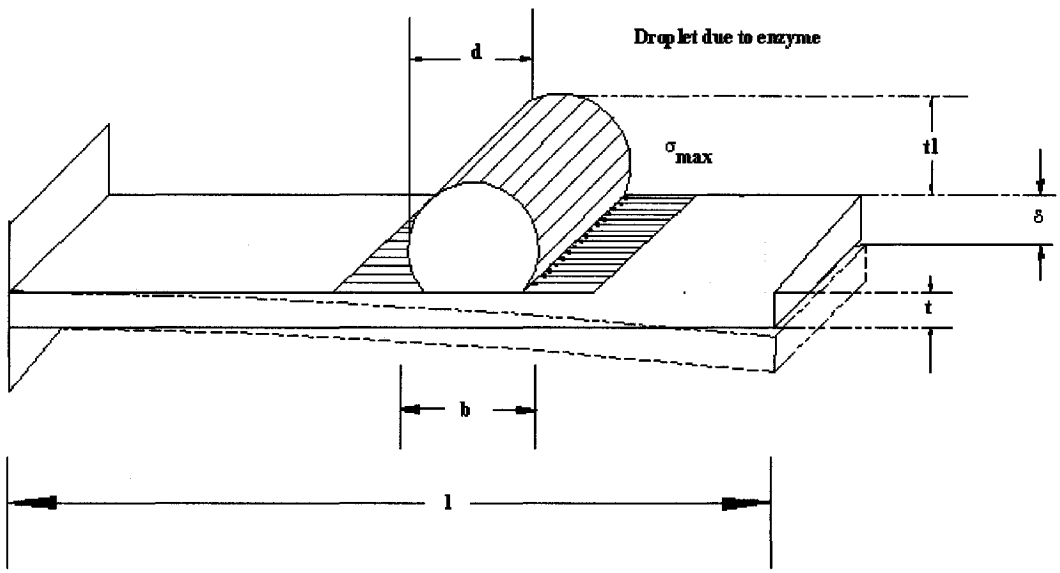

Figure 2.12: Behavior of cantilever beam under the action of the droplet due to the enzyme. The stress distribution is also denoted along side the droplet.

When a cantilever beam is deformed in pure bending (no axial load, no shear, no torsion), we expect a uni-axial stress that is applied at 3 different points of the beam (all along the thickness of the beam). All the other stress components are identically zero [69]. However, there is a small region adjacent to the points of load application where the internal stress distribution is complex. In discussing the pure bending of such beams we assume that cross sections of the beam remain plane during bending; hence elongations and contractions of the longitudinal fibers are proportional to their distances from the neutral surface. Taking this as a basis of discussion and assuming that during bending there exists the same relationship between stress and strain as in the case of simple tension and compression, it could be found that the stresses produced in the beam by a bending moment of any given magnitude [70].

Considering a beam of constant rectangular cross-section in which the radius of curvature R is been produced due to the two bending moments M as in Figure 2.2.

Again from the beam flexure equation (2.8)

$$\sigma_{max} = \frac{E * h}{2 * R} \tag{2.18}$$

Equation (2.18) can be re-arranged as follows

$$\frac{\sigma_{max}}{E} = \frac{h}{2R} \tag{2.19}$$

$$R = \frac{E * h}{2 * \sigma} \tag{2.20}$$

From Figure 2.5, the length MN is assumed to be b, which is equal to

$$R\alpha = b \tag{2.21}$$

Substituting equation (2.20) in (2.21) the following relation is obtained for α with stress

$$\alpha = \frac{2*b*\sigma}{E*h} \tag{2.22}$$

From Figure 2.5, the value of δ can be evaluated as follows:

$$\delta = R - R*\cos\alpha = R(1-\cos\alpha) \tag{2.23}$$

If on the cantilever beam b is the length of the wet portion due to the enzymes then the deflection is given by the following relation:

$$\delta = R\left[1-\cos\left(\frac{2*b*\sigma}{E*h}\right)\right] \tag{2.24}$$

2.2.3.2 Evaluation of Stress from Transcendental Equation

From Figure 2.13, we can estimate the relation between total deflection of the cantilever beam with the stress as follows:

$$\delta_{total} = \delta + \delta 1 \tag{2.25}$$

$\delta 1$ can be evaluated by using the angle α from Figure 2.15. The relation is given by

$$\delta 1 = (l-a-b) \ *\sin\alpha \tag{2.26}$$

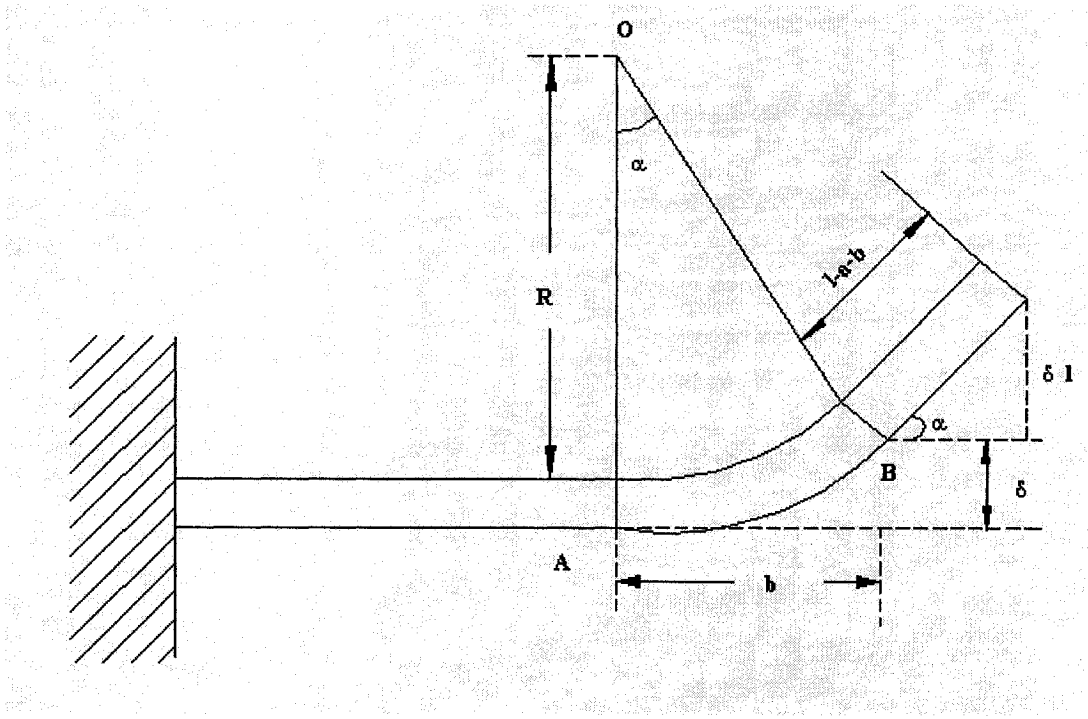

Figure 2.13: Schematic to evaluate the total deflection and stress

Substituting equation (2.24) and (2.26) in equation (2.25),

$$\delta_{total} = R\left[1-\cos\left(\frac{2*\sigma*b}{E*h}\right)\right]+(l-a-b)*\sin\left(\frac{2*\sigma*b}{E*h}\right) \qquad (2.27)$$

Substituting equation (2.6) in equation (2.13) and re-arranging the terms:

$$\delta_{total} = \frac{E*h}{2*\sigma}\left[1-\cos\left(\frac{2*\sigma*b}{E*h}\right)\right]+(l-a-b)*\sin\left(\frac{2*\sigma*b}{E*h}\right) \qquad (2.28)$$

The above equation is a transcendental equation involving both sin and cosine terms. The above equation will have more than one solution.

The stress was evaluated by varying the deflection due to the load by the following calculations:

Molecular weight of Troponin C = 18 KDa = 2.988 * 10^{-20} Kg (1 Da = 1.660540 * 10^{-24} Kg)

Number of moles = [Concentration] * Volume = 1 * 10^{-8} m^3

Mass of Troponin C = Number of moles * Molecular weight * Avogadro number

Mass of Troponin C = 1.8 * 10^{-4} Kg

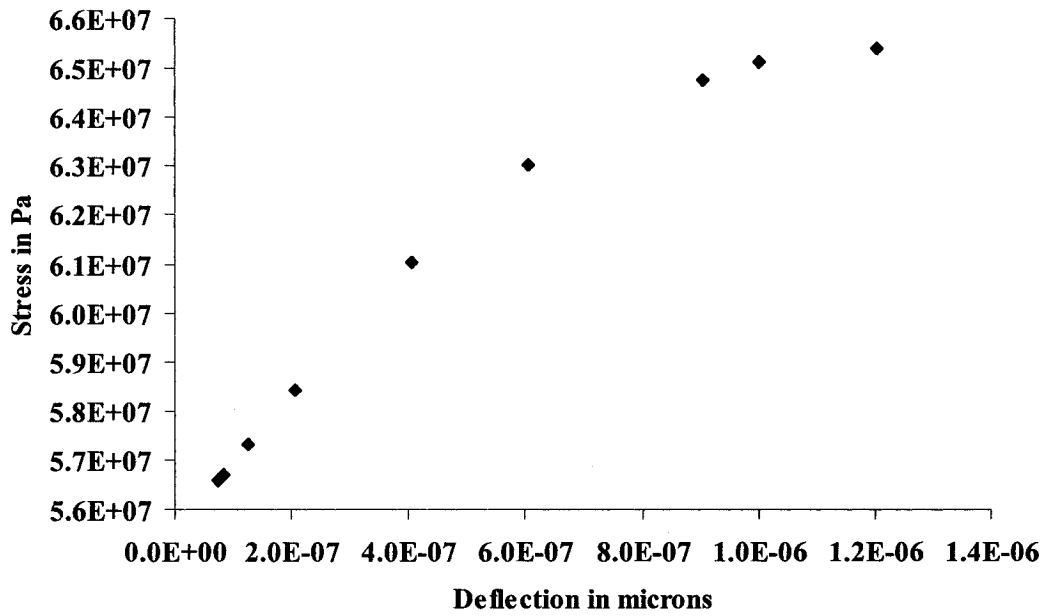

Figure 2.14: First solutions from transcendental equation showing stress vs. deflection for TnC-ME

Similarly the Mass of Melittin Bee was evaluated to be = 2.8504 * 10^{-5} Kg

From the total mass of the two proteins the total force was evaluated to be =2.04 * 10^{-3} N. For the corresponding force the stress was evaluated to be = 59 MPa which is closely obtained in the plot in Figure 2.14. This would be the stress that is required to bring the beam back to the original position after getting deflected. As the deflection is increased the stress also increases only on a particular segment of the cantilever beam.

Similar sort of calculations were also done for the other set of enzymes namely, Horseradish Peroxide (HRP) and Hydrogen Peroxide (H_2O_2). From the total mass of the two proteins the value of force was found out to be = 2.0594 * 10^{-5} N. From the correspo-

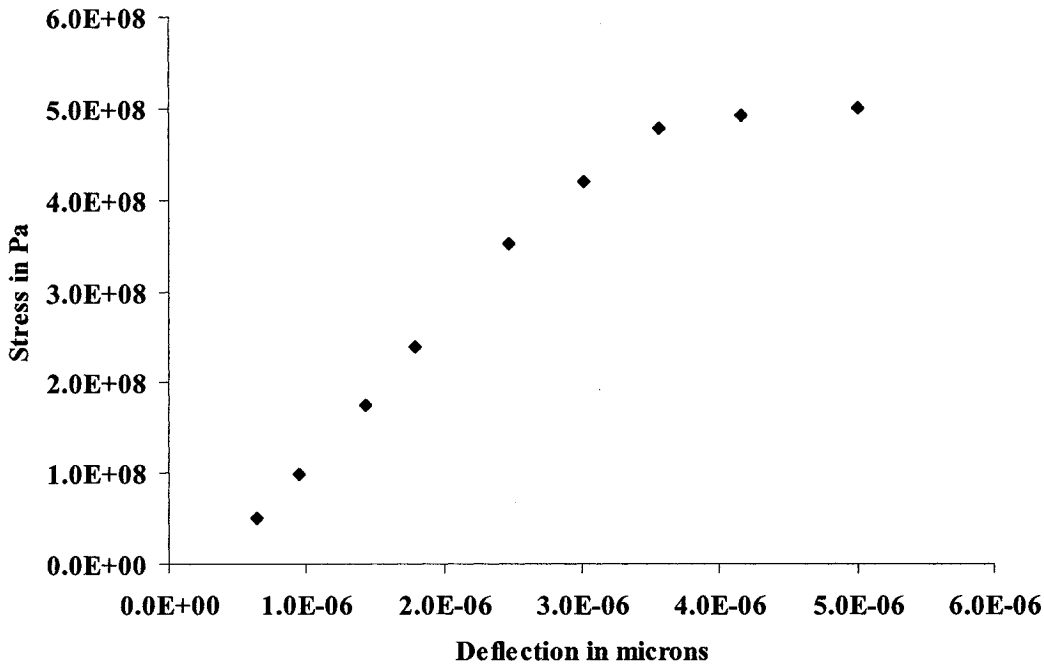

Figure 2.15: First solutions from transcendental equation showing stress vs. deflection for HRP-H_2O_2

-nding force the superficial tension was evaluated to be = 65 MPa. This would be the superficial tension required to bring the beam back to the original position after getting deflected due to the reaction. Figure 2.15 shows a linear variation of stress vs. deflection for a mass applied only on a particular segment on the beam. But the stress-deflection curve for HRP-H_2O_2 is less linear. This could be due to the fact that TnC-ME molecules interact at the same rate through out which pulls that particular segment of the beam inwards, but the HRP-H_2O_2 reaction does not take place at the same rate throughout the

reaction. The reaction is at the faster rate during the formation of the two electrons released from the oxidized first compound, which has Fe^{4+} and cation radical, and then steadies down after that. The oxidation of HRP was complete within 1 min at room temperature [71].

In the remaining portion of the beam the there could be stress caused due to the weight of the enzymes. The influence of the weight could be eliminated if the beam is set in a

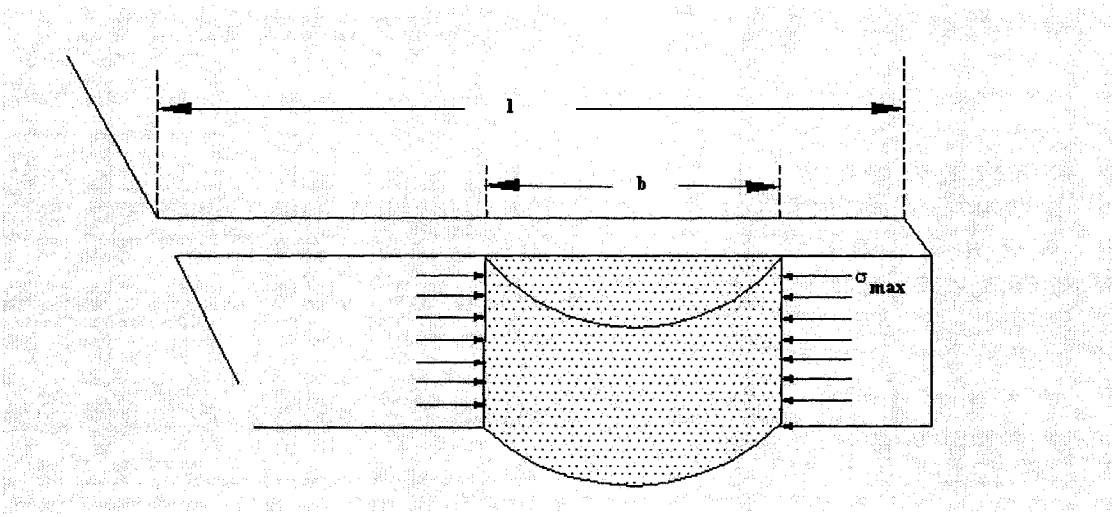

Figure 2.16: The influence of the weight could be compensated by applying the load in the vertical condition.

vertical position as shown in Figure 2.16. However, the beam may be subjected to torsion which might also influence the deflection of the tip.

2.2.4 Dynamic Behavior of the Beam subjected to Bio-reaction

In the dynamic analysis of the cantilever beam the natural frequency vs. amplitude is compared for three cases:

1. only the cantilever beam
2. cantilever beam with the extra mass
3. cantilever beam with the extra mass and the bending

The comparison is made by taking the ratio of the amplitude (deflection of the cantilever beam in this case) to the ratio of natural frequency. The ratio of the amplitude involves the ratio of amplitude at resonance to the static amplitude. The ratio of natural frequency involves the ratio of frequency at resonance to the natural frequency of the cantilever. It is expected that the signature of the bio-reaction to be relevant and sensitive to the measurement.

As seen in Figure 2.17, that ratio of amplitude for only the cantilever beam approaches a large number in comparison to the other two cases. The amplitude of a system is inversely proportional to the mass and hence when the beam is added with extra mass the shift in natural frequency takes place along a dip in the amplitude. This indicates that the natural frequency ω_n of the supported system must be small compared to that of the distributing frequency ω. The curves show that the mass factor has a large influence on the amplitude in the frequency region near resonance. For small values of ratio of freque-

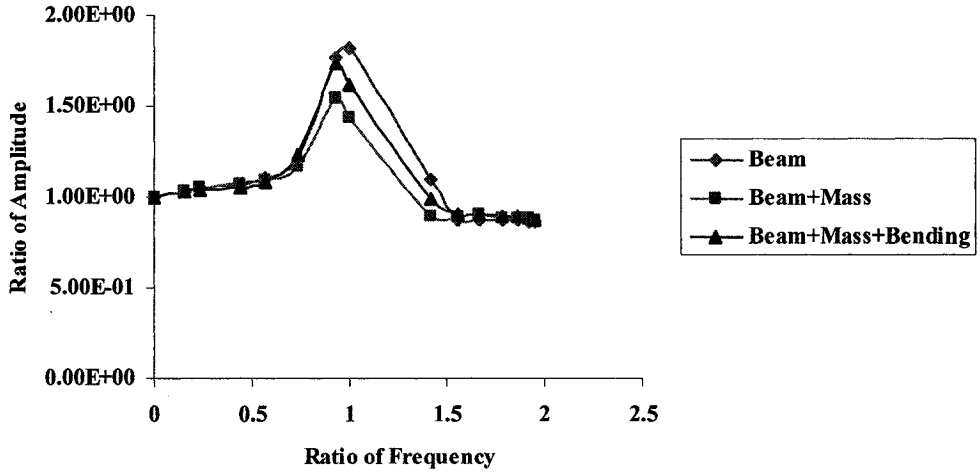

Figure 2.17: Relation between ratio of amplitude and natural frequency of the cantilever beam for three different cases.

-ncy$\left(\frac{\omega}{\omega_n}\langle\langle 1\right)$ the amplitudes for beam, beam+mass and beam+mass+bending remain more or less the same. In this case the inertia and damping forces are small. For $\left(\frac{\omega}{\omega_n}=1\right)$ the inertia force is larger than the damping force and is balanced by the spring force. At larger values of $\left(\frac{\omega}{\omega_n}\rangle 1\right)$ the inertia force is very large.

2.2.5 Modeling of Cantilever Beam for Harmonic Oscillations

Rayleigh-Ritz method of analysis has been applied to beam structures in order to obtain their natural frequency. In the present study, the vibration problem of a cantilever beam has been investigated by using a set of characteristic orthogonal polynomials in the classic Rayleigh-Ritz method. These orthogonal polynomials have been generated by using a Gram-Schmidt process [72] so as to satisfy at least the geometric boundary conditions of the cantilever beam.

When compared with the classic Rayleigh method, the Rayleigh-Ritz method replaces a single shape function by a series of shape functions multiplied by constant coefficients. The mode shapes of the system are characterized as a complete set of orthogonal polynomials, so the deflection function is usually expressed in a generalized Fourier series involving mode shapes. The assumed deflection in the Ritz method is a function of these shape functions and constant coefficients.

2.2.5.1 Boundary Characteristic Orthogonal Polynomials

Earlier literature [72] showed a simpler way to evaluate the natural frequencies of cantilever beams under various boundary conditions using boundary characteristic orthogonal polynomials in the Rayleigh-Ritz method. This method is better when compared to other methods that involve the use of trigonometric functions to evaluate the orthogonal polynomials, because it's much easier to differentiate or integrate an orthogonal polynomial than the trigonometric functions. The first polynomial is chosen so as to satisfy atleast the geometrical boundary conditions of the structure for use in Rayleigh-Ritz method. The example given below elaborates the construction of orthogonal polynomials for clamped-free beam whose boundary conditions are zero deflections and zero slopes at the clamped end.

For a clamped-free cantilever beam the deflections may be first assumed as

$$W(x) = \Phi(x)$$

The boundary conditions corresponding to the clamped-free beam are

$$\Phi_1(0) = \Phi_1'(0) = \Phi_1''(1) = \Phi_1'''(1) = 0 \tag{2.29}$$

Assuming a deflection function in the x-direction as

$$\Phi(x) = a_o + a_1(x) + a_2(x)^2 + a_3(x)^3 + a_4(x)^4 \tag{2.30}$$

Applying (2.16) and (2.17) the first normalized polynomial is obtained as

$$\Phi_0(x) = \frac{\left(6x^2 - 4x^3 + x^4\right)}{\int_0^1 \Phi^2(x)dx} \tag{2.31}$$

The second orthogonal polynomial is obtained in the interval $0 \leq x \leq 1$

$$\Phi_1(x) = (x - B_1)\Phi_0(x) \tag{2.32}$$

$B_2 = \dfrac{\int x\Phi_0^2 dx}{\int \Phi_1^2 dx}$ and from there Φ_3 and Φ_4 and so on.

In general

$$\Phi_k(x) = (x - B_k)\Phi_{k-1}(x) - C_k\Phi_{k-2}(x) \tag{2.33}$$

where

$$B_k = \frac{\int_0^1 xf(x)\Phi_{k-1}^2(x)dx}{\int_0^1 f(x)\Phi_{k-1}^2(x)dx} \tag{2.34}$$

$$C_k = \frac{\int_0^1 xf(x)\Phi_{k-1}(x)\Phi_{k-2}(x)dx}{\int_0^1 f(x)\Phi_{k-2}^2(x)dx} \tag{2.35}$$

The polynomials thus obtained satisfy the orthogonality condition

$$\int_0^1 f(x)\Phi_k(x)\Phi_1(x)dx = \begin{Bmatrix} 0 if k \neq 1 \\ a_{ij} if k = 1 \end{Bmatrix} \tag{2.36}$$

where f(x) is the weight function.

The Rayleigh-Ritz method provides an approximate solution of the eigen value problem for a cantilever beam whose deflection function is of the linear form given by a summation of n terms:

$$W(x) = \sum_{k=1}^{n} A_k \Phi_k \tag{2.37}$$

where A_k are the constant coefficients or the deflection constants and Φ_k are the shape functions that are generated by the Gram-Schmidt orthogonalization processes which are differentiable and which should satisfy at least the natural boundary conditions of the cantilever beam. The coefficients of the different terms of this Fourier series are general co-ordinates. The variable x defines the position along the cantilever where x = 0 corresponds to the fixed end of the cantilever and x = l corresponds to the free end of the cantilever [73]. The expression for Rayleigh's quotient is the ratio of the maximum potential energy, $U_{\max}$ to the maximum kinetic energy, $T^*_{\max}$ of the system. It is given by

$$\omega^2 = \frac{U_{\max}}{T^*_{\max}} = \lambda \tag{2.38}$$

Where the kinetic energy is expressed as $T_{\max} = \omega^2 T^*_{\max}$ and λ is the Eigen value. The use of Rayleigh's quotient (scalar quantity) is to estimate the lowest natural frequency in the Rayleigh's energy method [64]. The cantilever may not be perfectly conditioned under which either deflection or angle at the clamping point may be different from zero. This situation is illustrated in Figure 2.18.

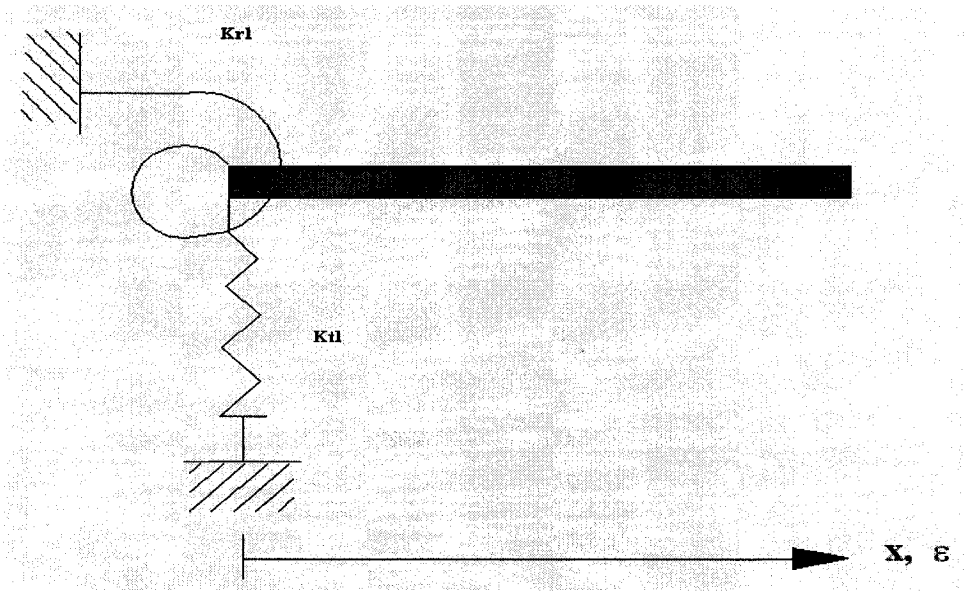

Figure 2.18: Cantilever beam showing the rotational and translational springs

The total energy of the cantilever beam includes the potential energy, the energy due to the springs and the kinetic energies. The total potential energy takes in to account the rotational and translation springs at the support end of the beam [74] as shown in the Figure 2.18. Hence the maximum potential energy of the system becomes $U_{\max} = U_b + U_s$. Here U_b is the strain energy of the cantilever and it's given by

$$U_b = \frac{EI}{2l^3}\int_0^l (W''(x))^2\,dx \tag{2.39}$$

U_s is the maximum potential energy due to the springs is given by

$$U_s = \frac{1}{2}K_T(W(0))^2 + \frac{1}{2}\frac{K_R}{l^2}(W'(0))^2 \tag{2.40}$$

T_b the maximum kinetic energy of the beam is given by

$$T_b = \frac{1}{2}\rho A l\omega^2\int_0^l (W(x))^2\,dx \tag{2.41}$$

Where ρ, A and L are the material density, cross-sectional area and the length of the beam respectively and ω is the natural frequency in radiance per second. Substituting the deflection function equation (2.24) in to the kinetic and potential energies (2.26), (2.27) and (2.28) the Rayleigh quotient in equation (2.25) is given in terms of the coefficients A_k minimizes in to the eigen value equation that is given in the form

$$\frac{\partial}{A_j}\left[U_b + U_s - \omega^2 * T_b^*\right] = 0 \tag{2.42}$$

The above equation is optimizing w.r.t A_m

$$\frac{EI}{l^3 2}\int_0^1 2\sum_m A_m \Phi_m''(x)\Phi_i''(x)dx + \frac{1}{2}\left[K_{T1}2\sum_m A_m \Phi_m(0) + \frac{K_{R1}}{l^2}2\sum_m A_m \Phi_m'(0)\right]$$

$$-\frac{1}{2}\rho A l\omega^2 \int_0^1 2\sum_m A_m \Phi_m(x)\Phi_i(x)dx$$

The above equation is further solved as

$$\sum_m \left[\frac{EI}{l^3}\int_0^1 \Phi_m''(x)\Phi_i''(x)dx + K_{T1}\Phi_m(0)\Phi_i(0) + \frac{K_{R1}}{l^2}\Phi_m'(0)\Phi_i'(0) - \rho A l\omega^2 \int_0^1 \Phi_m(x)\Phi_i(x)dx\right]A_m = 0$$

$$\sum_{m=1}^{10}\left[E_{mi}^{22} + \frac{K_{T1}l^3}{D}\Phi_m(0)\Phi_i(0) + \frac{K_{R1}l}{D}\Phi_m'(0)\Phi_i'(0) - \frac{\rho A l^4\omega}{D}E_{mi}^{00}\right]A_m = 0$$

$$\sum_m \left[E_{mi}^{22} + K_{T1}^*\Phi_m(0)\Phi_i(0) + K_{R1}^*\Phi_m'(0)\Phi_i'(0) - \lambda E_{mi}^{00}\right]A_m = 0$$

Where

$$E_{mi}^{22} = \int_0^L \left(\frac{d^2\Phi_n(x)}{dx^2}\right)\left(\frac{d^2\Phi_i(x)}{dx^2}\right)dx \tag{2.43a}$$

$$E_{m,i}^{0,0} = \int_0^L \Phi_n(x)\Phi_i(x)dx \tag{2.43b}$$

$$K_T^* = \frac{K_T l^3}{EI}, K_R^* = \frac{K_R l}{EI}, \lambda = \frac{\rho A \omega^2 l^4}{EI} \tag{2.43c}$$

$$D = EI \tag{2.43d}$$

The natural frequency of the cantilever beam then relates to the expression given below

$$\omega_n = \lambda_n \sqrt{\frac{EI}{\rho A l^4}} \tag{2.44}$$

Where the λ_n are the Eigen values, E is the Young's modulus of elasticity and I is the moment of inertia of the beam.

The load that is applied in the present case by the deposition of bio-chemicals actually acts as a droplet that remains stationary for a determined time. This droplet can be assumed to be a concentrated mass applied for simplicity in modeling at the free end of the cantilever beam as shown in the Figure 2.19. In many vibrational systems we can assume the mass to be lumped. A shaft transmitting torque for several pulleys along its length is an example. The kinetic energy of the system becomes

$$T_b = \frac{1}{2}\rho A l \omega^2 \int_0^L (W(x))^2 dx + \frac{1}{2} M (W(l))^2 dx \tag{2.45}$$

Here M is the concentrated mass that is applied at the free end of the cantilever beam as illustrated in the Figure 2.19.

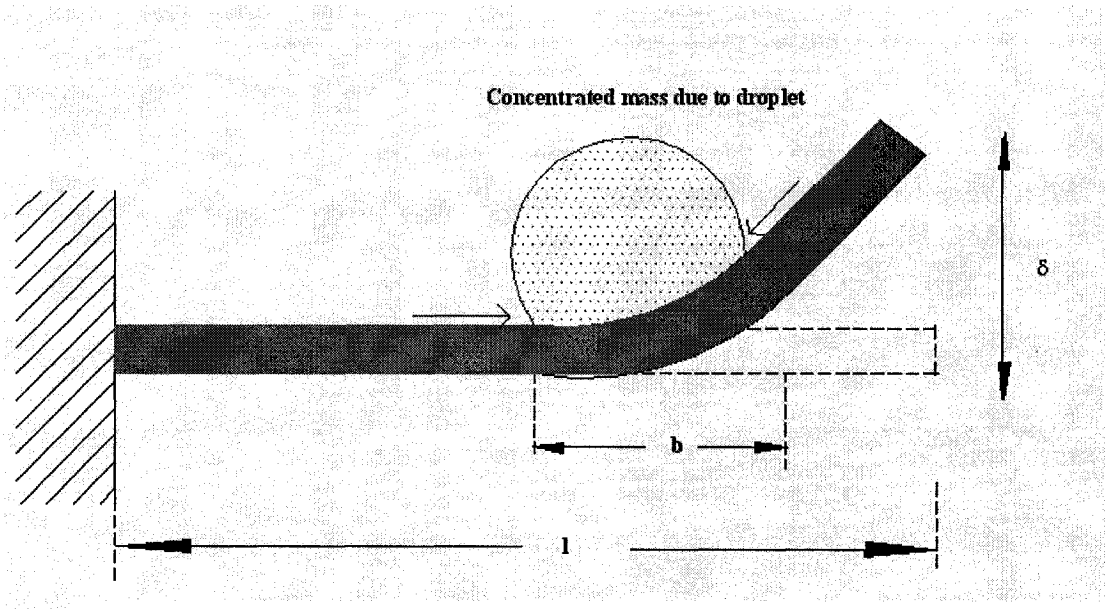

Figure 2.19: Concentrated mass (M) applied at the free end of the cantilever beam of length L1

Equation (9) can be written as follows

$$T_b = \frac{1}{2}\rho A l \omega^2 \int_0^l \sum_n \Phi_n(x)\Phi_i(x)dx + \frac{1}{2}\sum_n M\Phi_n(l)\Phi_i(l) \qquad (2.46)$$

$$T_b = \frac{1}{2}\rho A l \omega^2 \sum_n [\int_0^l \Phi_n(x)\Phi_i(x)dx + \frac{1}{2}M\Phi_n(l)\Phi_i(l)] \qquad (2.47)$$

Equation (2.34) gives an expression for the evaluation of concentrated mass at the free end of the cantilever beam. Due to the addition of this extra mass the natural frequency and second harmonics will go down. The cantilever beams used for modeling were PVDF beams of 2.5mm in length, 0.85mm in thickness and 25 μm in width respectively. The cantilever beams were made from silicon with aluminum coating of negligible thickness. While modeling the beam the boundary conditions for a clamped-free support were chosen. Since the cantilever beams are considered as continuous systems they have infinite number of degrees of freedom. The conditions for a valid mode shape depend on the boundary conditions of the beam.

2.3 SUMMARY

Mathematical and analytical modeling for characterization of mechanical stresses under the action of loads is essential for the reliable operation of many micromachines. In the present chapter modeling of cantilever beams was performed under static and dynamic conditions. In the static analysis of the cantilever beam validation of the experimental results were done by calculating the tip deflection of the beam from the PSD reading obtained from the experiment. The tip deflection was evaluated at different peaks in the signature reaction and from there the superficial tension was evaluated. In order to do so a simple relation between the total deflection of the beam and superficial tension was derived. In this relation the tip deflection was known. It was concluded that this superficial tension was responsible to move the cantilever beam up and down due to the reaction.

It is often very interested to note the shift in natural frequency in a cantilever beam when subjected to loading. So a comparison was made between the natural frequencies to the position of the extra mass on the load in ANSYS. The natural frequency was taken as the ratio of frequency of the beam with mass to the ratio of the frequency without mass. The extra mass was taken to be the ratio of the mass due to the load to the mass due to the cantilever. It was found that as the position of the mass moved from fixed end to the free end the natural reduced close to zero.

Due to the extra mass the molecules of the enzymes interact with each other pulling the surface of the cantilever (only on one segment of the beam) inwards causing a superficial

tension which further causes a deflection and hence bend the beam. A relation between the radius of curvature and stress was derived from simple geometry, which eventually ended as a transcendental equation relating the total deflection of the beam to the stress in terms of sine and cosine. The corresponding stress acting on the beam due to the different set of enzymes was analyzed for different deflections. It was found that the stress vs. deflection was a linear curve in the case of TnC-ME and also the stress was lower due to the smaller value of force acting on the beam. But in the case of HRP-H_2O_2 the stress vs. deflection was linear in the initial cases and then remained constant throughout. The stress evaluated in this case was higher.

In the dynamic analysis the behavior of the cantilever beam was analyzed for three different cases in ANSYS. For the first one, the ratio of amplitude vs. ratio of frequency was analyzed for a cantilever beam alone. In the second case ratio of amplitude vs. ratio of frequency was analyzed for cantilever with extra mass. In the third case it was analyzed for cantilever with the extra mass and also due to bending.

The dynamic analysis of the cantilever beam was further done using the classic Rayleigh-Ritz method. In modal analysis done here, the system is described in terms of the natural frequencies of the system. The modal analysis approach also reduces the time and effort and provides results for good engineering approximations and closer to the actual results. Derivation of orthogonal polynomials using the Gram-Schmit process was performed to find the first orthogonal polynomial. Although no experimental work on vibrations was

done modal analysis was performed to make accurate predictions for the dynamic behavior of the mechanical system.

CHAPTER 3

MICRO OPTO MECHANICAL BIOSENSORS FOR ENZYMATIC DETECTION USING CANTILEVERS BEAMS

3.1 INTRODUCTION

Micro Electro Mechanical Systems (MEMS) techniques integrated with biochemistry offers new exciting opportunities in biomedical analysis and bring unique characteristics. These micro mechanical transducers with biosensing applications have attracted considerable interest in the last few years. These transducers or biosensors employ a biological or biochemical detector, which can range from proteins/enzymes up to cells and microorganisms [75]. Biosensors of this type popularly make use of cantilevers that can transduce a chemical signal into a mechanical motion with high sensitivity. They provide a simple means for developing biosensors that are smaller, sensitive and lower at a cost [76]. The microcantilever based surface stress sensors have been successfully used to monitor different enzymatic detections in liquid environment [77].

The basis for detection is based on the fact that when the enzyme binds to the antibody on the surface of the cantilever, the chemical reaction between them creates a difference in surface stress that causes a deflection. Fritz et al., used two adjacent micromachined cantilevers to detect proteins [78]. Commercially available pipettes were used to functionalize the surface of these cantilevers with the corresponding enzymes. Chen et

al., used the AFM cantilevers to test biological samples and to detect their transient response [77]. He further comments that in liquid environments, the cantilever behavior is influenced by a large mass from the liquid. Binning et al., also investigated the behavior of AFM cantilevers under the influence of biological matter [39]. The liquid environment also considerably changes the mechanical response of the cantilevers [51]. Y. Arntz et al., demonstrated continuous label-free detection of two cardiac biomarker proteins using microcantilevers [33].

Biomarker proteins like Troponin's which are of increasing demand in the emergency departments were used for the detection of Acute Myocardial Infarction (AMI). They are a part of new generation of biochemical markers that provide an additional tool for assessment of the AMI. For medical applications, especially in an intensive care unit, it is desirable that many physiological parameters are monitored parallely and in real time. Detailed knowledge of these proteins levels would allow life saving treatments from AMI [31]. Method used in this work include the optical lever method for detection of these proteins on cantilever surfaces and monitor the deflection of the beam using a PSD and a laser source as shown in the Figure 3.1.

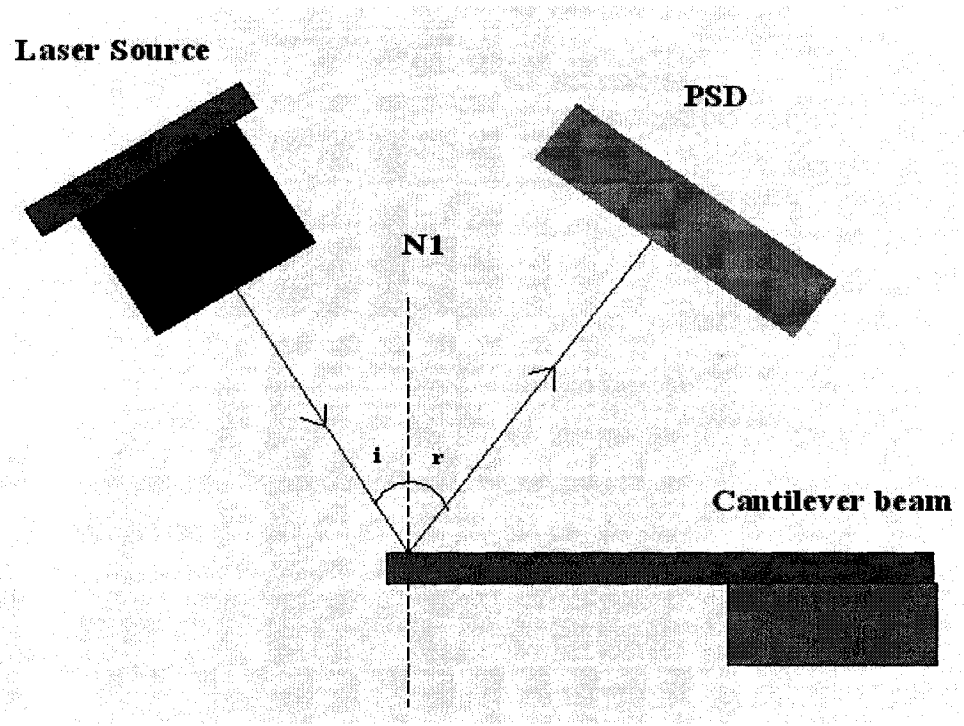

Figure 3.1: Schematic representation of the experimental set-up showing the position of laser source and PSD. N1 represents the normal, i and r represent the angle of incidence and reflection respectively.

The present chapter deals with PVDF cantilever beams of different lengths and widths whose behavior is been understood experimentally by functionalizing them with 2 set of proteins like Rabbit Skeletal Muscle Troponin C (TnC) and Honey Melittin Bee (ME) and Horse Raddish Peroxide (HRP) and Hydrogen Peroxide (H_2O_2). The cantilever deflection was monitored using a PSD. The behavior of the cantilever beams was also understood by functionalizing these enzymes on their surface under the influence of voltage. The voltage was kept at a constant 90 volts to do the testing as the touchdown voltage for the PVDF beams is around 110 volts and lesser voltages provide not much significant shift in time and deflection. The results obtained from the proteins were compared with that of TnC and water to show the variation in the results. Plots were obtained for deflection vs. time and deflection vs. concentration and compared with the

results in the literature [26] to evaluate the trend of the results. This experiment helps to characterize deflection and the results obtained here could well be useful in the development of a portable biosensor used for detection of AMI.

3.2 MATERIALS, EXPERIMENTAL SET-UP AND PROCEDURE

3.2.1 Materials and Chemicals used

The cantilevers were made of Poly Vinyl Dichloro Fluoride (PVDF) and cut into different sizes of $2.5\,mm$ x $0.8\,mm$ respectively. The thickness of 25 microns was constant for all the sizes. The SEM pictures of the cantilever beams can be seen in the Figures 3.2 and 3.3. Rabbit skeletal muscle Troponin C (TnC) which was used as enzyme was received from Life Diagnostics (USA). Honey bee Melittin (ME) which was used as an antibody was obtained from Sigma Aldrich (Canada).

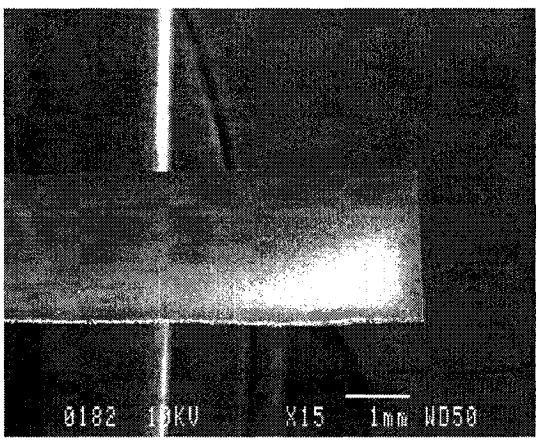

Figure 3.2: SEM image showing a PVDF cantilever

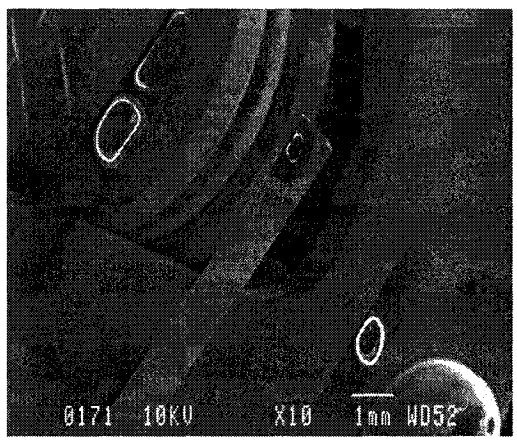

Figure 3.3: SEM image showing a PVDF cantilevers with enzymes deposited

Various concentrations of these proteins were made using a $50\,mM$ Potassium Chloride (KCl) and $50\,mM$ Tris-HCl at a pH of 7.5. The position sensitive detector (PSD) was obtained from Melles Griot (Canada). The enzymes were functionalized on the surface of the cantilever with the help of an electronic pipette purchased from Mandel Scientific (Canada).

A clear amber brown solution of Horse Raddish Peroxide (HRP) is obtained from 0.1mg per 1ml of 0.1M Potassium Phosphate (KH_2PO_4) with dilute Hydrochloric acid (HCL) to get a pH of 6.0 respectively. Hydrogen Peroxide (H_2O_2) was made of 30% by weight solution. The concentration of HRP used was 1% to the active ingredient in aqueous solution. 25mg/ml of HRP was used to react with H_2O_2. Both these chemicals were acquired from biochemistry laboratory of Concordia University.

A DC power supply ranging from 0-160V voltage and 0-2A current was used to vary the voltage, was obtained from Hewlett Packard (HP). Copper wire and stripes to provide the electrical connections was purchased from M-line accessories.

3.2.2 Experimental Set-up

Although bending of cantilevers can readily be determined by a number of means [78], this approach is focusing on the optical lever method. The experimental set-up is shown in Figure 3.4. The set-up makes use of a low power laser source of $1\,mW$ and a maximum wavelength of $632.8\,nm$ with a beam diameter at the focusing point of around 100 to

$200\,\mu m$, a spot-on Complimentary Metal Oxide Semi Conductor (CMOS) camera-the PSD with 3,50,000 pixels, wavelength sensitivity ranging from $350\,nm$ to $1100\,nm$. The

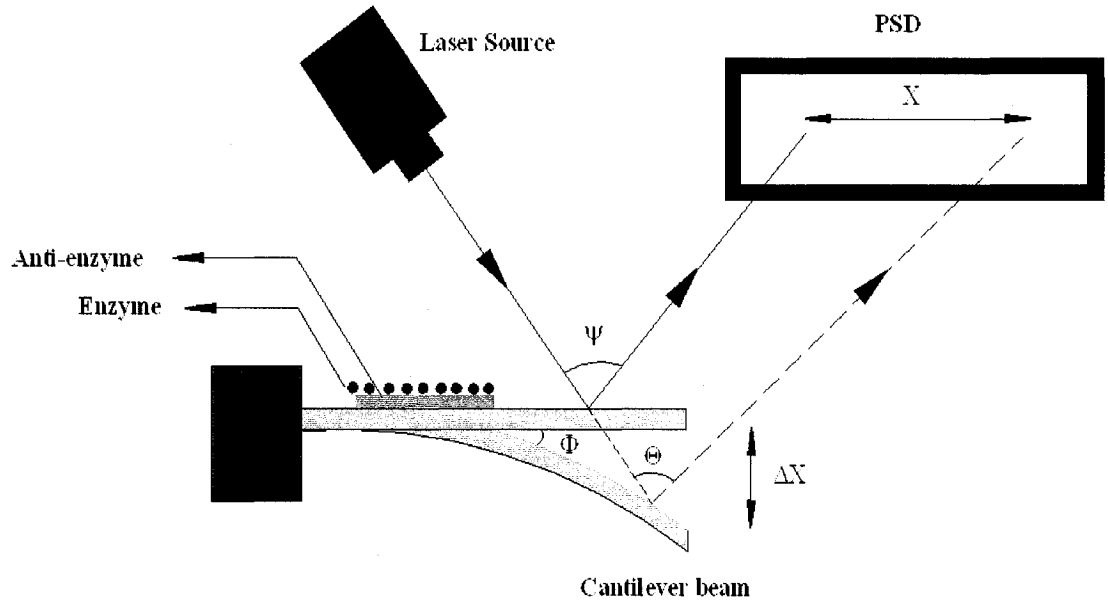

Figure 3.4: Schematic of the experimental set-up showing the bending of the cantilever under the action of the enzyme/anti-enzyme. The Position Sensitive Detector (PSD) is also shown.

position accuracy is less than $5\,\mu m$ with a sub micron resolution of less than $1\,\mu m$ which can accommodate a laser beam diameter from $100\,\mu m$ to $3\,mm$. The overall detector size is $4.7\,mm \times 3.4\,mm$ active area. PVDF coated aluminum beams of $2.5\,mm \times 0.8\,mm$ were used such that larger amount of reactants were deposited. The reactants were deposited using an electronic pipette that can take up a minimum volume of $0.2\,\mu l$ to a maximum volume of $2\,\mu l$. The error percentage was less that $0.012\,\mu l$. 2 broadband neutral density filters with 25% transmission at 633nm and an effective range from 400nm to 1100nm were used to get a focused spot of the laser.

Copper stripes were fixed on glass samples (one top and bottom) without making contact with each other. PVDF beams were glued on to the copper stripes. Copper wire was soldered to each contact to provide electrical connections with the bottom connection grounded.

3.2.3 Procedure

The experiment [67] was performed using a step by step procedure as follows:

1. PVDF beams of the required dimensions were cut and one of their edges was glued on a glass background in between 2 copper stripes. The glass was provided for support.
2. These glass supports were fixed on to xyz manual stage for fine adjustments of the specimen.
3. The laser source was set-up on V-grooves as an optical table such that the laser beam shines at angle on the top surface of the cantilever beam that is maintained in the horizontal position.
4. The PSD was trimmed and supported with a holder to receive the laser beam after reflected from the cantilever. The USB output of the PSD was connected to a PC.
5. ME, the antibody, is first deposited on the beam at a volume of $0.4\,\mu l$. This is followed by the deposition if TnC of the same volume. The timer is switched on before depositing the two proteins.
6. The PSD transmits the recorded x and y coordinate position of the cantilever beam and the data is stored in an excel file along side with time in seconds. A

total duration of 20 minutes was maintained for the entire reaction to take place with a time interval of 30 seconds. The sampling rate is thus 30 seconds while the sampling frequency is 0.0333 Hz. Similarly various concentrations of both the proteins were carried out and results obtained.

7. Special caution was taken with the proteins to keep them at low temperatures. They were refrigerated at -15° C.
8. TnC-ME was prepared using 50mM Tris HCL, 50mM KCl at pH of 7.5. Similarly HRP was prepared using 0.1M potassium phosphate with dilute HCl and -H_2O_2 was made of 30% by weight solution.
9. In order to compare the variation of two proteins, TnC was interacted with water to check for the deflection.
10. A similar approach was followed for both HRP and H_2O_2 as well.
11. A voltage of 90V was applied and the above methodology was repeated for both the enzymes and compared. The influence of the electrostatic field on the reaction signature was studied.

3.3 RESULTS AND DISCUSSION

3.3.1 Identification of Enzymatic Reaction for TnC-ME

The basic idea for increasing the dimensions of the cantilever beams is to deposit a reasonable amount of the enzymes on its surface and detect it. Additionally coating the micro-cantilevers with the enzymes only on one side was a great challenge. The pipette

used had a minimum volume of 0.2 μl which is about five times the volume of the AFM cantilever beam. Cantilever dimensions have effect on the performance of various sensors in liquid environment especially in the presence of enzymes. Earlier experiments were carried out using optical detection techniques on AFM cantilevers on a different set of enzymes [79]. However, for practical reason the size of the cantilever was selected in mm range such that the manipulation of the bio-materials to be performed easily with the available instruments. The present work strongly supports the previous results with more confidence [79, 80]. The TnC and ME proteins were mixed in a 1:1 proportions at different concentrations of 20mg/ml, 25mg/ml, 30mg/ml, 35mg/ml and 40mg/ml and applied over the PVDF cantilever beams.

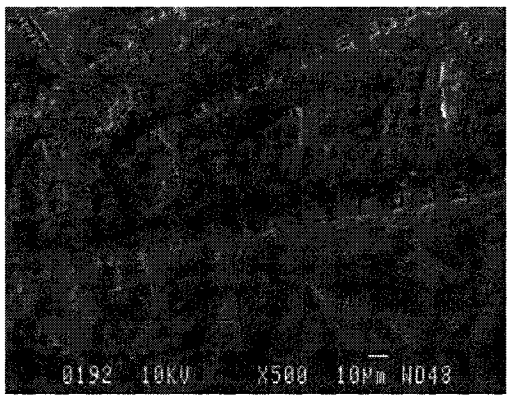

Figure 3.5: SEM image showing the surface of TnC on the cantilever after 2 weeks after deposition

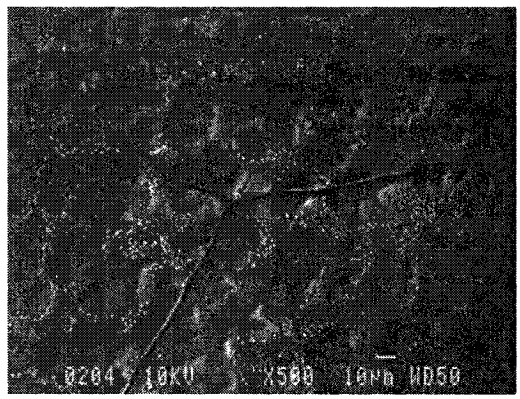

Figure 3.6: SEM image showing the surface of ME on the cantilever after 2 weeks after deposition

The concentration of Troponin is very low in the normal human serum (between 0 and 3.0 $\mu g / L$) but there is a large amount of Troponin in the myocardium, many times greater than the concentration of some other enzymes [81]. Therefore, the concentration of Troponin goes up to 158 times the discriminator in response to an AMI [82]. At the decisional concentration of 1 $\mu g / L$ for AMI, a good diagnostic efficiency with an

excellent clinical specificity could be made, even with patients for whom traditional biochemical markers of AMI are adversely influenced by diverse underlying clinical situations [82, 83]. Structural proteins are released into the circulation more slowly, but demonstrate elevations for longer periods of time. The actual life time of the circulating protein is relatively short; its prolonged diagnostic window is due to continued released from injured cells. The total amount of a marker protein released into the circulation as well as its rate of clearance may vary depending on the degree of reperfusion [83]. The reason to use high concentrations for the experiment was to understand the reaction much better on cantilever beams.

During the reaction between the enzyme and the anti-enzyme, the chains of enzyme molecules are opening followed by stretching such that it makes the cantilever beam to deflect [84]. This deflection is recorded using the PSD. Once the water in the buffer solution evaporates, the remaining solid phase on the beam arranges it self in a texture like configuration such that it will create a stress and therefore a strain in the cantilever. The SEM in the Figure 3.5 and 3.6 illustrates the structures of TnC and ME before reaction. The long chains in Figure 3.5 of the organic enzyme are observed being stretched and configured in a texture-like structure. TnC is a protein with a molecular weight of 18000 Daltons (1 Da = 1.660540 * 10^{-24} Kg) and about 70 Å long. It has an unusual dumbbell shape 75-Å-long molecule made up of two domains. The domains are connected through a nine-turn α helix, with no direct interaction between them [85]. On the other hand ME is a 26-residue membrane whose molecular weight is about 2850

Daltons obtained from the venom of honey bee. The SEM image in Figure 3.5 indicates the clusters of TnC are organized in uniform geometric structures in a branched form.

Bee venom melittin binds to skeletal muscle troponin C with a Ca^{2+}- dependant reaction. ME bound to troponin C irrespective of the presence or absence of Ca^{2+}in 50mM KCl and 50mM Tris-HCL at a pH of 7.5. The binding of TnC-ME mix is shown in the SEM picture after complete evaporation of the buffer solution. In order to explain the reaction between the two proteins Melittin is made to react with calmodulin because TnC resembles calmodulin (CaM) which forms a part of troponin complex, is another Ca^{2+} - binding protein, in both amino acid sequence and three dimensional structures [86]. The troponin C complex has four Ca^{2+} ions two with high affinity ($K_a = 10^7\ M^{-1}$) to the C-terminal domain of the molecule, and the other two with low affinity ($K_a = 10^5\ M^{-1}$) to the N-terminal domain [87].

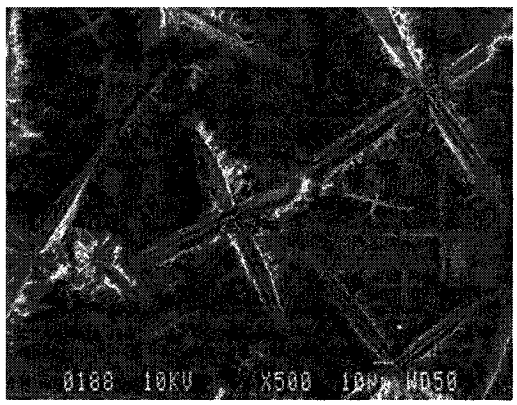

Figure 3.7: TnC-ME binding at 40mg/ml on the surface of cantilever. The SEM was taken after 2 weeks. The cross signs indicate the formation of ridges which tends to pull the surface inwards

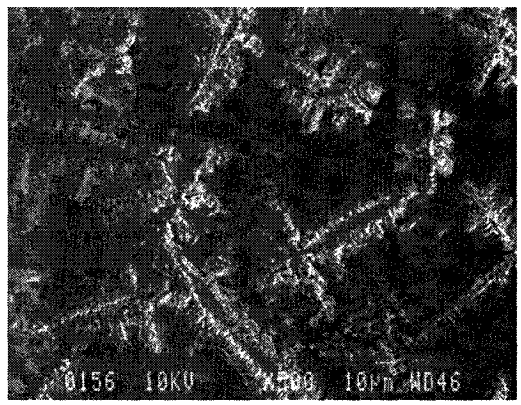

Figure 3.8: TnC-ME binding at 25mg/ml on the surface of cantilever. The SEM was taken after 2 weeks also has ridges protruding outward that pull the surface inwards

$$n\,Ca^{2+} + CaM \rightarrow CaM^{*}.Ca^{2+}{}_{n}$$

$$CaM^*.Ca^{2+}{}_n + E \rightarrow CaM^*.Ca^{2+}{}_n.E$$

The above reaction predicts that, upon binding of a certain number of Ca^{2+} ($1 \leq n \leq 4$); CaM undergoes a critical conformational change. The activated CaM* binds, then, to a target enzyme and modifies its activity. Blecher et al reported that when Ca^{2+} -saturated TnC bound to ME it assumed a significantly contracted structure compared to the free TnC-molecule [88]. That is, the dumbbell structure collapsed into a more globular structure. This can be clearly understood from Figures 3.7 and 3.8, where the molecules of both the proteins are attached to each other and the structure more or less collapsed. It can be concluded that the binding of calcium produces a conformational change which modulates the activity of other proteins. This is vital to the functioning of skeletal and cardiac muscles where formation of the complex triggers activation of contractile protein.

3.3.2 Identification of Enzymatic Reaction of HRP-H_2O_2

Further, another set of enzymatic reaction is analyzed in order to evaluate the uniqueness of the TnC-ME signature. Horse Raddish Peroxide (HRP) is a redox enzyme (biochemical catalyst) with approximately 40000 Da in size which catalyses the reduction of H_2O_2 into H_2O. It is a heme enzyme that is distributed in fungal, plant and mammalian organisms. These enzymes are involved in important physiological roles such as biosynthesis of hormones responses via the oxidation of various substrates at the expense of H_2O_2 [89]. The major advantage of using H_2O_2 as a substrate is its small activation volume [90] (ΔV=-1.5±0.5 ml/mol for peroxidase H_2O_2 and reaction) in determining the electrochemical potential and thus allowing a minimum volume reaction possible. Due to

these advantages H_2O_2 has been selected as a substrate for present study. SEM images of HRP and H_2O_2 are shown in Figure 3.9 and 3.10.

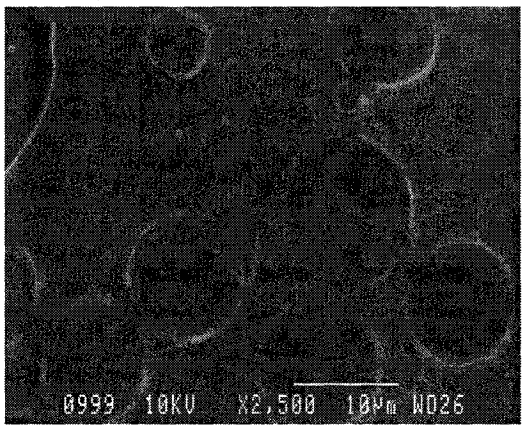

Figure 3.9: SEM image showing the surface of HRP on the cantilever after 24 hours. The holes in the surface are due to the presence of Fe^{4+} ions

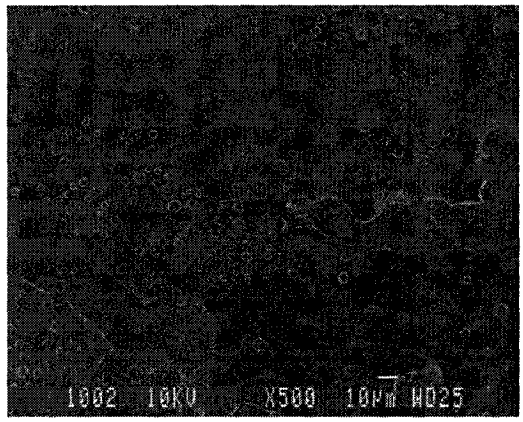

Figure 3.10: SEM image showing the surface of H_2O_2 on the cantilever after 24 hours. Bubbles on the surface indicates its slow decomposition to oxygen

HRP structurally resembles glycoprotein (a macromolecule composed of a protein and a carbohydrate and has a same molecular weight as HRP) with one mole of protohaemin. These enzymes exhibit different iso-forms and are generally isolated from the roots of horseradish. Stability of the enzyme is in the range of 5.00 to 10.00 pH and can withstand up to 50° C for at least 10 minutes. Kinetic analysis indicate that there are two kinetic influencing, ionizable groups on the enzyme with pKa (pH value corresponding to higher dissociation rate. The dissociation rate is the number of events the antibody- antigen react per unit time) of 3.2 and 3.9 [91].

When HRP comes into contact with selected substrate H_2O_2, it basically reduces the substrate. This spontaneous reaction can produce superoxide or the ROS (reactive oxygen

species) by the reduction of Hydrogen Peroxide. The major enzymatic reaction that contributes to transduction is

$$H_2O_2 \rightarrow H_2O + \frac{1}{2} O_2$$

Because of this H_2O_2 clings on to HRP and forms like a "cotton structure" as shown in the Figure 3.11 and 3.12. The property of HRP is such that it whenever it reacts with any

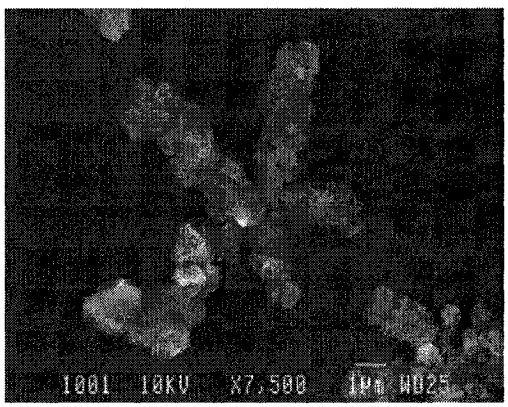

Figure 3.11: SEM image showing the surface of HRP-H_2O_2 after binding at 25mg/ml on the cantilever after 24 hours

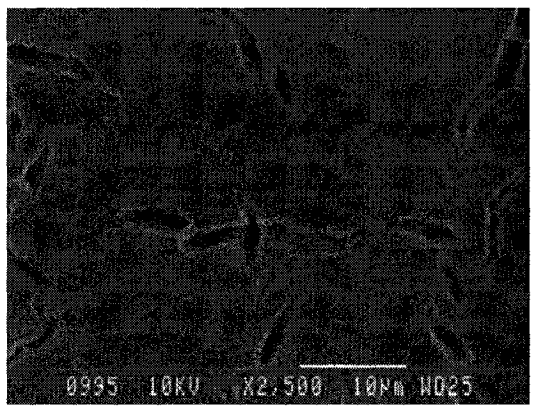

Figure 3.12: SEM image showing some cracks occurred on the surface of HRP-H_2O_2 at 25mg/ml due to molecular interaction

peroxides, it elucidates the effect of small increase in chain length while maintaining free carboxyl groups [92]. It can be concluded that hydrogen peroxidase catalyzed H_2O_2 reaction can thermodynamically yield results in a very wide pH ranges. The reaction between HRP and H_2O_2 results in the formation of a two-electron oxidized species known as compound I, which has a Fe^{4+} and a cation radical. This rapid formation of compound I oxidizes the substrate molecule like H_2O_2 [93]. This compound oxidizes a substrate molecule to become the next intermediate, compound II, which returns to the resting state by oxidizing another substrate molecule [94].

3.3.3 Comparison of Enzymatic Reaction between TnC-ME with and without Electric Field

Measurement of cantilever deflection was performed under the circumstances like temperature (~22°C) and humidity (55%) and for concentrations of TnC-ME ranging from 20mg/ml to 40mg/ml. The pattern of measurement regardless the concentration is always almost the same and is illustrated in Figure 3.13 and consists of a significant bound of the beam for about 2 minutes after about 12 minutes from the reaction. The displacement in μm at the PSD scanner in the vertical axis is given with respect to time in seconds in the horizontal axis. The Figure 3.13 indicates that the loading with the organic fluid solution of the beam will create a deflection of about 10 μm that is translated to the PSD in a negative (downward) displacement of the laser spot by 400 μm. Further reactions will stretch the beam more due to configuration of the enzyme molecules on the surface of the cantilever. The reactions count for 5 to 6 more μm of deflection at the

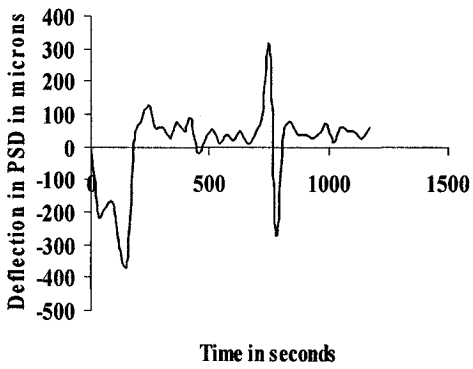

Figure 3.13: PSD reading of cantilever deflection for 20mg/ml TnC-ME at 0.4 μl

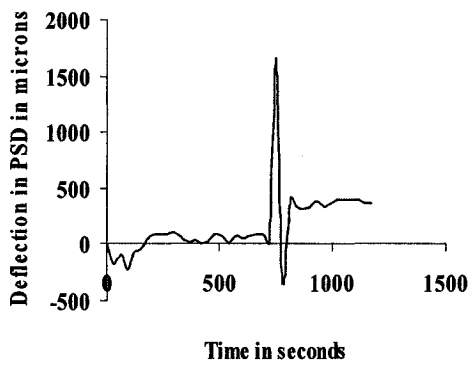

Figure 3.14: PSD reading of cantilever deflection for 40mg/ml TnC-ME at 0.4 μl

cantilever which occur about one minute. The time duration is not quite relevant since the volumes used in the experiments were quite large. However, the displacements of 5 to 6 μm may be very easily detected in a microstructure [84]. Further, the beam starts moving up by 27 μm with respect to the lowest previous occupied position. This motion is slow at a rate of about 1 μm per second. This curving up is associated to the adhesion of the enzymes molecules on the surface of the cantilevers which phenomenon produces a tension in the bottom surface of the beam. A long duration of about 500 seconds, almost steady condition occurs before an up, down and again up of 25 μm jolt is seen in the PSD, followed by a steady state as same as the initial condition. The approach for the preferential immobilization of active antibodies onto one side of the cantilever shows great promise for the development biosensors that could also detect differential stress changes upon the reaction with the appropriate antigen.

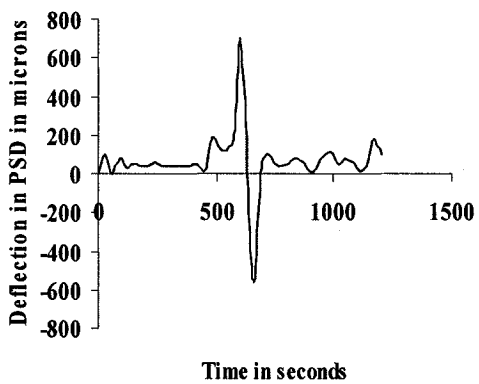

Figure 2.7: PSD reading of cantilever deflection for 25mg/ml TnC-ME at 0.4 μl at 0 volts. From chapter 2.

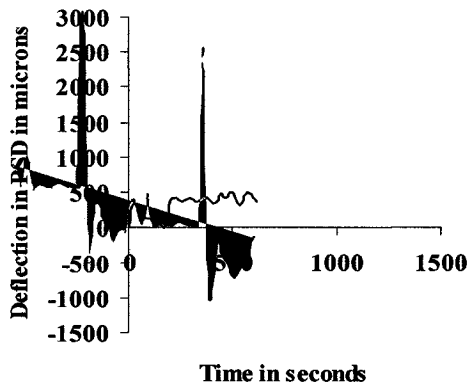

Figure 3.15: PSD reading of cantilever deflection for 25mg/ml TnC-ME at 0.4 μl at 90 volts

Figures 2.7 (taken from chapter 2) and 3.15 indicate the interaction between the two proteins at 25mg/ml with and without the application of voltage. The pattern remains the

same more or less for all the concentrations. Further, due to the application of 90 volts the deflection increases to 2600 μm on the PSD and moves downwards to about -1000 μm in the negative y-direction followed by a steady state as same as the initial condition. From the two plots one can clearly see a difference of 250 seconds along the x-axis and 250 μm deflection along the y-direction. From here we conclude that the electrical potential might acts as a catalyst to the chemical reaction between the two proteins.

This signature of TnC-ME reaction was compared with that of TnC-water of different concentrations. Significant differences were recorded in the pattern of displacement and amplitude. The patterns are presented in Figures 3.16 and 2.1 respectively. Similar trend in the signature was found at different concentrations. From the experimental set-up it was noticed that there was a time-dependant drift present in the deflection signal and the drift in the measured signal depended almost linearly on time.

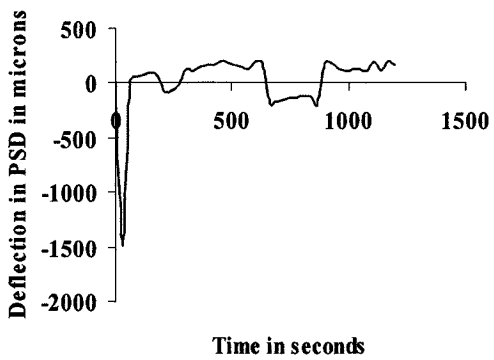

Figure 3.16: PSD reading of cantilever deflection for 20mg/ml TnC-Water at 0.4 μl

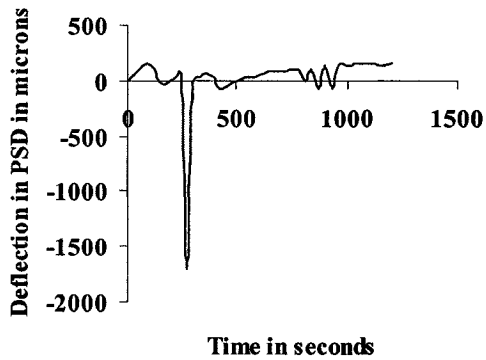

Figure 2.1: PSD reading of cantilever deflection for 40mg/ml TnC-Water at 0.4 μl . From chapter 2.

In order to understand this downward displacement pattern in the plots, a calibration was done on the optical system .The set-up was arranged as earlier with the laser spot

focusing on the cantilever and its image clearly absorbed by the PSD and seen on the computer. By adding load (a droplet of water in this case) the movement of the laser spot on the computer was monitored. It was noticed that if the cantilever moves downwards (due to the load) the spot also moves upward. After the drop dries, the spot comes back to the original position and moves downwards to some distance and rests there. But in the case of a reaction the spot moves well upwards, which means the cantilever moves downwards in the negative direction and then moves well up. This explanation may be used to describe the downward movement of the curves in the plots.

Further curiosity in confirming the signature reaction for TnC-ME, the individual signatures for TnC and ME are shown in plots 3.17 and 3.18 respectively. Both the

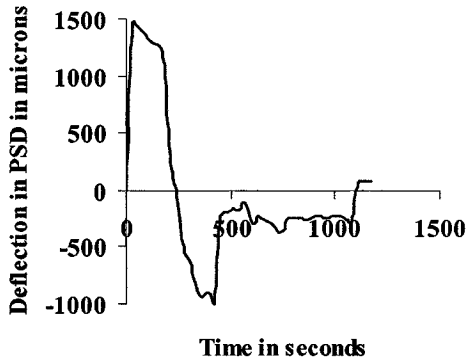

Figure 3.17: PSD reading of cantilever deflection for 25mg/ml TnC at 0.4 μl

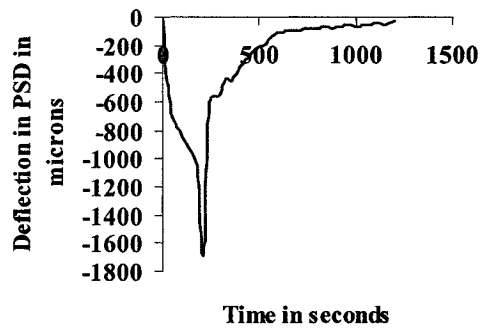

Figure 3.18: PSD reading of cantilever deflection for 25mg/ml ME at 0.4 μl

individual proteins have different signatures at the same concentration. In the case of TnC, the cantilever beam moves down due to the load and then moves a little up. This could be due to the fact that the water could have started to dry up due to the laser intensity leaving the TnC molecules behind to stick onto the surface of the cantilever that could pull the surface inwards. But in the case of ME the signature is quite similar to that

of water. The molecular weight of ME is quite less than TnC and hence even it could one of the reasons for a different signature as shown in the Figure 3.18.

3.3.4 Comparison of PSD deflection of the Cantilever with Concentration of Enzymes and the Time taken for the Reaction

As the concentration (mass) increases deflection also increases linearly as shown in Figure 3.19. The final deflection of the microcantilever as a function of the concentration of TnC-ME is plotted. The measured deflection of the microcantilever exhibits a linear

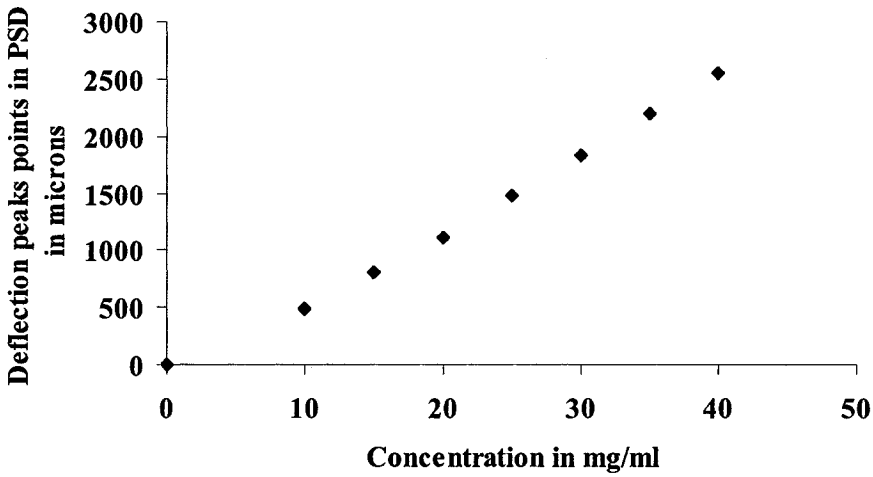

Figure 3.19: Plot showing the deflection peak points in PSD for TnC-ME interaction with respect to concentration in mg/ml

dependence on the concentration of TnC-ME. It can be seen that the PVDF cantilevers responds very sensitively to the presence of TnC-ME in the concentrations range of 20mg/ml. Given the above findings, a comparison was made for the deflection with respect to time in order to find the sensitivity of PVDF cantilevers to the presence of TnC-ME as these molecules adsorb on the PVDF surface forming chain of molecules

[26]. The time t=0 corresponds to the time when 0.4 μl of TnC and 0.4 μl of ME was deposited on the cantilever surface at room temperature. The PVDF cantilever exhibited a deflection of ~ 2500 μm at time t=1100. As seen in the Figure 3.20, the deflection rate becomes constant at t=900 when the liquid phase in TnC-ME evaporate completely from the surface of the cantilever. This duration is much dependant on the environment conditions. The data presented in this figure demonstrates both the high sensitivity and large dynamic range of PVDF cantilevers to TnC-ME reaction.

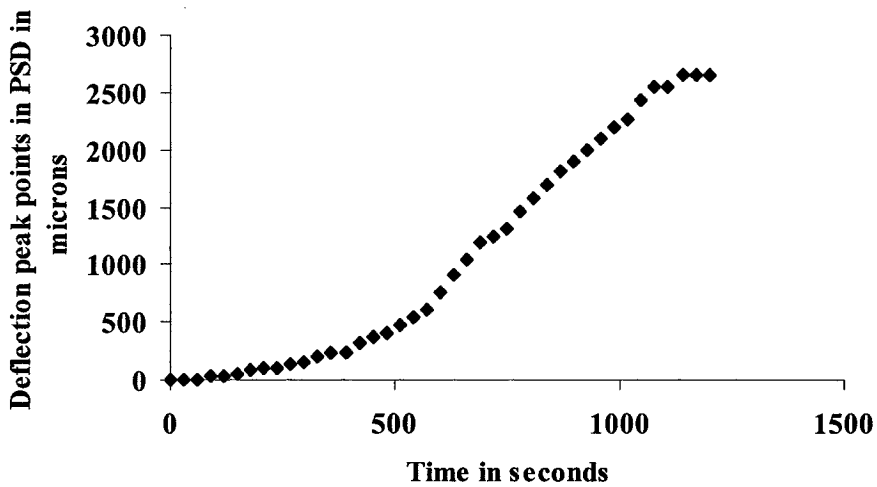

Figure 3.20: Plots showing the deflection peak points in PSD for TnC-ME interaction at various concentrations with respect to time

3.3.5 Comparison of Enzymatic Reaction between HRP-H_2O_2 with and without Electric Field

A similar approach was adopted in the case of HRP-H_2O_2 interaction. 0.4 μl of H_2O_2 was deposited on the cantilever surface at 0 voltage followed by HRP. Figure 2.8 indicate that there is a recorded PSD reading of 1450 μm when no voltage is applied to the device. The initial two peaks of 300 μm and 480 μm are due to the load of deposition of the two

proteins. After the huge peak of 1450 μm is recorded, there is a steady state up till the end of 20 minutes indicating that the reaction between the two proteins has taken place. The reaction between HRP-H_2O_2 takes lesser time and smaller deflection when compared to

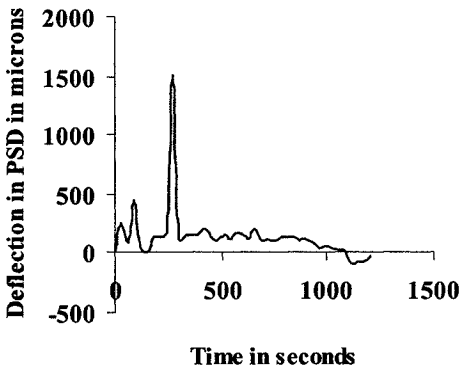

Figure 2.8: PSD reading of cantilever deflection for 25mg/ml of HRP-H_2O_2 at 0.4 μl at 0 volts

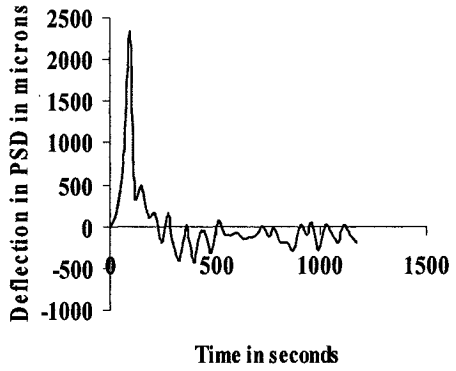

Figure 3.21: PSD reading of cantilever deflection for 25mg/ml of HRP-H_2O_2 at 0.4 μl at 90 volts

that of TnC-ME. That might be due to the reason that HRP reduces its substrate H_2O_2 in the even of an instantaneous reaction. The reaction between HRP and H_2O_2 at room temperature takes place rapidly, which indicates the presence of compound I as mentioned earlier in this chapter. But in the case of TnC-ME, ME interacts with the Ca^{2+} ions of TnC which in turn converts the shape of TnC into a dumbbell shape which is assumed to be time consuming. Application of the voltage hastens the reaction even further with a higher jump of 2450 μm in the PSD reading. But there is no steady state up till the 20^{th} minute as seen in Figure 3.21. This could be assumed to be due to the voltage applied. Clearly the above two plots show a difference in deflection in the PSD reading which is about 1000 μm and also a difference in time of about 300 seconds.

Although, in the present experiments an optical detection system is used, the deflection of a cantilever can be measured using capacitive, piezoresistive, or piezoelectric detection methods. These detection systems have some advantage over optical detection system such as elimination of optical set-up and alignment, and compactness [95].

The bending of a microcantilever is extremely sensitive to the adsorption of biomolecules on the surface and the results show that monitoring of the bending as analytes adsorb on the microcantilever surface can provide powerful bio-analytical tool in the development of a biosensor. In the present experiments immobilization of the antibody and antigen have been only on one side of the cantilever. This is done to get an optimal transducer response with only one side of the cantilever, reacting as a sensing surface, thus optimizing the change in surface stress. The cantilever response is quantitative (concentration of the analyte proteins) and qualitative (multiple proteins). Proteins are been detected in real time in less than 10 minutes.

3.4 SUMMARY

In recent years micro-cantilever beams have become important structures that have found usage in diverse applications as sensors and actuators especially in biomedical applications. Identification and quantitative analysis of biological molecules are critical in disease detection and monitoring of health associated problems. The bending of a micro-cantilever is very sensitive to changes in the environment of the cantilever and, more interesting, to changes at the surface of the cantilever. This can be used to detect changes upon structural changes in the layer of surface adsorption. This will lead to a new, fascinating bio-analytical tool which will give dynamic structural information about the bio-enzymes on the surface. However, a biosensor in the classical sense should detect unknown biomolecules in the liquid phase. Generally the bending process associated with biological reactions in the cantilever beam are quite complicated and often not completely understood. So, it is quite impossible to build accurate models while measurements are always a probability and large variance. Another problem of the bending compared to frequency measurements is that they are prone to disturbances of the environment like temperature and vibrations.

In the present chapter, experiments were conducted to show the enzymatic reactions between Troponin C and Melittin Bee and Horse Raddish Peroxide (HRP) and Hydrogen Peroxide (H_2O_2) on PVDF coated cantilevers with and without the application of voltage. A novel protein assay for a biomedical environment was developed. Real-time protein detection is been demonstrated. The ability to measure specific signals in a background

reflects the reliability and specificity of cantilever array sensors. The optical set-up was arranged so as to identify the enzymatic reactions on the surface of the cantilever of different length by monitoring a change in their deflection. The carried out work was compared to that done previously using different enzymes on microcantilevers. The use of Troponin C as an antigen and Melittin Bee as an antibody were seen to have enhanced the deflection of the cantilever beam. The fact that the immobilized antibodies are active was confirmed by their ability to bind to the appropriate antigens. The SEM images of TnC-ME and HRP-H_2O_2 reactions showed that the anti-enzymes were predominantly bound to the enzymes and formed different patterns over the entire coating. This method is able to detect enzymes involved in the diagnosis of myocardial infarction. Continuous monitoring of biochemical markers will allow the earliest possible biochemical diagnosis of myocardial infarction. Shortening the time to treatment as well as reducing the time to exclusion of infarction in this deadly disease has the potential of minimizing the risk for the patient.

The bending of the cantilever is very sensitive to changes in the environment. This will lead to a new, and promising bio-analytical tool which will give dynamic structural information about known biomolecule. Often bending occurrences cannot be explained in full detail, and therefore it is nearly impossible to make quantitative analysis. Another problem of the bending compared to frequency measurements is that they are very prone to disturbances of the environment like temperature changes or vibrations. In spite of these problems results provided in the chapter could be useful in giving information towards the development of a biosensor that could detect AMI. The combination of

results obtained gives important information on the operational characteristics of the biosensor and for future working of the sensor.

CHAPTER 4

ENZYMATIC DETECTION THROUGH STANDARD PHYSICAL PROCEDURES

4.1 INTRODUCTION

The work presented in the previous chapter indicates that a bio reaction might produce a mechanical effect on a micro-cantilever beam. However, there is no evidence that indeed, the reaction occurs at the specific time. The objective of the present chapter is to investigate through standard physical means the signature of the bio reaction of TnC-ME and HRP-H_2O_2 using other means of detection such as Fourier Transform Infrared Spectrometer (FTIR), Fluorescence Spectrometer (FS) and Mass Spectrometer (MS). These methods have advantages like less electric noise, being compatible with use under liquid and lack of contact to the sensing element [98]. These procedures are currently used in microbiology labs to assess the reaction among various bio-molecules.

4.2 FOURIER TRANSFORM INFRARED SPECTROMETER (FTIR)

4.2.1 Introduction to FTIR

4.2.1.1 Definition

Infrared (IR) spectroscopy is a chemical analytical technique, which measures the infrared intensity versus wavelength (wavenumber) of light. Based upon the wavenumber, infrared light can be categorized as far infrared (4 ~ 400 cms^{-1}), mid infrared (400 ~ 4000 cms^{-1}) and near infrared (4000 ~ 14000 cms^{-1}).

Infrared (IR) spectroscopy detects the vibration characteristics of chemical functional group in a sample. When an infrared light interacts with the matter, chemical bonds will stretch, contract and bend. As a result, a chemical function group tends to adsorb IR radiation in a specific wavenumber range regardless of the structure of the rest of the molecule. For example, the C=O stretch of a carbonyl group appears at around 1700cms^{-1} in a variety of molecules [99]. Hence the correlation of the band wavenumber position with the chemical structure is used to identify a functional group in a sample. The wavenumber positions where functional groups adsorb are consistent, despite the parts of the molecules. Thus the presence of specific functional groups can be monitored by these types of infrared bands, which are called as group wavenumbers.

4.2.1.2 Principle of FTIR

A FTIR obtains IR spectra by first collecting an interferogram of sample signal with an interferometer, which measures all of IR frequencies simultaneously. A FTIR acquires and digitizes the interferogram, performs the Fourier transform (FT) function and outputs the spectrum. An interferometer utilizes a beam splitter to divide the incoming IR beam into 2 optical beams. One beam reflects off a flat mirror which is fixed in place. Another beam reflects off a flat mirror which travels a very short distance (a few mm) away from the beam splitter. The 2 beams reflect off their respective mirrors and are recombined when they meet together at the beam splitter. The recombined signal results from the "interfering" with each other. Consequently, the resulting signal is called the interferogram, which has every IR frequency "encoded" into it. When the interferogram

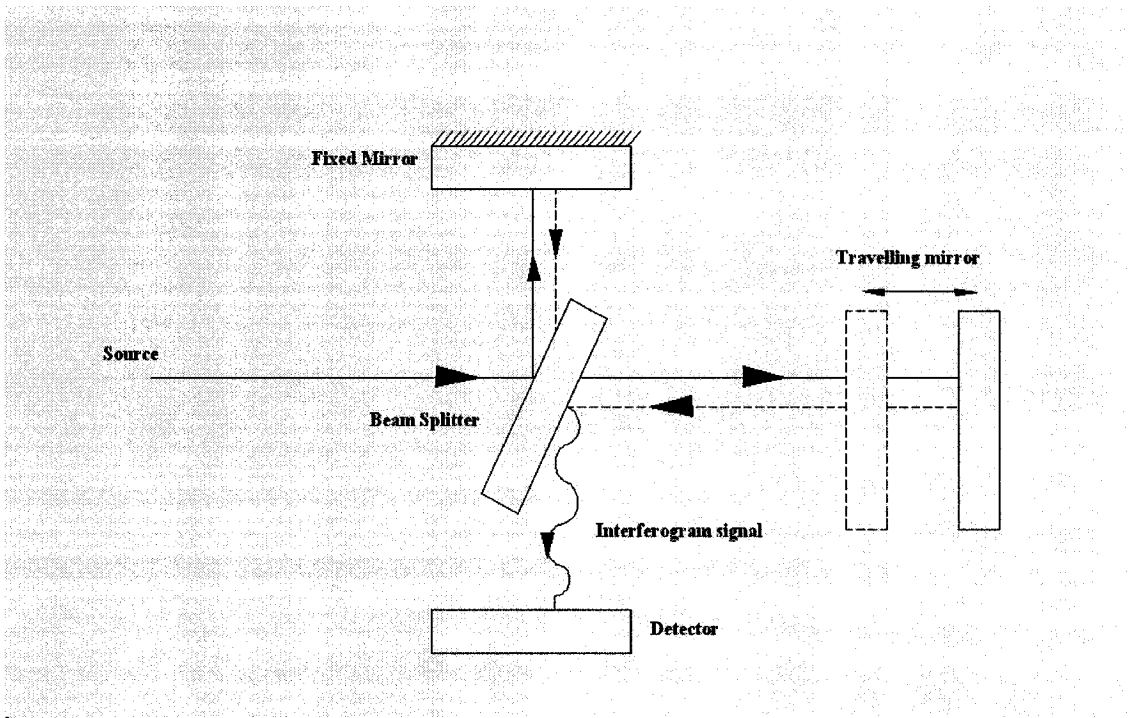

Figure 4.1: Principle of the Fourier Transform Infrared Spectrometer (FTIR)

signal is transmitted through or reflected off the sample surface, the specific frequencies of energy are adsorbed by the specimen due to the excited vibration of the functional groups in molecules. The IR signal after interaction with the sample is uniquely characteristic of the sample. The beam finally arrives at the detector and is measured by the detector as shown in Figure 4.1. The detected interferogram cannot be directly interpreted. It has to be "decoded" with a well-known mathematical technique in terms of Fourier transform (FT). The computer can perform the FT calculation and present an IR spectrum, which plots absorbance (or transmittance) versus wavenumber.

When an interferogram is Fourier transformed, a single beam spectrum is generated. A single beam spectrum is a plot of raw detector response versus wavenumber. A single beam spectrum obtained without a sample is called a background spectrum, which is induced by the instruments and environments.

4.3 FLUORESCENCE SPECTROSCOPY

4.3.1 Introduction to Fluorescence Spectrometer (FS)

4.3.1.1 Definition

Fluorescence spectroscopy (FS) or fluorometry is a type of electromagnetic spectroscopy used for analyzing fluorescent spectra. It involves using a beam of light, usually ultraviolet light, that excites the electrons in molecules of certain compounds and causes

them to emit light of a lower energy, typically, but not necessarily, visible light. The main advantage of fluorescence detection compared to absorption measurements is the greater sensitivity achievable because the fluorescence signal has a very low background. The resonant excitation provides selective excitation of the analyte to avoid interferences. A hollow-cathode lamp or laser provides the resonant excitation to promote the atoms to higher energy levels.

4.3.1.2 Principle of Spectroscopy

Molecules have various states referred to as energy levels. Fluorescence Spectroscopy (FS) is primarily concerned with electronic states and vibrational states. Generally, the species being examined will have a ground electronic state (a low energy state) of interest, and an excited state of higher energy. Each of these electronic states has vibrational states.

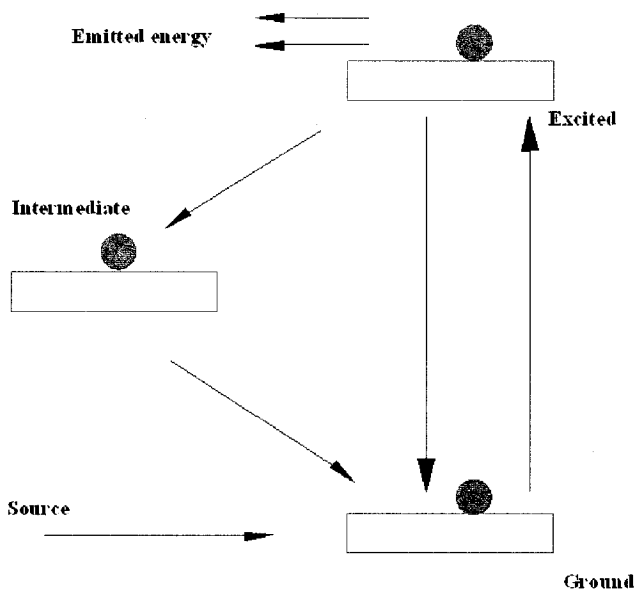

Figure 4.2: Excitation of an electron in a molecule to a higher state when a photon of energy is absorbed by the electron in the ground state.

Photons of light are small "packets" of energy, each of which are energy proportional to its frequency; photons of high frequency light have higher energy than those of low frequency light. These can be absorbed by molecules, with the molecules gaining the energy of the photon, or emitted by molecules, with the photon carrying source of energy of the molecule away.

In Fluorescence Spectroscopy (FS), the species is first excited, by absorbing a photon of light, from its ground electronic state (10^{-9} seconds) to one of its various vibrational states in the excited electronic state (10^{-15} seconds). Collision with other molecules cause the excited molecule to lose vibrational energy until it reaches the lowest state of the excited electronic state (10^{-12} seconds) as shown in Figure 4.2.

The molecule then drops down to the various vibrational levels of the ground electronic state again, emitting a photon in the process. As molecules may drop down into any of the vibrational levels of this ground state, the photons will have different energies, and thus frequencies. Therefore, by analyzing the different frequencies of light emitted in Fluorescence Spectrometer (FS), the structure of these different vibrational levels can be determined.

4.4 MASS SPECTROSCOPY (MS)

4.4.1 Introduction to Mass Spectrometer (MS)

4.4.1.1 Definition

A mass spectrometer (MS) is an analytical tool for measuring the molecular weight (MW) of a sample. For large samples such as biomolecules, molecular weight (MW) can be measured to within an accuracy of 0.01% of the total molecular weight (MW) of the sample. For smaller organic molecules the molecular weight (MW) can be measured to within an accuracy of 5 ppm, which is often sufficient to confirm the molecular formula of a compound. The physics behind Mass spectrometer (MS) is that a charged particle passing through a magnetic field is deflected along a circular path on a radius that is proportional to the mass to charge ratio (m/e).

4.4.1.2 Principle of a Mass Spectrometer (MS)

A very low concentration of sample molecules are allowed to leak into the ionization chamber (which is under a very high vacuum) where they are bombarded by a high-energy electron beam. The molecule fragments and the positive ions produced are accelerated through a charged array into an analyzing tube. The path of the charged molecules is bent by an applied magnetic field. Ions having low mass (low momentum) will be deflected mostly by this field and will collide with the walls of the analyzer.

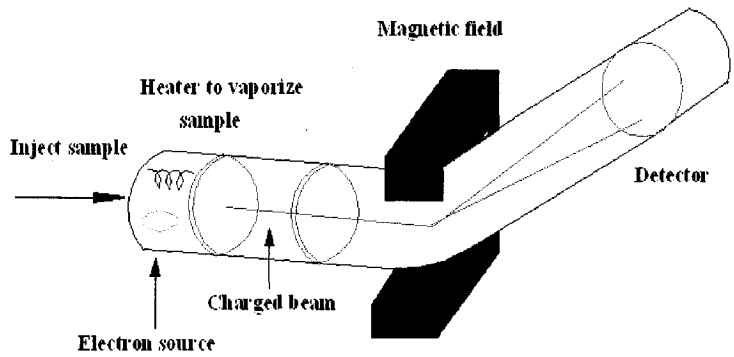

Figure 4.3: Principle of a Mass Spectrometer (MS) in which the charged beam is split into 2 by a magnetic field depending on their mass-to-charge ratio (m/e)

Likewise, high momentum ions will not be deflected enough and will also collide with the analyzer wall. Ions having the proper mass-to-charge (m/e) ratio, however, will follow the path of the analyzer, exit through the slit and collide with the collector as shown in Figure in 4.3. This generates an electric current, which is then amplified and detected. By varying the strength of the magnetic field, the mass-to-charge (m/e) ratio which is analyzed can be continuously varied.

The output of the mass spectrometer (MS) shows a plot of relative intensity vs the mass-to-charge (m/e) ratio. The most intense peak is termed as the base-peak and all others are reported relative to its intensity.

4.5 Experimental set-up and Procedures for Optical Techniques

4.5.1 Experimental set-up for FTIR

The Perkin Elmer model 16 PC spectrophotometer as shown in Figure 4.4 is provided with a rapid data acquisition over a total range of 7800 to 100 cm^{-1} (wavelength number), with better than 2 cm^{-1} resolution, and good signal-to-noise was used. The system includes a helium-neon laser of 633nm wavelength with power less than 0.3mW. 22*22mm glass samples were used to perform tests with enzymes like TnC-ME, HRP-

Figure 4.4: Experimental test set-up for FTIR

H_2O_2 and pure water were to observe the variation in transmittance and absorption spectrums respectively.

4.5.1.1 Preparation of HRP-H_2O_2 Sample from Buffer Solution

4.5.1.1.1 Preparation of Buffer

Potassium phosphate, dibasic (K_2HPO_4) is a white powder in appearance whose molecular weight is 174.18 gram per mol is placed in a weighing pan. 0.5 liters of water is taken in a beaker. By taking the product of the molecular weight of potassium phosphate and weight of water we get the actual weight of the buffer to be added to HRP (8.71 g). A slightly hazy colorless solution is obtained. The buffer is diluted with strong hydrochloric acid (HCL) in order to get a pH of 6.0. To check for the pH, a pH tester is used.

4.4.1.1.2 Procedure for Preparation of Horse Radish Peroxide (HRP) along with Potassium Phosphate, Dibasic:

The solid HRP is taken in a pan and weighed in physical balance and placed in small test tubes. The buffer solution is added to HRP to get a liquid solution of the enzyme with a pH of 6.0. A clear amber brown solution of HRP is obtained at 10mg per 1ml of 0.1M potassium phosphate. 250 to 330 units* per mg solid HRP is added to the buffer to get enzymatic activity. (*One unit will form 1.0 mg purpurogallin from pyrogallol in 20 sec at pH 6.0 at 20°C).

4.4.1.2 Experimental Procedure for FTIR

1. 22*22 mm square glass samples are taken and cleaned with acetone and water. They are dried using nitrogen gas.
2. Two glass specimens were taken together and placed inside a square hole made in a substrate to place there in the FTIR analyzer.

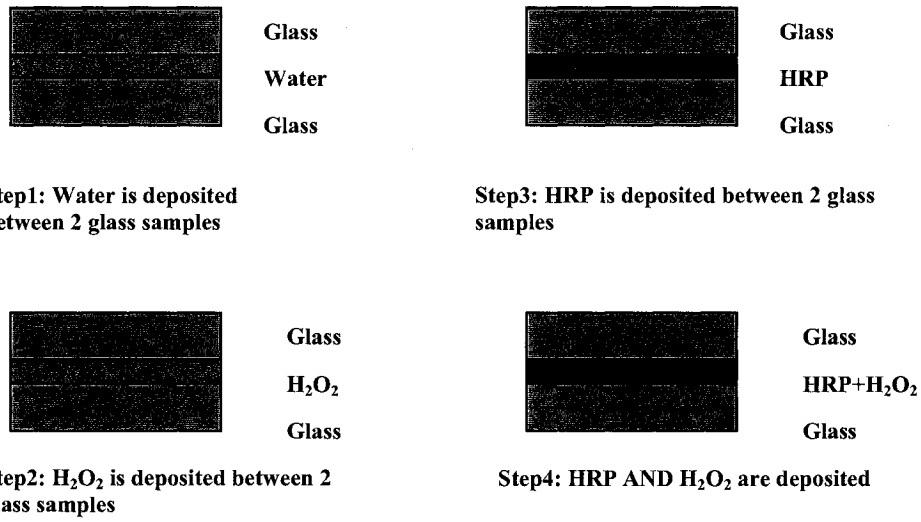

Figure 4.5: Experimental steps for FTIR which makes use of HRP-H_2O_2 and water sandwiched between two glass samples

3. The two glass samples are first scanned together to get a background spectrum. (The first spectrum that is acquired after start-up must be a background. They are placed in the background memory region of the instrument. Subsequent sample spectra are ratioed to the background)
4. The glass samples are now scanned to get a sample, so that a straight line is obtained on the screen. This is to make sure that there is no noise occurring while scanning the samples.

5. Pure water is deposited in between the glass samples as shown in Figure 4.5 and checked for scanning. The output is recorded in the computer.
6. Dry the samples with nitrogen gas and deposit hydrogen peroxide (H_2O_2) on its surface and scanned.
7. The samples are washed with water and acetone and dried with N_2 gas.
8. The horse radish peroxide is deposited on the samples and checked for scanning and the results are recorded.
9. The specimens are washed as done before and the mix of H_2O_2 and HRP are depo--sited together on the samples are scanned and results are recorded.
10. Similar tests were done for TnC-ME at a different concentration.

4.5.2 Experimental set-up for Fluorescence Spectroscopy (FS)

The equipment used in this study to determine the enzymatic reactions between TnC and ME was fluorescence spectrometer purchased from AMINCO Bowman series 2, U.S.A, as shown in Figure 4.6. The spectrofluorometer has a range of 220-850 nm range, Xenon source, excitation and emission wavelength scans, spectral bandwidth 1-16 nm and a Photomultiplier tube (PMT) detector. It has a scan rate of 3-6000 nm/min. It also includes a grating monochromatic. A 50 mm cylindrical IR quartz cuvette, constructed of high-purity infrared (IR) quartz with minimal OH content was used. They provide a maximum sampling versatility for transmission studies from the near infrared to 2500 cm^{-1}. The above equipment was used at biochemistry laboratory at CONCORDIA University Loyola campus.

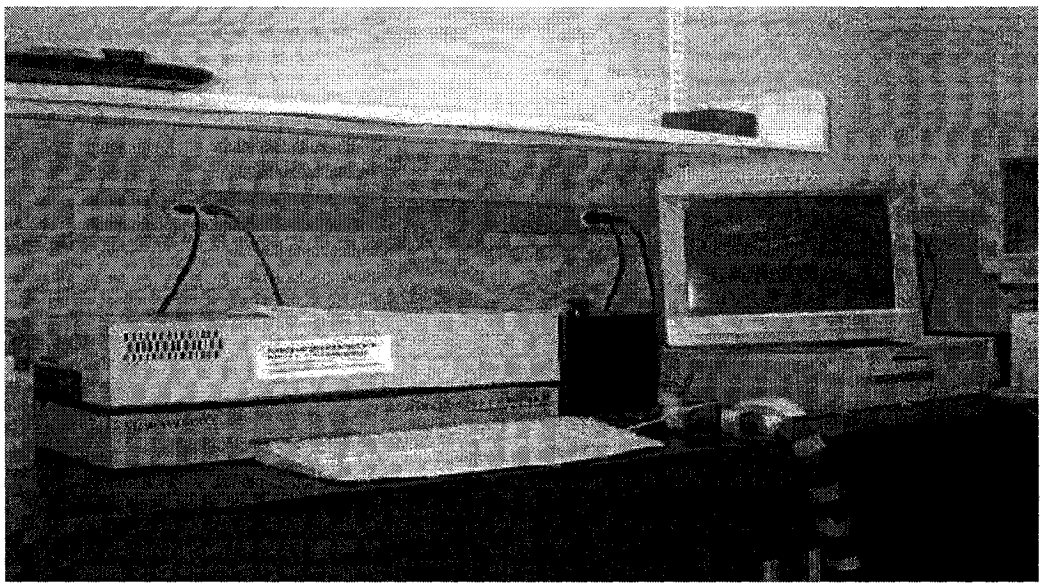

Figure 4.6: Shows the luminescence spectrometer from AMINCO Bowman series II, with 120 volts in the biochemistry laboratory at Loyola campus

Different concentration ratios of both TnC and ME were tried at an excitation voltage with a wavelength of 350 nm, speed rate of 2 nm/sec and a voltage of 740 volts. Initially 5μM concentrations of TnC (mixed with buffer) were taken in the quartz cuvette and the spectrum obtained. Similarly, a fluorescence spectrum was obtained for 5μM of ME (mixed with buffer). At a ratio of 1:1, both TnC and ME were mixed in the quartz cuvette. The fluorescence spectrum was obtained for the mixture. Fluorescence for the buffer solution alone was also taken to check for the variation in enzymes. The above procedure was repeated for different ratios like 10μM of ME with 1μM TnC and 10μM ME with 6μM TnC respectively.

4.5.2.1 Experimental Procedure for Fluorescence Spectroscopy (FS)

4.5.2.1.1 Preparation of TnC and ME with the Buffer Solution

Rabbit skeletal muscle Troponin C (TnC) was prepared in a buffer comprising of 0.5 M Tris, 0.5 M KCl at a pH of 7.5. 30.3 grams of Tris and 18.64 grams of KCl was prepared (M1 = C * V * MW) and mixed with 400ml of distilled water. The solution is titrated with 10M HCl to get a pH of 7.5 respectively. Stock troponin C (TnC) concentration obtained from the supplier (Life Diagnostics, Inc, U.S.A) 12.25 mg per ml is mixed with the buffer to get concentrations of around $2\,\mu M$, $20\,\mu M$ and $200\,\mu M$ with a total volume of $14.7\,\mu l$ respectively.

$100\,\mu g$ of ME was obtained from Sigma Aldrich, Canada. ME concentration was determined using a molar coefficient of 5470 M^{-1}. cm^{-1} at an absorbance value of 280 nm [55]. The absorbance value at 280 nm was determined using a Fluorescence spectrometer. The measurement is carried in a quartz cuvette since the wavelength of interest is expected at an absorbance of 280 UV range (plastics absorb in this range, while quartz does not). The absorbance value was found out to be 0.00761. The path length was assumed to be 1 cm. The path length is the distance between the laser source to quartz cuvette. To evaluate the concentration of melittin we have;

$$A1 = \nu * g * C$$

Where, A1 = absorbance value

ν = extinction coefficient or molar absorptivity

g = path length

C = concentration of melittin

To measure optical density (OD) or absorbance, add 120 μL (the lowest amount that yields a signal) into 1980 μL (for example) of the buffer. This gives a total volume of 2100 μL. To find the dilute factor one has; Dilute factor = final volume/volume of initial sample added

= 2100/120 = 17.5

$C = A1/\nu g = (0.00761)/ (5470\ M^{-1}.\ cm^{-1} * 1\ cm)$

$C = 1.39 * 10^{-6}\ M = 1.39\ \mu M$

Stock C = 1.39 * 17.5 = 24.32 μM

4.6 RESULTS

4.6.1 Identification of Enzymatic Reaction using the FTIR

The spectrum is plotted for wavenumber along the x axis and percentage transmittance along the y axis. Transmittance is given as the ratio of intensity of the beam before hitting the sample to the intensity of the beam after leaving the sample. Percentage transmittance is measured as how a particular frequency gets through the compound. Figure 4.7 shows the spectrum of glass on the addition of water, Horseradish Peroxidase (HRP), Hydrogen Peroxide (H_2O_2) and antigen-antibody (HRP-H_2O_2) reaction. The peak intensity (%T or absorbance value) clearly changes for water, HRP and H_2O_2. After reaction the % transmittance has reached 40% for HRP and H_2O_2. The increase in % transmittance is

about 25% between water, HRP, H_2O_2 and the reaction itself. The value of wavelength remains the same for water and HRP, but extends in the case of H_2O_2 and antibody-antigen reaction.

From a frequency range of 4000 per cms to 400 per cms the maximum variation is found along the 3300 per cms value of wavenumber. In this case the background spectrum was taken for that of glass.

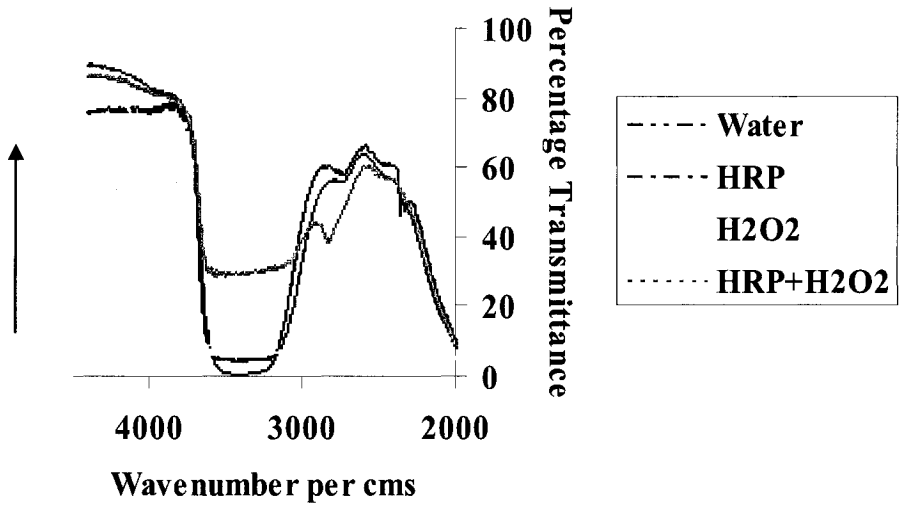

Figure 4.7: A comparison of FTIR Spectrum for HRP and H_2O_2 at 2μM concentration and water at the same concentration

Each frequency of light has some certain energy including that of Infrared. If a particular frequency is being absorbed as it passes through the compound being investigated it means that its energy is being transferred to that compound. In this particular case one of the frequencies of IR could have matched the frequencies of the sample (in each of the four cases) and caused the excitation of the atoms to a higher state. The bonds holding these atoms vibrate with different energies for each of the samples.

There was some variation found even at different wavenumbers and at different concentrations as shown in Figures, 4.8, 4.9, 4.10 and 4.11 respectively. This could be due to the reason that more than one frequencies of the IR could have matched the respective samples and causing the bonds to vibrate.

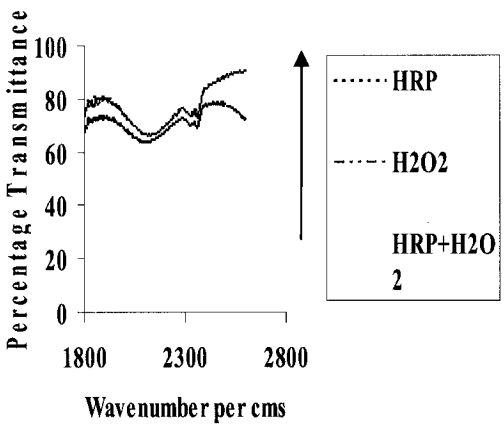

Figure 4.8: FTIR spectrum for HRP-H_2O_2 at different wavenumber at 5μM concentration

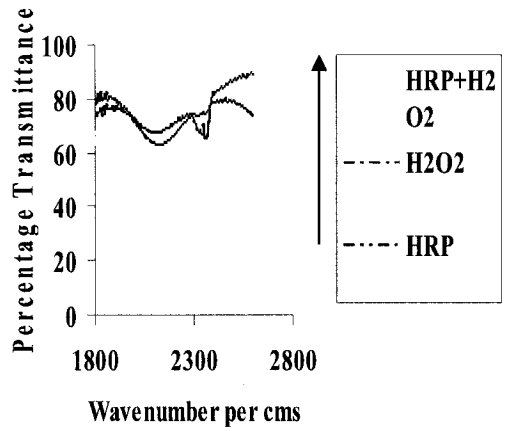

Figure 4.9: FTIR spectrum for HRP-H_2O_2 at different wavenumber at 10μM concentration

The change in concentration (in microns) does not seem to have a significant effect although a slight change in transmittance is observed at 100μM and 200μM respectively.

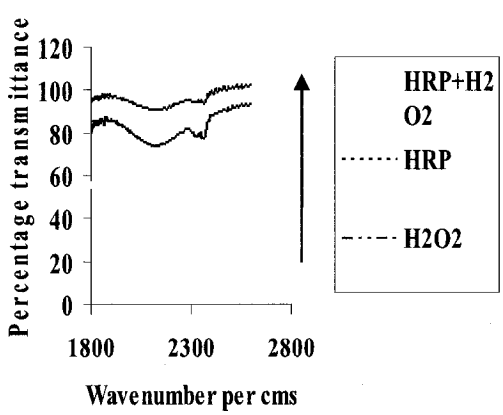

Figure 4.10: FTIR spectrum for HRP-H_2O_2 at different wavenumber at 100 μM concentration

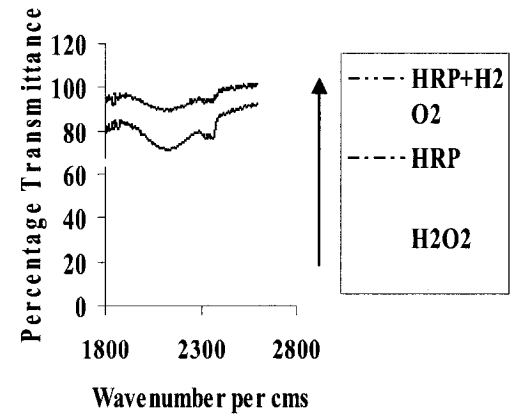

Figure 4.11: FTIR spectrum for HRP-H_2O_2 at different wavenumber at 200 μM concentration

4.6.2 Dynamic Characteristics

The objective of the dynamic characteristics was to know the stability of the enzymes and their longevity after the reaction has taken place. The dynamic analysis was performed with a horizontal set-up (beam condenser accessory) specifically made for the FTIR spectrometer. It consists of 2 flat mirrors placed at 45° to each other and parallely across them there are 2 concave mirrors (one ellipsoid and other hyperboloid) which are also placed 45° to each other. It has a horizontal support to hold the glass samples as shown in the Figure 4.12. The condenser accessory allows analyzing smaller quantities of material than can be sampled by conventional methods. Because the beam condenser reduces the source image at the sample to one-fifth its normal size, it is possible to collect spectra on microgram or sub-microgram amounts of sample.

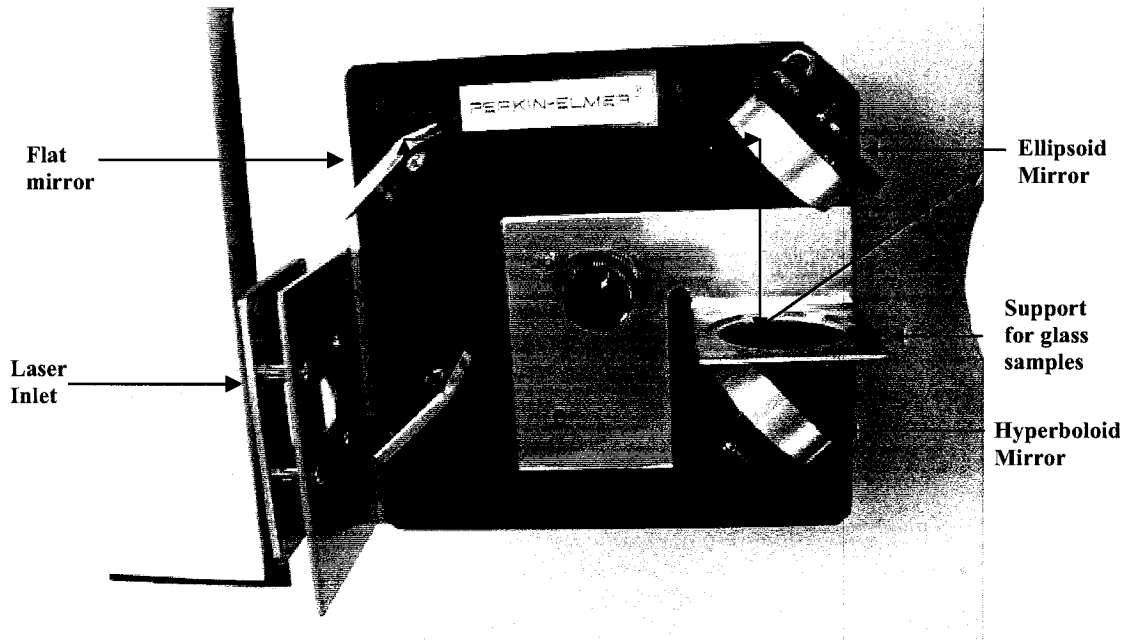

Figure 4.12: Horizontal set-up for TnC-ME reaction using the FTIR to analyze the dynamic characteristics of the enzymes

When used with the FTIR, the beam condenser provides extremely high throughput. This gives high signal-to-noise spectra; with minimal signal averaging needed. The laser light from the FTIR passes through the inlet on the left of the mirrors and gets reflected 3 times back and forth between the flat and concave mirrors to let the light pass through the glass samples containing the enzymes. The light reflects between the two glass samples and then passes through the other concave mirror which allows the light pass to the scanner present in the FTIR.

4.6.2.1 Results for TnC-ME and HRP-H_2O_2 in Dynamic Characteristics

The dynamic characteristics where taken between the antibody-antigen reaction for an interval of every 5 minutes. Results show a high change in the value of peak intensity (%T or absorbance value). The reaction after the first 5 minutes and next 5 minutes prod-

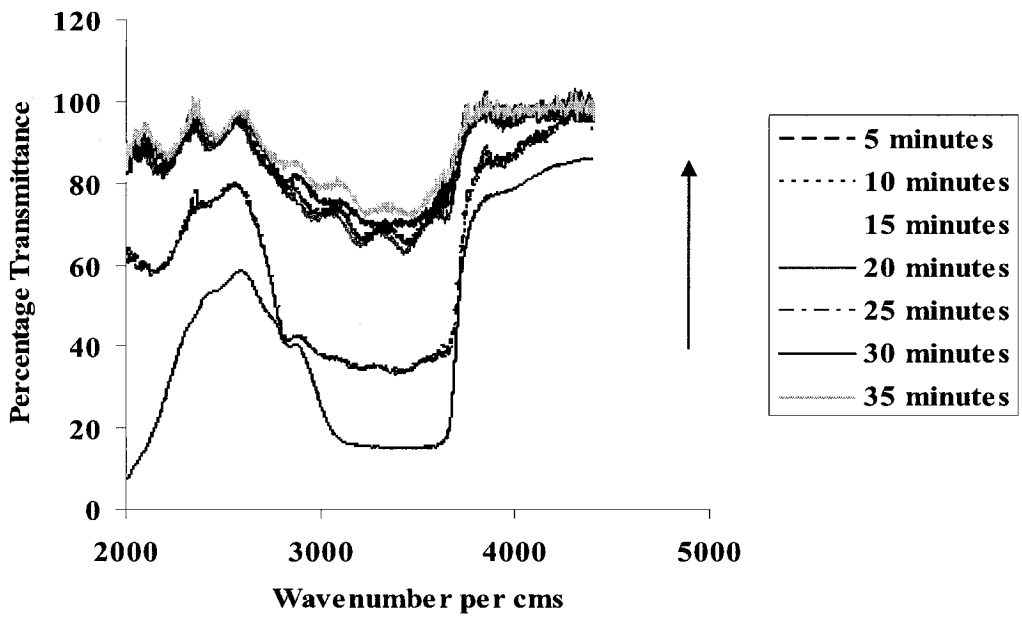

Figure 4.13: FTIR spectrum for dynamic characteristics of HRP-H_2O_2 at 2μM concentration for every 5 minutes

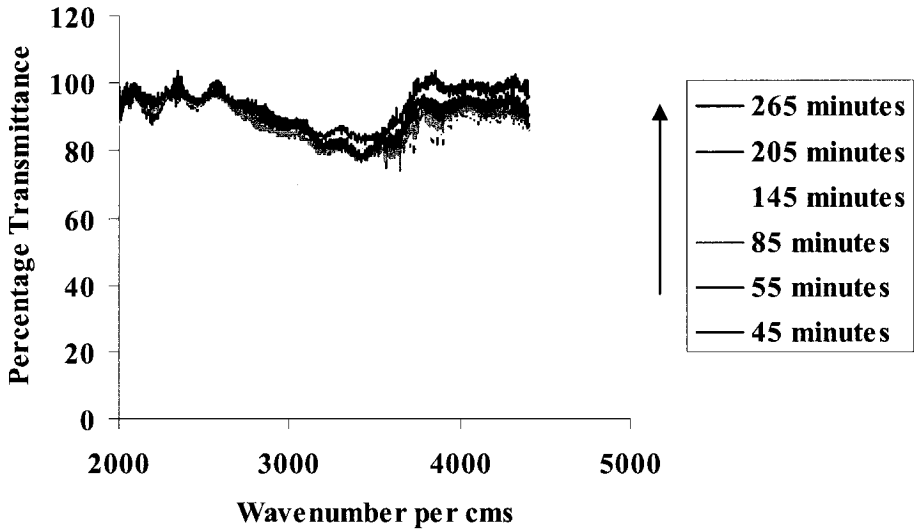

Figure 4.14: FTIR spectrum for dynamic characteristics of HRP-H_2O_2 at 2μM concentration for every 10, 30 minutes and 1 hour respectively

-uced a change in % transmittance of about 20%. This change could partially be due to a small proportion of the IR wave getting reflected off the sample and the remaining getting transmitted and partially due to the evaporation of the sample due to IR radiation. As the time keeps increasing there is a change in of about 45% transmittance from the first 5 minute spectrum to the 15 minute spectrum and from them on the transmittance is more or less constant with a very slight change as shown in Figure 4.13. By observing the results in Figure 4.13 and 4.14, one may conclude that the HRP-H_2O_2 (antibody-antigen) reaction creates a noticeable change in the peak intensity (%T).

Since solutions of pure substances do not absorb the energy of all wavelengths of light equally, a substance may be identified by the unique pattern of wavelengths absorbed. Absorbance is measured as logarithm of inverse of transmittance. The area under the absorbance spectra corresponds to the percentage absorbance of the IR frequencies by the

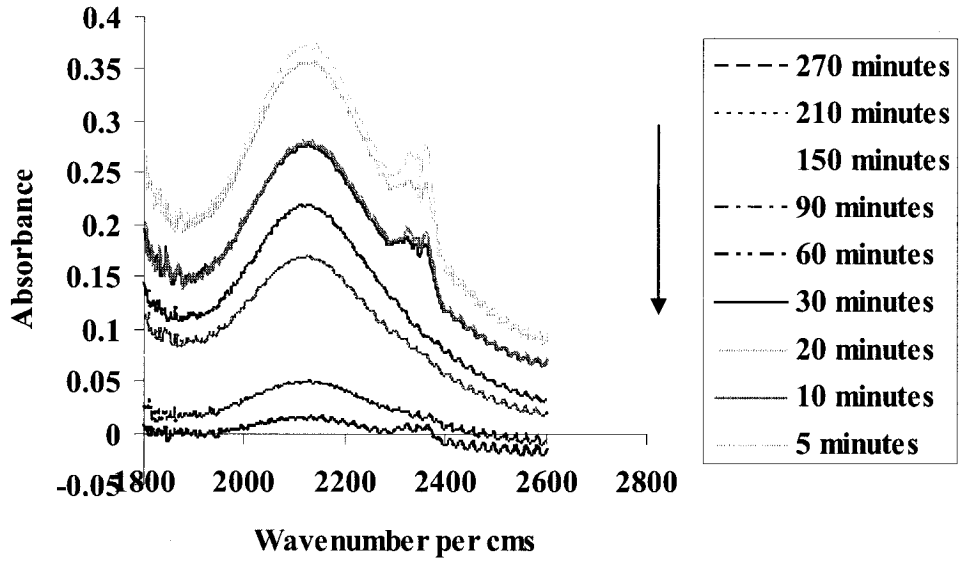

Figure 4.15: Absorption spectrum of HRP-H_2O_2 for every 5, 10, 30 and 60 minutes. The absorbance of visible light by HRP-H_2O_2 is measured as a function of wavenumber which is maximum at about 2100 per cms

sample. The absorption maximum of any sample in solution is the wavelength or wavenumber where the absorption is greatest. Although there were a couple of absorption peaks, in the present case the absorption spectrum was found to be maximum at 2100 per cms. Clearly from Figure 4.15 the maximum absorption takes place at 2100 per cms, which illustrates lesser percentage of reflectance. The increase in % absorption could be due to more and more electrons are absorbing energy and reaching the excitation states.

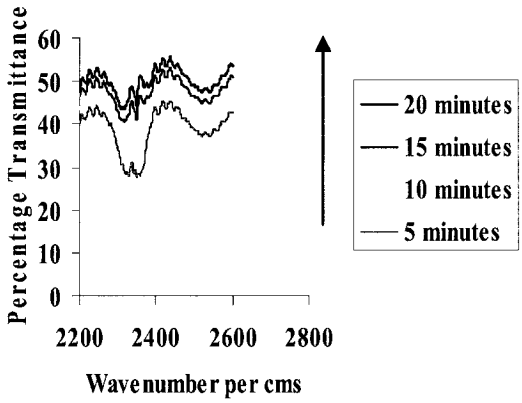

Figure 4.16: FTIR spectrum for dynamic characteristics of TnC-ME at 25mg/ml concentration for every 5 minutes

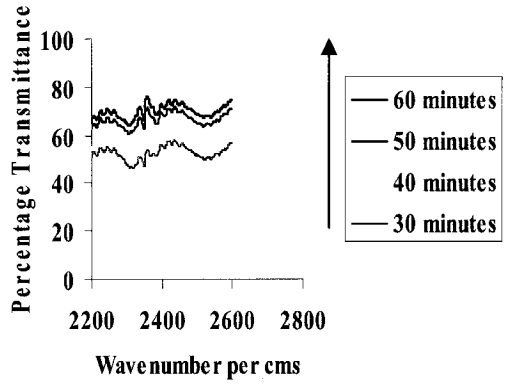

Figure 4.17: FTIR spectrum for dynamic characteristics of TnC-ME at 25mg/ml concentration for every 10 minutes

In the case of TnC-ME the concentration of the sample had to be increased to at least 25mg/ml to record a transmittance spectrum. The reason could be that at a lower concent-

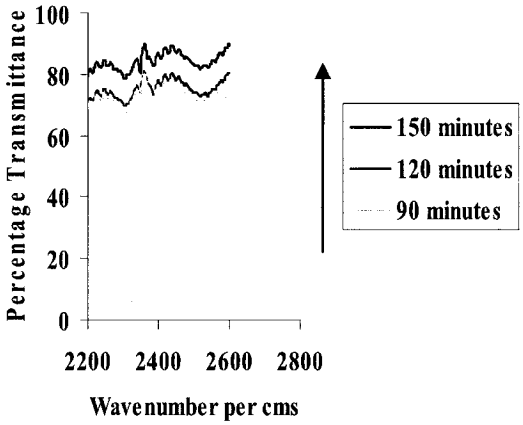

Figure 4.18: FTIR spectrum for dynamic characteristics of TnC-ME at 25mg/ml concentration for every 30 minutes

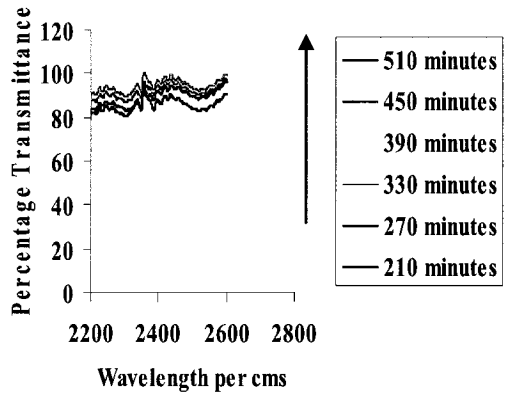

Figure 4.19: FTIR spectrum for dynamic characteristics of TnC-ME at 25mg/ml concentration for every 1 hour

-ration the sample could not have the desired frequencies of that of IR radiation. The electrons could not have absorbed the photon of energy from the IR radiation and hence stayed at the ground state.

The wavenumber or frequency is significantly less in the case for TnC-ME when compared to HRP-H_2O_2. In the case of HRP-H_2O_2 molecular vibrations shift to higher

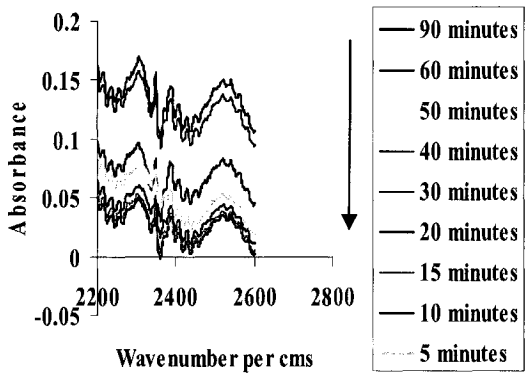

Figure 4.20: FTIR spectrum showing % absorption for TnC-ME at 25mg/ml concentration for 5, 10 and 30 minutes

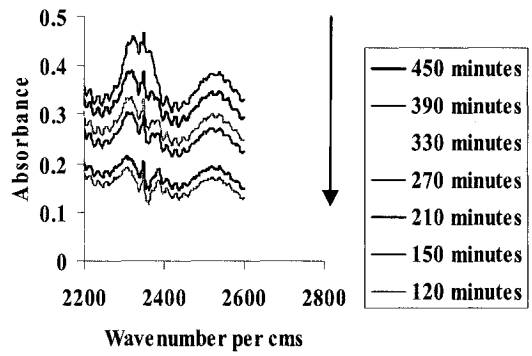

Figure 4.21: FTIR spectrum showing % absorption for TnC-ME at 25mg/ml concentration for 60 minutes

frequencies as the hydrogen bond weakens, the covalent OH bonds strengthen causing the molecules to vibrate at higher frequencies. But in the case of TnC-ME due to the absence of covalent OH bonds the intramolecular vibrations shift to a lower frequency [91]. The structural change in TnC due to the binding of Ca^{2+} ions could also have lead to the shift in wavenumber to a lower value. But otherwise the % absorption is more or less the same.

4.6.3 Identification of Enzymatic Reaction using Fluorescence Spectroscopy (FS)

Figure 4.22 shows the comparison between ME and ME-TnC complex. It clearly shows that there is an increase in fluorescence intensity of 15 arbitrary units (au) between both the curves. Melittin contains a single tryptophan group, Trp-19, because of this, the addition of TnC to ME in the presence of excess Ca^{2+} causes an enhancement and shift to

higher fluorescence intensity of tryptophan fluorescence band. In the absence of TnC the tryptophan fluorescence of melittin is quenched by acrylamide with relatively high efficiency [100].

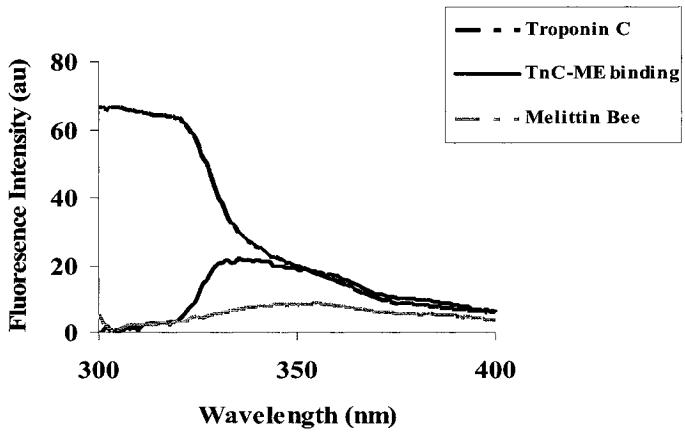

Figure 4.22 Fluorescence emission spectrum of Melittin (5μM) TnC (5 μM) and TnC-Melittin mix.

While it is not possible beforehand to make a conclusion to the contribution of the two components in the increase in helical content, but it are unlikely that a major portion of the change arise from TnC. Since the structure of TnC is largely α-helical, any further increment in helical content would have to be at the expense of the four Ca^{2+} -binding loops.

In Figure 4.23 a much more clear variation is shown between the TnC-ME reaction and ME alone for 5 μM . The flexibility of the protein molecule is important for the biological function of the protein [101]. Babu et al. [94] reported that the deletion of up to seven amino acids from the central helix of TnC does not inhibit its biological function. If the structure of TnC is rigid, the deletion of one amino acid in the central helix induces a 1.5

A° decrease in the length of the central helix and about 100 degree rotation of the N-terminal domain relative to the C-terminal domain. The N-terminal domain has been called the regulatory domain and contains one or low affinity Ca^{2+} binding sites [101]. So in Figure 4.22 it is evident that TnC molecule has as different fluorescence intensity. The above figure also reveals that ME binding to divalent cation-free TnC induced contracti-

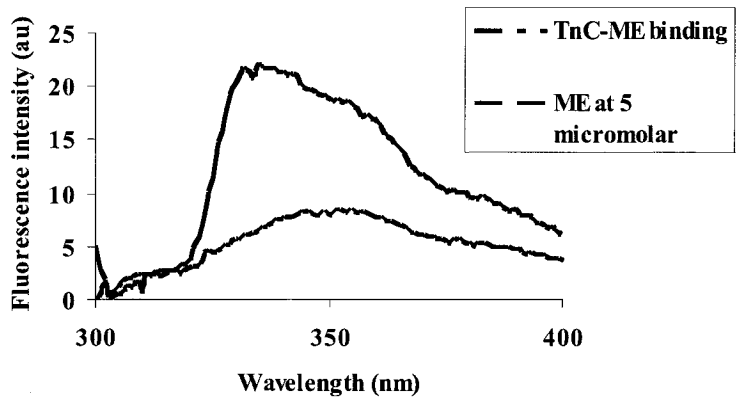

Figure 4.23: Fluorescence emission spectrum of Melittin (5μM) and TnC-Melittin mix.

-on of the TnC molecule, resulting in a reduction in size of the TnC. On the other hand, the C-terminal domain has been called the structural domain and contains two affinity sites.

In the presence of excess TnC, melittin develops a strong positive difference spectrum in Tryptophan (Trp) region, 350 nm, as shown in Figure 4.23. It remains uncertain whether the effect results from the direct involvement of Trp 19 (Tryptophan is the 19^{th} amino acid residue to ME) in the region of contact, or whether it arises indirectly, from the altered conformation of melittin. There is substantial evidence [102] that the interaction

of TnC-ME involves extensive contact of the helical melittin strand with both halves of the molecule combines with the N and C lobes of TnC.

Addition of an equimolar amount of TnC to this ME solution induced an increase in fluorescence of about 8 percent. Further addition of TnC increased the fluorescence to

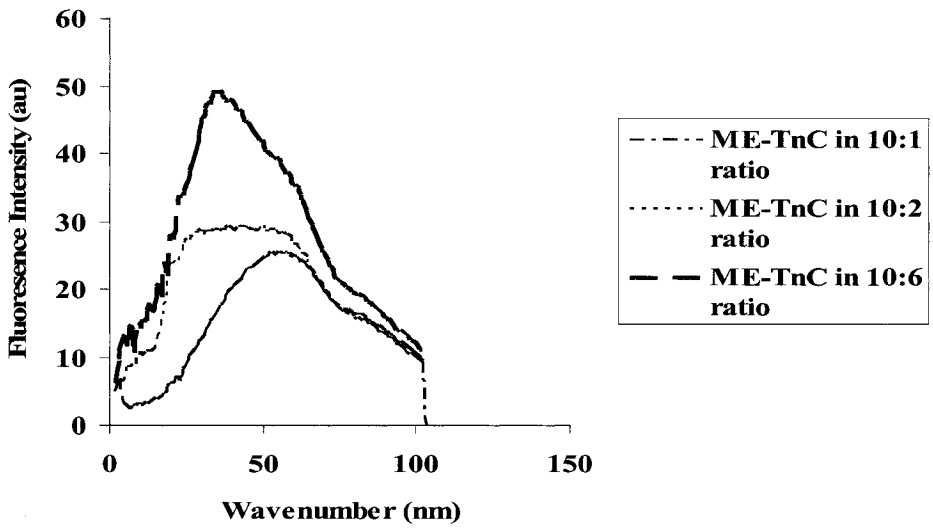

Figure 4.24: Fluorescence emission spectrum of TnC and melittin at different ratios

about 50 percent as is evident from Figure 4.24. The increase in fluorescence intensity is largely due to the removal of quenching factors, such as quenching small molecules and quenching (the definition of quenching is any process that reduces the life time of the excited state) amino acids. The most common use of quenching in the study of proteins is to determine the residues in a structure due to the conformational changes. ME binding to TnC strengthen the binding of Ca^{2+} to the TnC of the complex [103]. So, the TnC-Melittin complex is not rigidly maintained but undergoes a transition upon the Ca^{2+} -binding to the low affinity Ca^{2+} -binding sites. Also an increase in ME to Ca^{2+}-liganded TnC results in a further major increase in the intensity of fluorescence spectrum. The

more obvious explanation for this is one of the 26 amino acids of ME comes in direct involvement in the zone of contact and a consequent shift to a less polar environment [104].

4.6.4 Enzymatic Detection through Mass Spectroscopy

The enzymatic samples were individually deposited using a pipette onto a 5*5 mm

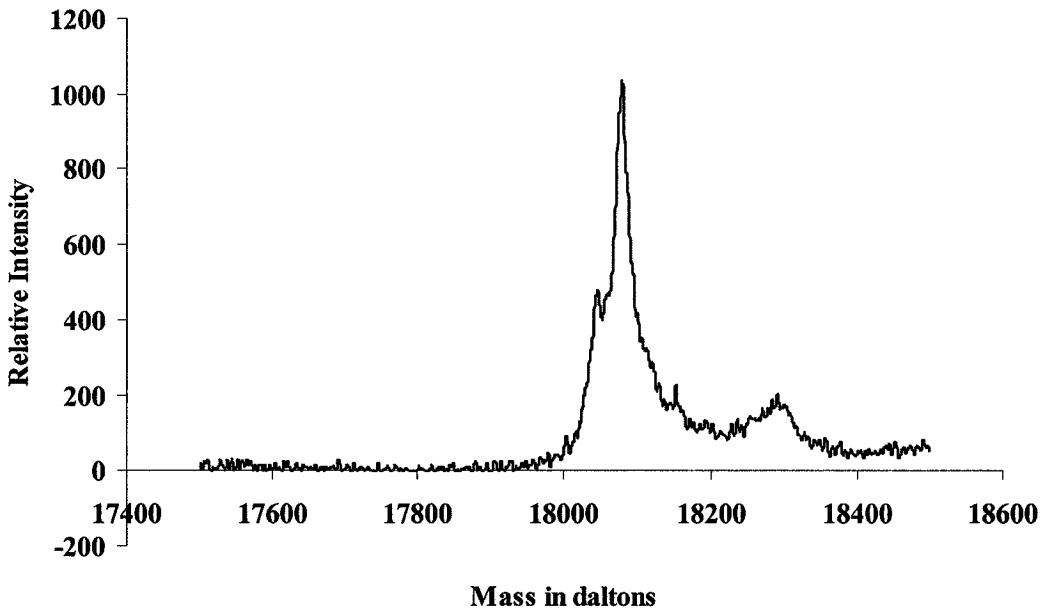

Figure 4.25: Mass spectrum of TnC molecule confirming its molecular weight

aluminum plate containing many channels or opening of 0.2 mm diameter. These enzymes were accompanied with a protein whose mass spectrum is already known. This process is done to calibrate the device to the right settings. The aluminum plate is placed inside a vertical chamber which includes the laser beam.

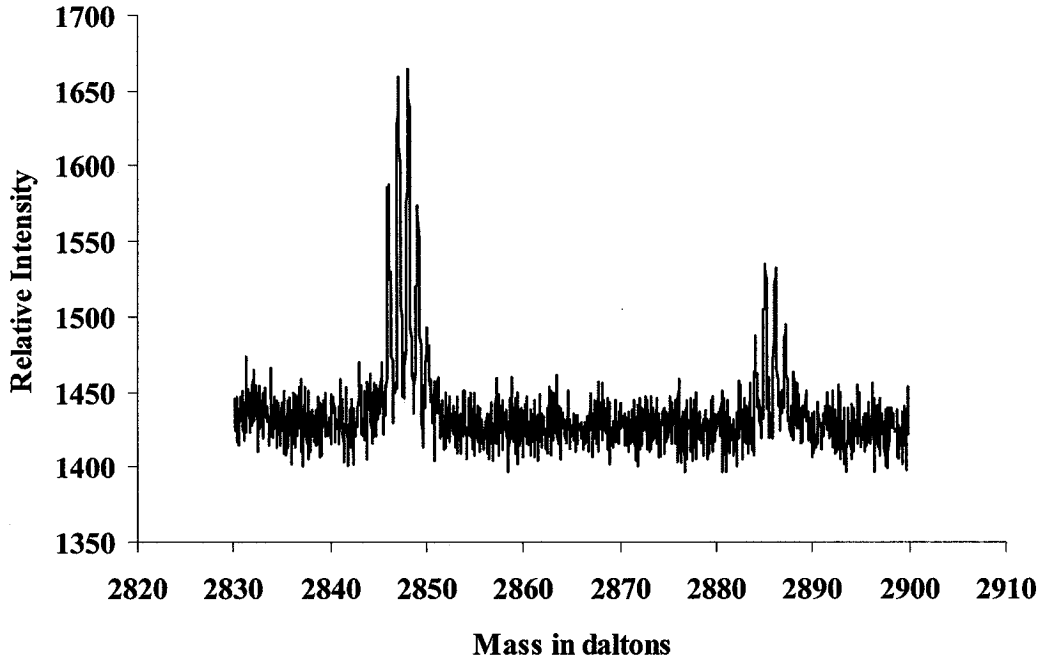

Figure 4.26: Mass spectrum for ME molecule confirming its molecular weight. The other peak at 2885 Da could be due to the buffer solution. But in the case of two peaks, the one giving the highest relative intensity is selected to give the MW of the sample

The laser beam is focused on the required channel by viewing the corresponding channel through the computer and hence the spectrum. As the ultra-violet light falls on the sample, the electrons from the sample gather energy, get excited and enter into a high vacuum chamber under the influence of a magnetic field. Electrons having the right mass-to-charge ratio (18100 Daltons in Figure 4.25 and 2845 Daltons in Figure 4.26) are made to pass through the chamber and collected at the detector.

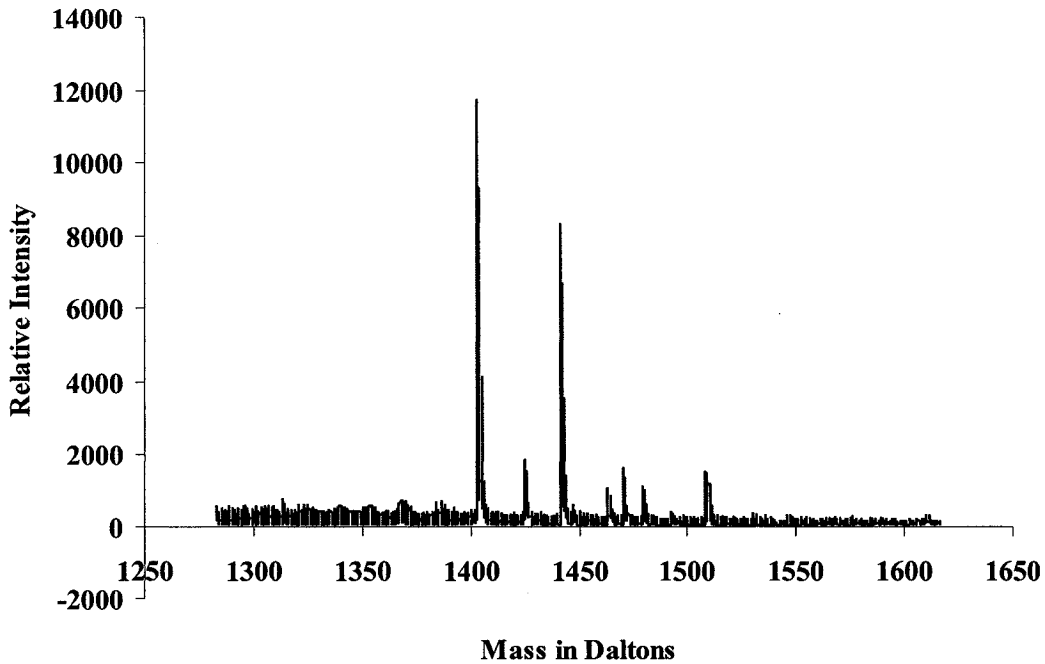

Figure 4.27: Mass spectrum for TnC-ME interaction at 1400 Daltons. The reduction in molecular weight (MW) could be due to influence of mass-to-charge ratio (m/e) and thus confirming the reaction has taken place

When the UV light is made to strike at the hole in the aluminum plate containing the mixture of both the proteins, the TnC-ME electrons having the mass-to-charge-ratio (m/e) in the range of 1400 Daltons are made to pass through the high vacuum chamber through the magnetic field as shown in Figure 4.27. There are two individual peaks that are closer to each other because the molecular weight is same for both the peaks, those with more charges appear at lower m/e values than those with fewer charges.

The reduction in molecular weight (MW) in the case of HRP-H_2O_2 interaction could be due to the fact that the higher molecular weight (MW) molecules do not cause fragmentation of the covalent bonds so the maximum relative intensity occurs at a lower m/e ratio as in Figure 4.29.

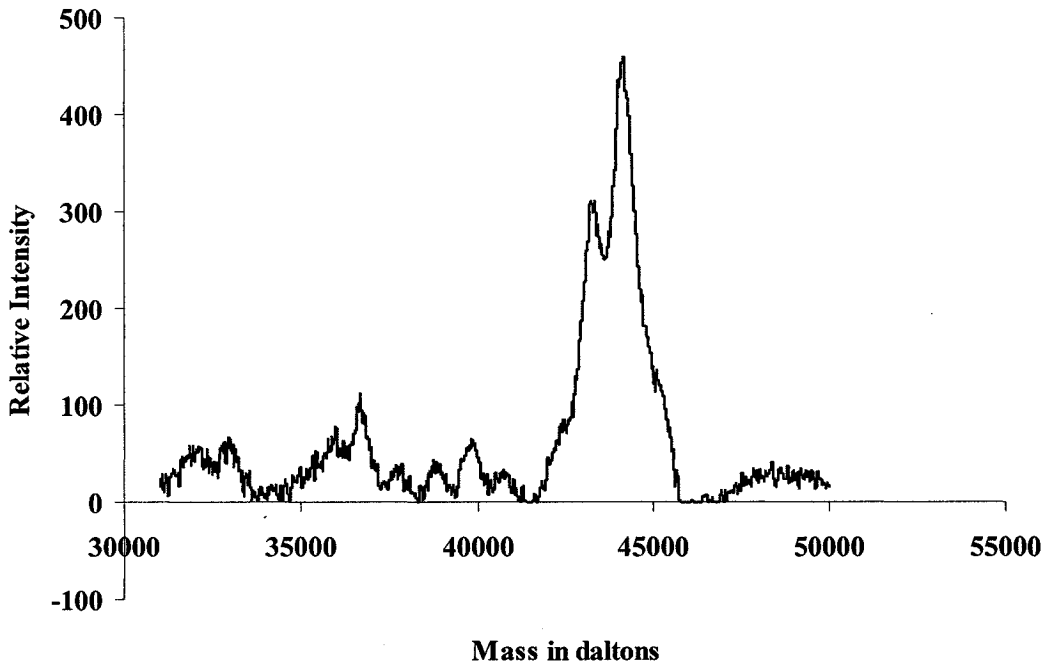

Figure 4.28: Mass spectrum for HRP clearly indicating its molecular weight (MW). The increase in MW could be due to the salts in the buffer solution which could be having the same m/e ratio as HRP molecule

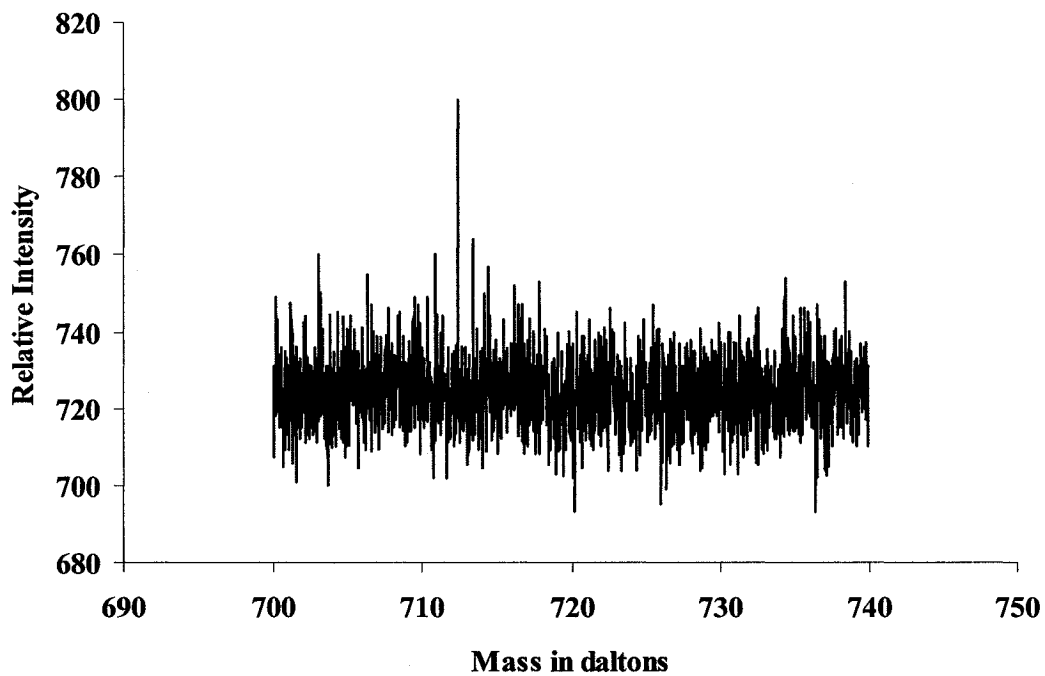

Figure 4.29: Mass spectrum for HRP-H_2O_2. The reduction in relative intensity compared to TnC-ME could be due to lesser mass-to-charge (m/e) ratio. The mass spectrum is also associated with disturbances due to the wrong pH solution and over addition of water and dilute HCl

4.7 SUMMARY

Continuous monitoring of multiple cardiac markers will allow the earliest possible biochemical diagnosis of myocardial infarction. Shortening the time to treatment as well as reducing the time to exclusion of infraction in this deadly disease has the potential to minimize the risk for the patient. During the last few years the use of optical techniques to detect biomarkers has met this challenge and is now acknowledged by the scientist as the standard for technology advances. Precision measurements of minute amounts of biological material could be performed by optical means with a remarkable accuracy with optical methods. Although available in medical laboratories, such analyzers are making their way directly to the users as they are easy to use. The versatility of some of these optical detection techniques is their high sensitivity and long wavelength of radiation which minimizes scattering problems.

Considered as one of the fast growing techniques in medical care they are expected to provide even a broader platform to integrate protein markers with infectious disease testing. In the present chapter a few of the standard optical techniques like Fourier Transform Infrared Spectrometer (FTIR), Fluorescence Spectrometer (FS) and Mass Spectrometer (MS) are employed to investigate the signature of the bio reaction for enzymes like TnC-ME and HRP-H_2O_2 interaction. A clear description is given about each of the above mentioned methods and their use in medical care.

Results on the FTIR were recorded to get both the transmittance and absorbance spectrums for each of the enzymes to understand the variation in reaction signals. The results gave a clear insight about the behavior of the atoms inside the molecules when they are excited with energy. An effort was made to comprehend the dynamic characteristics for each of the enzymes with a beam condenser accessory (horizontal support) in the FTIR. The concentration of the enzymes was varied in order to record at what frequencies (or wavenumbers) were the infrared (IR) radiation was absorbed by the samples.

A completely different procedure was explained earlier in the chapter to excite atoms to higher energy levels in fluorescence spectroscopy (FS). A clear variation of signal was found to be plotted for TnC-ME interaction at 350nm wavelength. This method proved to be more sensitive because even at small concentrations it could detect TnC-ME interactions. The ratio of concentrations was also varied for the proteins to understand the variance in interaction. The change in fluorescence intensity was concluded due to the conformational change in TnC owing to the Ca^{2+} binding.

Mass spectroscopy was based on mass-to-charge (m/e) ratio of the samples. This method was basically employed to confirm the molecular weight (MW) for the proteins before and after the reaction. The MW tends to reduce drastically in both the cases indicating the influence of mass-to-charge (m/e) ratio.

The interest for optical techniques is expected to grow annually with specific areas such as cardiac markers. The future of blood analysis is at the patient's side and what was once thought of as a passing has become nothing short of a revolution in patient care.

CHAPTER 5

CONCLUSIONS AND RECOMMENDATIONS FOR FUTURE WORK

5.1 CONCLUSIONS

In the present work an attempt is made to monitor bio-enzymatic reaction by various optical detection techniques. Microcantilever structures are some of the simplest MEMS structures that can be used to identify the enzymatic reactions between various proteins given their high sensitivity and mass production. PVDF cantilever beams were used to analyze these enzymatic reactions using the optical lever method (OLM). The results in this work provide enough validation that could help building a portable biosensor that will detect Acute Myocardial Infarction (AMI).

The experimental plots produced signature reaction having peaks at different time intervals. The first peak occurred before 25 seconds due to the mass of the droplets and the second peak occurred when the chemical reaction took place. The third occurred when the chemical reaction was over and so on. Validation on the experimental results was done by evaluating the superficial tension that is responsible for making the beam move up and down. A simple relation was derived between the tip deflection and superficial tension. The tip deflection was evaluated from the PSD readings. Due to this load there could be a possible shift in the natural frequency of the beam. The ratio of position of the load was also varied on the entire length of the cantilever to find the shift

in natural frequency. The ratio of natural frequency was observed to be higher when the ratio of load was at the fixed end of the beam and gradually reduced close to zero when the load moved close to the tip of the beam.

The relation between the total deflection of the cantilever beam and the stress acting on the surface of the beam was obtained using the beam flexure formula. The stress was evaluated only at the particular segment where the enzyme was dropped and not at the entire length of the beam. The force that is acting on the surface of the beam due to the enzymatic droplet was evaluated and from there the corresponding superficial tension acting on that segment of the beam was calculated for both the enzymes. It was found that HRP-H_2O_2 produced a larger force and hence a larger stress. This is could be largely due to the formation of compound one and the instantaneous reaction between the two compounds. The stress vs. deflection plot produced a linear relationship. But in the case of TnC-ME the force produced was comparatively smaller with a smaller stress. This could be due to the change in structure in TnC and also due the reaction time.

Dynamic analysis of the cantilever beam was done for three different conditions. The first included the cantilever beam with no load, the second the cantilever beam with extra mass and the third the cantilever beam with extra mass and bending. Resonance occurred at three different positions for all the three cases. There is a dip in amplitude and shift in natural frequency when the extra mass is added on the system. Amplitude due to the cantilever beam with extra mass and bending was seen to be higher than the case with cantilever with extra mass on it.

Further dynamic analysis for the PVDF cantilever beams were carried out using the classic Rayleigh-Ritz method to find out their natural frequencies. The load due to the enzymes was incorporated into the model. Although there was no experimental work done for dynamic analysis, modeling was done in order to validate the experimental work that would be done in the future.

Experimental analysis was done using two sets of enzymes on PVDF cantilever beams and the deflection was monitored using the PSD. The first set of enzyme namely Horseradish Peroxide (HRP) and Hydrogen Peroxide (H_2O_2) at 25mg/ml were used to understand the enzymatic reaction between them using optical detection technique and PVDF cantilever beams with and with out the influence of voltage. The reaction without voltage took place at around 250 seconds stating the ability of HRP to reaction faster with its substrate. The deflection was about $1450\,\mu m$. At a voltage of around 90 volts the reaction took place at around 100 seconds and deflection at $2450\,\mu m$. The influence of the electric field acts as a catalyst to the reaction that hastens the reaction. Dynamic characteristics on HRP-H_2O_2 were done for every 5 minute time interval using the Fourier Transform Infrared Spectrometer (FTIR). As the time interval increases there is a significant difference in the peak intensity values. Mass spectroscopy (MS) was done to confirm their molecular weight before and after the reaction. Mass Spectroscopy (MS) confirmed a clear change in molecular weight of the two proteins indicating a reaction has taken place.

The second set of enzymes used were more cardiac specific namely, Rabbit Skeletal muscle Troponin C (TnC) and Melittin Honey Bee (ME) at 25mg/ml. When compared with the earlier enzymes the reaction took place at a much slower pace. This is because when TnC and ME react at a pH of 7.5, TnC which is globular in structure undergoes a transition in to a dumbbell like structure. The entire reaction took almost 600 seconds to complete and then maintain a steady state. The deflection was 750 μm which is much lower than the earlier enzymes used. The application of voltage hastens the reaction to about 350 seconds and a much higher deflection of about 2600 μm.

In order to verify the enzymatic reaction between TnC and ME, a fluorescence study was done on them. TnC and ME were made to react with each other at a pH of 7.5 and that could be detected at a wavelength of 350nm for a 1:1 ratio. Various concentrations of 20mg/ml, 25mg/ml, 30mg/ml, 35mg/ml and 40mg/ml at different ratios were tried for fluorescence study. The increase in fluorescence intensity (FI) was around 50% for a ME-TnC 10:1 ratio. It reduced to 30% for a 10:2 ratio and a further reduction of 25% for a 10:6 ratio. The reduction in FI is due to the quenching of small molecules and amino acids of ME. The more obvious explanation for this is that one of the 26 amino acids of ME comes into direct involvement with the two lobes of TnC. FTIR study has been applied to examine the percentage transmittance and absorption spectrums for the two sets of proteins used. For HRP-H_2O_2 the maximum wavelength was found to be at 3400 per cms and that for TnC-ME was found to be at 2400 per cms. This could be due to the absence of OH bonds the intramolecular vibrations shifts to a lower frequency. Dynamic characteristics for the two enzymes on the FTIR showed that as the time interval

increases a large variation in %absorption and %transmittance increased was found. This could be partially due to more excitation of electrons and partially due to evaporation. But the results concluded that the set of enzymes are steady are reaction.

Conclusions based on the results from the present study were outlined at the respective chapters. From a global point of view the conclusions drawn from the present study can be summarized in the following way:

1. The micro-cantilevers are appropriate for enzymatic detection and can be incorporated in a biosensor as they respond to chemical stimuli.
2. The signature reaction from the two sets of proteins for both with and without the application of voltage is different and that is clearly shown in the variation in spectrum in the results in the corresponding chapters.
3. Optical detection in conjunction with the strain of the cantilever beam due to the induced reaction is simple and less expensive methodology than other techniques in the enzymatic detection.
4. FTIR, Fluorescence Spectroscopy (FS) and Mass Spectroscopy (MS) clearly indicate the existence of an enzymatic reaction that was detected through the cantilever beam deflection method.
5. There is a significant change in the first natural frequency at different load positions on the cantilever beam that could be detected and used for the enzymatic reaction detection.
6. Stress increases linearly with the increase in deflection for the concentrated load.

7. The ratio of amplitude dipped when cantilever was added with the extra mass on its surface and hence the change in resonance.

5.2 RECOMMENDATION FOR FUTURE WORK

Bio-MEMS is a vast field and each of the applications in it require rapid and reliable test systems. There are significant challenges in the development of such systems. The implication of having an optical detection system and a cantilever beam in combination is that any analyte can be detected provided that there is a suitable biocomponent and a solvent in which the analyte is soluble. There are a few future recommendations for the present work done:

1. The sensitivity of Troponin C in the human blood is about $1\ \mu g/l$ or lower. The next step is to aim a sensitivity of $1\ ng/l$ so that that might reveal serious medical conditions well before they may happen.
2. Frequency response modification due to the stress induced into the micro-cantilever.
3. Smaller size of cantilever beams must be tried to evaluate the enzymatic detection of biomolecules.
4. Another significant challenge for the future of Bio-MEMS is the deposition of reactants on one side of the cantilever beam so that no damage to the beam has caused.

5. The above findings indicate towards a hybrid system that would contain various commercial technologies and some dedicated processes to build the highly sensitive cantilever beams.
6. The possible architecture of the enzyme detection system may include a fluidic circuit made from Pyrex 7740 glass in which the fluid is handled through capillary electrophoresis, laser diode and optical positioning system; a micro-controller could be implemented in a Bi-CMOS technology. The overall sensitivity of the device is expected to be very good although a large number of experiments should be run to validate the cross-sensitivity. Figure 5.1 illustrates the architecture of the system that could be accomplished by three to four comme-

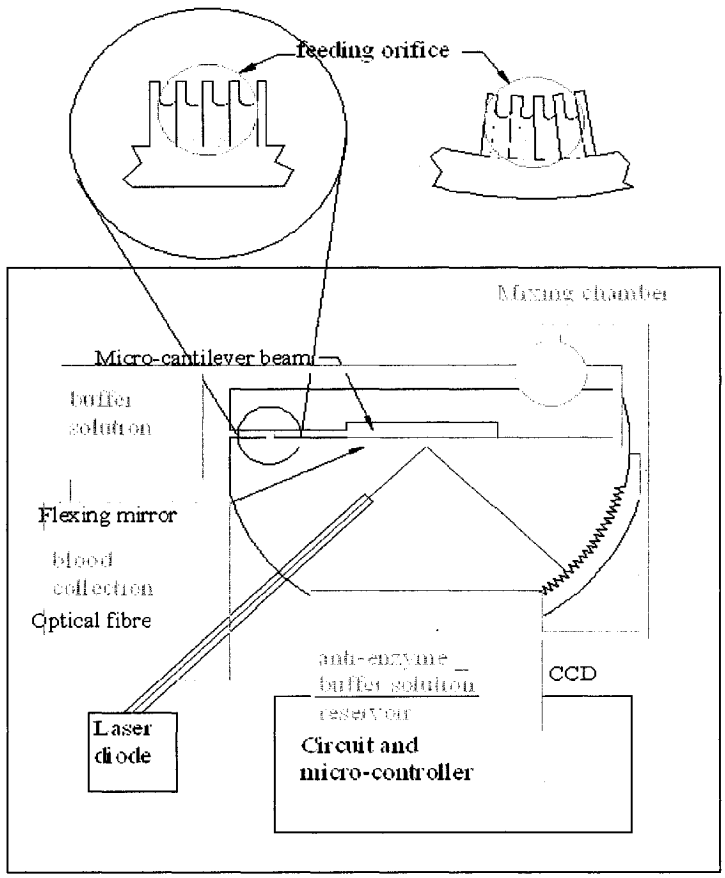

Figure 5.1: Possible architecture of the bio-sensor [84]

-rcial technologies, a Deep Reactive Ion Etching (DRIE) and a Xenon Di-Fluoride (XeF_2) selective release of the mirror. The micro-fluidic device has to be filled in advance with the buffer solution and the anti-enzyme for easy usage. Power could be attached as a long lasting Li-ion battery. The device as conceived could be built in $5000 \times 5000\,\mu m^2$ ship surface.

7. The cross sensitivity of the method should be also systematically investigated.

REFERENCES

[1]. Wachter E.A, Thundat T, "Micromechanical sensors for chemical and physical measurements", *Rev. Sci. Instrum.*, **Vol 66 (6),** June 1995.

[2]. Kovacs G.T.A, "Micromachined Transducers Sourcebook", McGraw Hill, New York, 1998.

[3]. Nadim M, "An Introduction to Microelectromechanical Systems Engineering", Arctech House, New York, 1999.

[4]. Cornnor K. A, "Silicone-grease-based immobilization method for the preparation of enzyme electrodes", *Analyst*, **Vol 114**, 1989, pp. 1427-1429.

[5]. Yang Y, "Glucose sensor with improved haemocompatibilty", *Biosensors and Bioelectronics*, **Vol 15**, 2002, pp. 221-227.

[6]. Amritsar J, Stiharu I, Packirisamy M, Balagopal G, Li X, "MOEMS based cardiac enzymes detector for Acute Myocardial Infarction", Optical components and Devices, Proceedings of the SPIE, **Vol. 5578**, Editors: Armitage John C, Fafard Simon, Lessard Roger A, Lampropoulos George A, 2004, pp. 91-98.

[7]. Flannery A. F, Mourlas N, Storment C, Tsai S, Tan S, Kovacs G.T.A, "PECVD Silicon Carbide for Micromachined Transducers", Proc. 1997 Int. Conf. on Solid-State Sensors and Actuators, Chicago, IL, **Vol. 1**, June 16-19, 1997, pp. 217-220.

[8]. Jobst G, "Thin film microbiosensors for glucose-lactate monitoring", *Anal. Chem. A*, **Vol 68**, 1996, pp. 3173-3179.

[9]. Min Y, "A 2-D Microcantilever Array for multiplexed Biomolecular Analysis", *JMEMS*, **Vol 13 (2),** April 2004, pp. 290-299.

[10]. Pope J.H, Aufderheide T.P, Ruthzaer R, "Missed Diagnosis of Acute Cardiac Ischemia in the Emergency Department", *New Eng. J. Med*, **Vol 342**, 2000, pp. 1163.

[11]. Helen J, "Current and future hospitalization after heart attacks", Health Reports, autumn, **Vol 10 (2),** 1998.

[12]. Ivnitski D, Rishpon J, "A one-step, separation-free amperometric enzyme immunosensor", *Biosensors and Bioelectronics*, **Vol 11 (4),** 1996, pp. 409-417.

[13]. Ryan G. M, "Cardiac Markers and Point-of-Care Testing: A perfect Fit", *Crit Care Nurs Q*, **Vol 24 (1),** 2001, pp. 54-61.

[14]. O'Regan T.M, George G, "Direct detection of myoglobin in whole blood using a disposable amperometric immunosensor", *Analytica Chimica Acta*, **Vol 460**, 2002, pp. 141-150.

[15]. Adams III J.E, 'A Comparaison of Reteplase with Alteplase for Acute Myocardial Infarction', *New Eng. J. Med*, **Vol 337**, October 16th 1997, pp. 1118-1123.

[16]. Aravind S, 'Comparison of techniques for enzymes immobilisation on silicon supports', *Enzyme and Microbial Technology*, **Vol 24**, 1999, pp. 26-34.

[17]. Janata R, "Principles of chemical sensors", Plenum press, New York, 1989.

[18]. Donald W.M, "Role of cardiac markers in evaluation of suspected myocardial infarction", *Postgraduate medicine*, **Vol. 102 (5),** Nov 1997.

[19]. Jesse E. A, "Clinical application of markers of cardiac injury: basic concepts and new considerations", *Clinica Chimica Acta*, **Vol 284**, 1994, pp. 127-134.

[20]. Emil D.M, "Clinical insights on the use of highly sensitive cardiac troponin assays", *Clinica Chimica Acta*, **Vol 284,** 1999, pp. 175-185.

[21]. Christopher H, "Evaluation of a Rapid Whole Blood ELISA for Qualification of Troponin I in patients with Acute Chest Pain", *Clinical Chemistry*, **Vol 45(10),** 1999, pp. 1789-1796.

[22]. Christopher H, "Analytical performance and clinical application of a new rapid bedside assay for the detection of serum cardiac troponin I", *Clinical Chemistry,* **Vol 44**, 1998, pp. 1925-1930.

[23]. Rishpon J, Ivnitski D, "An amperometric enzyme-channeling immunosensor", *Biosensors and Bioelectronics*, **Vol. 12(3),** 1997, pp. 195-204.

[24]. Athey D, "Homogeneous amperometric immunoassay of theophylline in whole blood", *Biosensors and Bioelectronics*, **Vol. 8,** 1993, pp. 415-419.

[25]. McNeil C.J, "Direct electron transfer bioelectronic interfaces: application to clinical analysis", *Biosensors and Bioelectronics*, **Vol. 10**, 1995, pp. 75-83.

[26]. Datskos P.G, Isidor S, "Detection of 2-mercaptoethanol using gold-coated micromachined cantilevers", *Sensors and Actuators*, **Vol. B61**, 1999, pp. 75-82.

[27]. Petrou P.S, Moser I, Jobst G, "BioMEMS device with integrated microdialysis probe and biosensor array", *Biosensor and Bioelectronics*, **Vol. 17**, 2002, pp. 859-865.

[28]. Henry C, "Getting under the skin: Implantable electrochemical glucose sensors are moving closer to commercialization", *Anal. Chem. A*, **Vol 70**, 1998, pp. 594-598.

[29]. O'Regan Tina M, George G, "Development of a disposable immunosensor for detection of human heart fatty-acid binding protein in human whole blood using screen-printed carbon electrodes", *Talanta,* **Vol 57**, 2002, pp. 501-510.

[30]. Wilson G.S, "Fundamentals of amperometric sensors", Biosensors: fundamentals and applications", Oxford University Press, New York, 1987.

[31]. Bruce Jacobson K, "Biosensors and other medical and environmental probe", Center of microbiology, www.ornl.gov

[32]. Nicolini C, "Biosensors: A step to bioelectronics", *Physics world*, **Vol 5**, May 1992, pp. 30-34.

[33]. Arntz Y, Seelig J.D, "Label-free protein assay based on a nanomechanical cantilever array", *Nanotechnology*, **Vol. 14**, 2003, pp. 86-90.

[34]. Oden P.I, "Gravimetric sensing of metallic deposits using an end-loaded microfabricated beam structure", *Sensors and Actuators*, **Vol. B53**, 1999, pp. 191-196.

[35]. Taylor E.H, "Measurement of Forces between a metal surface and molecules adsorbed on it", in: Report No. ORNL-5297, Oak Ridge National Laboratory Chemistry Division Annual Report, 1997, pp. 11-12.

[36]. Hai-Feng J, Thundat T, "In situ detection of calcium ions with chemically modified microcantilevers", *Biosensors and Bioelectronics*, **Vol. 17**, 2002, pp. 337-343.

[37]. Butt H.J, Raiteri R, Grattarola M, "Changes in surface stress measured with an atomic force microscope", *Scanning Microscopy*, **Vol. 12(1)**, 1998, pp. 243-251.

[38]. Guanghua W, Ram H.D, Thundat T, "Bioassay of prostate-specific antigen (PSA) using microcantilevers", *Nature Biotechnology*, **Vol. 19**, 2001, pp. 856-860.

[39]. Binnig G, "Atomic Force Microscope", *Phys. Rev. Lett*, **Vol. 56**, 1986, pp. 930.

[40]. Barnes J.R, Stephenson R.J, Woodburn C.N, O'Shea S.J, Welland M.E, 'A femtojoule calorimeter using micromechanical sensors', *Rev. Sci. Instrum*, **Vol 65**, 1994, pp. 3793.

[41]. Christopher T. B, "Acute Myocardial Infarction", The Cleveland Clinic Foundation, May 30th 2002.

[42]. Bhayana V, Henderson A.R, "Biochemical markers of myocardial damage", *Clin. Biochem*, **Vol 28**, 1995. pp. 1.

[43]. Keffer J.H, "Myocardial markers of injury: Evolution and Insights", *Am. J. Clin. Pathol*, **Vol 105**, pp. 305.

[44]. Adams III J.E, Abendschein D.R, "Biochemical Markers of Myocardial Injury", *Circulation*, **Vol 88**, 1993, pp. 750.

[45]. Selkar H. P, "Coronary care unit triage decision aids: How do we know when they work?", *Am J Med*, **Vol 87**, 1989, pp. 491-493.

[46]. Zimmerman J, Fromm R, Meyer D, "Diagnostic marker co-operative study for the diagnosis of myocardial infarction", *Circulation*, **Vol 99 (13),** Apr 6, 1999, pp. 1671-1677.

[47]. Brogan G. X, "Evaluation of cardiac STATus CK-MB/myoglobin device for rapidly ruling out acute myocardial infarction", *Clin Lab Med*, **Vol 17**, 1997, pp. 655-668.

[48]. Emmanuel. I, "Organic phase enzyme electrodes: kinetics and analytical applications", *Biosensors and Bioelectronics*, **Vol. 12 (1),** 1997, pp. 53-75.

[49]. Grogan C, Raiteri R, O'Connor G.M, Glynn T.J, Cunningham V, Kane M, Charlton M, Leech D, "Characterization of an antibody coated microcantilever as a potential immuno-based biosensor", *Biosensor and Bioelectronics*, **Vol 17,** 2002, pp. 201-207.

[50]. Brynda E, Houska M, Brandenburg A, Wikerstal A, "Optical biosensors for real-time measurement of analytes in blood plasma", *Biosensors and Bioelectronics*, **Vol 17**, 2002, pp. 665-675.

[51]. Butt H.J, "A sensitive method to measure changes in the surface stress of solids", *J. Colloid Interface Sci,* **Vol 180**, 1996, pp. 251-260.

[52]. Seiki I, "Analysis of the resonance characteristics of a cantilever vibrated photothermally in a liquid", *J. Appl. Phys.* **Vol 73(6),** 1993, pp. 2654-2658.

[53]. Pelton J.T, "Spectroscopic methods for analysis of protein secondary structure", *Anal. Biochem*, **Vol 277**, 2002, 167-176.

[54]. Hiroki S, "Fluorescence Energy Transfer Study of Troponin C-Melittin Complex", *J. Biochem*, **Vol 118**, 1995, pp. 996-1000.

[55]. Robert F.S, "The interaction of Melittin with Troponin C", Archives of *Biochemistry and Biophysics*, **Vol 254 (1),** April 1987, pp. 342-352.

[56]. Takuhiro N, "Static and Kinetic Studies on Rabbit Skeletal Muscle Troponin", *J. Biochem*, **Vol 94,** 1983, pp. 745-754.

[57]. Ryan G. M, "Cardiac Markers and Point-of-Care Testing: A Perfect Fit", *Crit Care Nurs Q*, **Vol 24(1),** 2001, pp. 54-61.

[58]. Chiu A, "Troponin-I, myoglobin, and mass concentration of creatine kinase-MB in acute myocardial infarction", *Q J Med*, **Vol. 92**, 1999, pp. 711-718.

[59]. Xu W, "Structure of the C-domain of human cardiac Troponin C in complex with the Ca^{2+} sensing drug EMD 57033", *The Journal of Biological Chemistry*, **Vol. 276(27),** 2001, pp. 25456-25466.

[60]. Madou M.J, "Fundamentals of Microfabrication", Boca Raton, FL: CRC, 2002.

[61]. Senturia S.D, "Microsystems Design", Norwell: Kluwer, 2001.

[62]. Chen K.S, "Controlling and Testing the strength of Silicon on the mesoscale", *J. Amer. Ceram. Soc*, **Vol 83**, 2000, pp. 1467-1484.

[63]. William T, "Theory of Vibrations with Applications", Fifth Edition, Prentice Hall, Inc. 1998.

[64]. Leonard M, "Elements of Vibrational Analysis", Second Edition, McGraw-Hill, Inc. 1986

[65]. Srikar V.T, Senturia S.D, "The reliability of microelectromechanical systems in shock environments", *JMEMS.*, **Vol. 11**, 2002, pp. 206-214.

[66]. Srikar V.T, Mark S, "Materials selection in micromechanical design: An application of the ashby approach", *JMEMS.*, **Vol. 12**, Feb 2003, pp. 3-10.

[67]. Amritsar J, Stiharu I, Packirisamy M, "Micro Electro Mechanical Systems (MEMS) for enzymatic detection", Proceedings of SPIE, Optical Biochips and Biosensors for Nucleic Acids and Proteins, **Vol 5969-26**, Editors: Ulrich J. Krull, Paul A. Piunno, 2005.

[68]. Srikar V.T, Anna K. Swan M, Selim U, Bennett B.G, Mark S, "Micro-Raman Measurement of bending stresses in Micromachined Silicon Flexures", *JMEMS.*, **Vol. 12**, Dec 2003, pp. 779-787.

[69]. Shanley F.R, "Strength of Materials", McGraw-Hill, New York, 1957.

[70]. Timoshenko S, "Strength of Materials", Huntington, New York: Robert E. Krieger Publishing company, 1976.

[71]. Dunford H.B, "Horseradish Peroxidase: structure and kinetic properties. In Peroxidases in Chemistry and Biology, **Vol 2**, J. editors: Everse, K.E. Everse, and M.B. Grisham, CRC press, Boca Raton, FL, pp. 1-24.

[72]. Rama B, "Natural Frequencies of Rectangular Plates using Characterization Orthogonal Polynomials in Rayleigh-Ritz Method", *J. Sound and Vibrations*, **Vol 102**, 1985, pp. 493-497.

[73]. Gino R, Packirisamy M, Stiharu I, "Experimental investigation on the dynamics of MEMS structures", Proceedings of SPIE, **Vol 12**, 2004.

[74]. Packirisamy M, Stiharu I, Rama B, "Application of Boundary Conditioning to the Synthesis of Microsystems", Micro Electro Mechanical Systems Conference, Berkeley, California, USA, 24-26 August 2001, pp. 83-86.

[75]. Wachter E.A, Thundat T, Oden P.I, Warmack R.J, "Remote optical detection using microcantilevers", *Rev. Sci. Instrum.* **Vol 67 (10),** October 1996, pp. 3434-3439.

[76]. Sarid D, "Scanning Force Microscopy with applications to Electric, Magnetic and Atomic Forces", Oxford University Press, New York, 1991.

[77]. Chen G.Y, "Transient response of tapping scanning force microscopy in liquids", *J. Vac. Sci. Technol.* **Vol B 14(2),** March 1996, pp. 1313-1317.

[78]. Fritz J, "Translating Biomolecular recognition into nanomechanics", *Science*, **Vol 288**, April 2000, pp. 316-318.

[79]. Amritsar J, Packirisamy M, Stiharu I, Ganesharam B, "Micro Electro Mechanical Systems (MEMS) for enzymatic detection", Proceedings of SPIE, MEMS, MOEMS and Micromachining. **Vol 5455**, Editor(s): Hakan Urey, Ayman El-Fatatry, 2004, pp. 101-109.

[80]. Amritsar J, Stiharu I, Packirisamy M, "Enzymatic detection of Troponin C and Melittin Bee", Proceedings of SPIE, Nanophotonics and Biomedical applications II, **Vol. 5705**, Editors: Alexander N, Cartwright, Marek Osinski, pp. 40-51.

[81]. Jingyan W, Ying M, Daqian S, Xuexun F, Xia L, Lisha B, Hanqi Z, Guizhen Z, Jiahua D, Weizhong W, Qinhan J, Guimin L, "A novel sandwich immunosensing method for measuring cardiac troponin I in sera", *Analytical biochemistry*, **Vol 321**, 2003, pp. 209-216.

[82]. Katagiri T, "Alterations in cardiac troponin subunits in myocardial infarction", *Jpn. Heart J*, **Vol 22**, 1987, pp. 653-664.

[83]. Li D, "Greater frequency of increased cardiac troponin T than increased cardiac troponin I in patients with chronic renal failure", *[Letter], Clin. Chem*, **Vol 42**, 1996, pp. 114-115.

[84]. Stiharu I, Rakheja S, Packirisamy M, Amritsar J, "MEMS Based Cardiac Bio-enzyme Detection for the Acute Myocardial Syndrome Recognition", *WSEAS Transactions on Systems*, **Vol. 4, issue 5**, May 2005, pp. 577-584.

[85]. Dawson C. R, Drake A. F, Helliwell J, Hider R. C, "The interaction of Bee Melittin with lipid bilayer membranes", *Biochem. Biophys. Acta*, **Vol 510**, 1978, pp. 75.

[86]. Dolman D, Newell G. A, Thurlow M. D, "A Kinetic study of the reaction of horseradish peroxidase with hydrogen peroxide", *Can J Biochem.* **Vol 53(5),** 1975, pp. 495-501.

[87]. Motomasa T, Koji M, Shiro Y, Satoshi T, Koichiro I, Hiroshi H, Isao M, "Activation of Hydrogen Peroxide in Horseradish Peroxidase Occurs within ~200 μs observed by a new freeze-quench device", *Biophysical Journal*, **Vol. 84**, March 2003, pp. 1998-2004.

[88]. Robert K.D, David H.D, "Substituted Hemins as probes for Structure-Function Relationships in Horseradish Peroxidase", *The Journal of Biological Chemistry*, **Vol. 256**, issue 13, July 10th 1981, pp. 6903-6912.

[89]. Senesac L . R, Farahi R. H, Corbeil J. L, Earl D. D, Rajic S, Datskos P. G, "Fabrication of integrated diffractive micro-optics for MEMS application", Proceedings of SPIE, **Vol 4451,** 2001.

[90]. Datskos P.G, Thundat T, Nickolay V.L, "Micro and Nano-cantilevers Sensors", *Encyclopedia of nanoscience and nanotechnology*, **Vol 10**, 2004, pp. 1-10.

[91]. Xia L, Jingyan W, Daqian S, Ziwei Z, Hanqi Z, Guimin L, "Determination of affinities and antigenic epitopes of bovine cardiac troponin I (cTnI) with monoclonal antibodies by surface plasmon resonance biosensor", *Analytical Biochemistry*, **Vol 314**, 2003, pp. 301-309.

[92]. Comte M, Maulet Y, Cox J.A, "Ca^{2+} -dependant high-affinity complex formation between calmodulin and Melittin", *Biochem. J*, **Vol 209**, 1983, pp. 26.

[93]. Amritsar J, Stiharu I, Packirisamy M, "MOEMS for Bio-Enzymatic Detection", Technical Review of the Canadian Institute for Photonic Innovations (CIPI), **Vol 3 (1),** Spring 2005.

[94]. Babu A, Rao V.G, Su H, Gulati J, "Critical minimum length of the central helix in troponin C for the Ca^{2+} switch in muscular contraction", *J. Biol. Chem*, **Vol 268,** 1993, pp. 19232-19238.

[95]. Walters D.A, Cleveland J.P, Thompson N.H, Hansma P.K, Wendman M.A, Gurley G, Elings V., "Short cantilevers for atomic force microscopy", *Rev. Sci Instrum*, **Vol 67**, 1996, pp. 3583-3590

[96]. Kakiuchi S, Yamazaki R, Teshima Y, and Venishi K, "Regulation of Nucleoside Cyclic 3:5 –Monophosphate Phosphodiesterase Activity from Rat Brain by a Modulator and a Ca^{2+}", *Proc. Natl. Acad. Sci. U.S.A.,* **Vol 70,** 1973, pp. 3526.

[97]. Clague M. J, and Cherry R. J, "A comparative study of band 3 aggregation in erythrocyte membranes by melittin and other cationic agents", *Biochim. Biophys. Acta*, **Vol 980**, 1989, pp. 93-99.

[98]. Marco V. W, Parvez I. H, Wim E. H, Daan J.A.C, "Fourier Transform Infrared Spectrometric Analysis of Protein Conformation: Effect of Sampling Method and Stress Factors", *Analytical Biochemistry*, **Vol 297**, 2001, pp. 160-169.

[99]. Spigia O, Bernini A, Scarselli M, Ciutti A, Bracci L. L, Lelli B, Maro D.D, Calamandrei D, Niccolai N., "Peptide-protein interactions studied by surface Plasmon and nuclear magnetic resonances", *FEBS Lett*, **Vol 511**, 2002, pp. 33-35

[100]. Frey S, Tamm L.K, "Orientation of melittin in phospholid bilayers: a polarized attenuated and total reflection infrared study", *Biophys J*, **Vol 60**, 1991, pp. 922-930

[101]. Berneche S, Nina M, Roux B, "Molecular dynamics simulation of melittin in a dimyristoylphosphatidylcholine bilayer membrane", Biophys. J, Vol 75, 1998, pp. 1603-1618.

[102]. Yves M, Jos A. C, 'Structural changes in melittin and calmodulin upon complex formation and their modulation by calcium', Biochemistry, Vol 22, 1983, pp. 5680-5686

[103]. Comte M, Maulet Y, Jos A C, 'Ca^{2+} -dependant high affinity complex formation between calmodulin and melittin', *Biochem. J*, **Vol 209**, 1983, pp. 26

[104]. Malencik D.A, Anderson S.R, "Association of melittin with the isolated myosin light chains", Biochemistry, Vol 27, 1988, pp. 1941-1949